



Subthalamic Nucleus Neural Synchronization and Connectivity during
Limbic Processing of Emotional Pictures: Evidence from Invasive
Recordings in Patients with Parkinson's Disease

Synchronisierung und Konnektivität des Nucleus subthalamicus während
limbischer Bearbeitung affektiver Bilder: Evidenz aus invasiven
Aufzeichnungen in Patienten mit Morbus Parkinson

A dissertation for the degree of

Doctor rerum naturalium

submitted by

Uri Eduardo Ramírez Pasos

at the Graduate School of Life Sciences,
Julius-Maximilians-Universität Würzburg,
Section Neuroscience

Würzburg, 2018



Submitted on:

Office stamp

Members of the *Promotionskomitee*:

Chairperson: Prof. Dr. Paul Pauli

Primary Supervisor: Prof. Dr. Jens Volkmann

Supervisor (Second): Prof. Dr. Erhard Wischmeyer

Supervisor (Third): Prof. Dr. Muthuraman Muthuraman

Date of Public Defence:

Date of Receipt of Certificates:

ABSTRACT

In addition to bradykinesia and tremor, patients with Parkinson's disease (PD) are known to exhibit non-motor symptoms such as apathy and hypomimia but also impulsivity in response to dopaminergic replacement therapy. Moreover, a plethora of studies observe differences in electrocortical and autonomic responses to both visual and acoustic affective stimuli in PD subjects compared to healthy controls. This suggests that the basal ganglia (BG), as well as the hyperdirect pathway and BG thalamocortical circuits, are involved in affective processing. Recent studies have shown valence and dopamine-dependent changes in synchronization in the subthalamic nucleus (STN) in PD patients during affective tasks. This thesis investigates the role of dopamine, valence, and laterality in STN electrophysiology by analyzing event-related potentials (ERP), synchronization, and inter-hemispheric STN connectivity. STN recordings were obtained from PD patients with chronically implanted electrodes for deep brain stimulation during a passive affective picture presentation task. The STN exhibited valence-dependent ERP latencies and lateralized 'high beta' (28–40 Hz) event-related desynchronization. This thesis also examines the role of dopamine, valence, and laterality on STN functional connectivity with the anterior cingulate cortex (ACC) and the amygdala. The activity of these limbic structures was reconstructed using simultaneously recorded electroencephalographic signals. While the STN was found to establish early coupling with both structures, STN-ACC coupling in the 'alpha' range (7–11 Hz) and uncoupling in the 'low beta' range (14–21 Hz) were lateralized. Lateralization was also observed at the level of synchrony in both reconstructed sources and for ACC ERP amplitude, whereas dopamine modulated ERP latency in the amygdala. These results may deepen our current understanding of the STN as a limbic node within larger emotional-motor networks in the brain.

ZUSAMMENFASSUNG

Neben Bradykinese und Tremor weisen Patienten mit Morbus Parkinson (PD) bekannterweise nicht-motorische Symptome auf wie Apathie und Hypomimie, aber auch Impulsivität, welche durch Dopaminersatztherapien bedingt ist. Viele Studien belegen außerdem Unterschiede von kortikalen und autonomen Reaktionen auf sowohl visuelle als auch akustische Reize bei Patienten mit PD im Vergleich zu gesunden Kontrollgruppen. Dies legt nahe, dass sich die Basalganglien (BG), und auch die hyperdirekte Verbindung sowie die BG-thalamokortikalen Schleifen, an der Affektbearbeitung beteiligen. Jüngere Studien haben Valenz- und Dopamin-bedingte Veränderungen der Synchronisierung im Nucleus subthalamicus (STN) von Parkinson-Patienten bei affektiven Aufgaben belegt. Diese Promotionsarbeit untersucht die Rolle von Dopamin, Valenz und Lateralität in der STN-Elektrophysiologie mittels Analysen von ereigniskorrelierten Potentialen (ERP), Synchronisierung und interhemisphärischer funktioneller Konnektivität. STN-Aufzeichnungen wurden von Patienten mit dauerhaft implantierten Elektroden für die Tiefenhirnstimulation während einer passiven Aufgabe abgeleitet, bei den ihnen Bilder mit emotionalen Inhalten gezeigt wurden. Der STN wies Valenz-bedingte ERP-Latenz und lateralisierte ereigniskorrelierte Desynchronisierung in ‘hohem Beta’ (28–40 Hz) auf. Diese Dissertation untersucht auch die Rolle von Dopamin, Valenz und Lateralität bezüglich der funktionellen Konnektivität zwischen dem STN und dem Gyrus cinguli pars anterior (ACC) sowie der Amygdala. Die Aktivität dieser Strukturen wurde aus simultanen elektroenzephalographischen Aufzeichnungen rekonstruiert. Obwohl eine STN-Kopplung mit beiden Strukturen auftritt, war die STN-ACC-Kopplung im ‘Alpha’-Bereich (7–11 Hz) und die Entkopplung im ‘niedrigen Beta’-Bereich (14–21 Hz) lateralisiert. Lateralisierung wurde auch an der Synchronisierung in beiden rekonstruierten Quellen und an der ACC-ERP-Amplitude festgestellt, wohingegen Dopamin die ERP-Latenz in der Amyg-

dala modulierte. Diese Ergebnisse mögen das gegenwärtige Wissen vom STN als limbischem Knoten innerhalb größerer affektiv-motorischer Schleifen im Gehirn vertiefen.

Table of Contents

I. Affidavit.....	viii
II. Acknowledgements	ix
III. Abbreviations	x
IV. List of Figures.....	xii
V. List of Tables	xiii
1. Introduction	1
1.1. Emotion and Parkinson's Disease	1
1.2. Parkinson's Disease and its Neuropathology.....	1
1.3. The Basal Ganglia.....	3
1.4. The Subthalamic Nucleus	4
1.5. The STN and Oscillations.....	6
1.6. Deep Brain Stimulation	9
1.7. Emotion Circuits in the Brain	10
1.8 Understanding the Limbic Brain through Affective Pictures.....	12
2. Methods	15
2.1. Data Collection	15
2.2. Recordings and Paradigm	15
2.3. Preprocessing	18
2.4. STN Event-Related Potentials	18
2.5. STN Power Analysis	20
2.6. Inter-STN Coupling	22
2.7. Source Reconstruction	24
2.8. Event-Related Potentials with Reconstructed Sources	26
2.9. Power Analysis with Reconstructed Sources.....	26
2.10. Coherence with STN-LFPs and Reconstructed Sources.....	27
3. Results	28
3.1. Event-Related Potentials in the STN	28
3.2. Power Analysis in the STN.....	30
3.3. STN-STN Coupling	31
3.4. Event-Related Potentials in Reconstructed Sources	33
3.5. Power Analysis for Reconstructed Sources	34
3.6. STN-Reconstructed Sources Coherence.....	36

4. Discussion	39
4.1. STN ERP Analysis	39
4.2. STN Power Analysis	41
4.3. STN Coherence Analysis	43
4.4. Analysis of Reconstructed Sources	44
5. Concluding Remarks	48
6. Future Directions	51
7. References	53
8. Appendix	66
9. Curriculum Vitae	69

I. Affidavit

I hereby confirm that my thesis entitled *Subthalamic Nucleus Neural Synchronization and Connectivity during Limbic Processing of Emotional Pictures: Evidence from Invasive Recordings in Patients with Parkinson Disease* is the result of my own work. I did not receive any help or support from commercial consultants. All sources and/or materials applied are listed and specified in the thesis.

Furthermore, I confirm that this thesis has not yet been submitted as part of another examination process neither in identical nor in similar form.

Würzburg, July 20th of 2018

Eidesstattliche Erklärung

Hiermit erkläre ich an Eides statt, die Dissertation *Synchronisierung und Konnektivität des nucleus subthalamicus während limbischer Bearbeitung affektiver Bilder: Evidenz aus invasiven Aufzeichnungen in Patienten mit Morbus Parkinson* eigenständig, d.h. insbesondere selbstständig und ohne Hilfe eines kommerziellen Promotionsberaters, angefertigt und keine anderen als die von mir angegebenen Quellen und Hilfsmittel verwendet zu haben.

Ich erkläre außerdem, dass die Dissertation weder in gleicher noch in ähnlicher Form bereits in einem anderen Prüfungsverfahren vorgelegen hat.

Würzburg, den 20.07.2018

II. Acknowledgements

I would like to express my gratitude to my *Doktorvater* Prof. Jens Volkmann of the University of Würzburg, as well as my other supervisors, Prof. Muthuraman Muthuraman of the University of Mainz and Prof. Erhard Wischmeyer of the University of Würzburg. Their vast knowledge, patience, kindness, and constant support made this dissertation possible. Dr. Andreas Keil provided valuable input on experimental design. I would also like to thank Dr. Isaias, Dr. Reich, and Dr. Steigerwald for their generous help with technical and administrative aspects concerning my experiments with PD patients.

I would like to thank my wonderful colleagues Virginia Maltese, Chiara Palmisano, Lisa Rauschenberger, and Susanne Knorr, who enriched my time at the hospital and often lent a hand when I needed it. Special thanks to Nicolás Pozzi, whose unequalled moral-boosting prowess made a difference.

I would like to take the opportunity to thank the patients who kindly agreed to participate in my lengthy experiments and who allowed me to get to know them during the long data download periods of the PC+S devices.

Many thanks to the incredibly helpful staff at the Graduate School of Life Sciences as well as to the Graduiertenkolleg ‘Emotions’, which exposed me to a truly multifaceted research milieu and funded the research presented here.

Lastly, my gratitude goes to my family and friends from Mexico for their unremitting love and support. Special thanks to Jorge, Valeria, Atenea, Lorena, and Emilia for accompanying me in one way or another and for helping me in the most unexpected ways. I am thankful to Daniel for being a most loving friend. The last few years have run less smoothly than expected, yet Yannick stuck through it by my side and created the closest thing to family that I had in Germany. I am lucky.

Uri Ramírez Pasos

III. Abbreviations

ACC	Anterior cingulate cortex
BG	Basal ganglia
BLA	Basolateral complex of the amygdala
CeA	Central nucleus of the amygdala
dACC	Dorsal anterior cingulate cortex
DBS	Deep brain stimulation
DD	Dopaminergic denervation (factor)
DOP	Dopaminergic medication state (factor)
DRT	Dopamine replacement therapy
EEG	Electroencephalography
ERD	Event-related desynchronization
ERP	Event-related potential
ERS	Event-related desynchronization
fMRI	Functional magnetic resonance imaging
GABA	gamma-Aminobutyric acid
GPe	Globus pallidus externus
GPi	Globus pallidus internus
Hz	Hertz
IAPS	International Affective Picture System
LFP	Local field potential
MEG	Magnetoencephalography
ML	midpoint latency
ms	millisecond

MSN	Medium spiny neurons
M1	Primary motor cortex
MW	Measurement window
PD	Parkinson's disease
PFC	Prefrontal Cortex
pgACC	Pregenua anterior cingulate cortex
sgACC	Subgenual anterior cingulate cortex
SNpr	Substantia nigra pars compacta
STN	Substantia nigra pars reticulata
SNpc	Subthalamic nucleus
UPDRS	Unified Parkinson's disease rating scale
VAL	Valence (factor)

IV. List of Figures

2.1 Schematic of picture presentation paradigm	16
3.1 STN waveforms	29
3.2 Normalized STN waveforms	30
3.3 STN-ERP and valence	31
3.4 STN time-frequency analysis	32
3.5 Laterality effect on low beta ERD in STN.....	33
3.6 Inter-hemispheric STN coherence	34
3.7 Waveforms of reconstructed sources	35
3.8 Dopamine and laterality effects in ERP analysis of reconstructed sources	36
3.9 Laterality in time-frequency analysis of reconstructed sources	37
3.10 Functional connectivity between the STN and reconstructed sources	38
5.1 Motor-affective information processing schematic	49

V. List of Tables

Table 2.1 Normative ratings of IAPS stimuli used in this study	17
Table 2.2 Patient ERP ‘flipping’	19
Table A1 Patient information	65
Table A2 STN Signed Area Amplitudes	65
Table A3 STN 50% area latencies. Mean values per condition combination, SD in parentheses	66
Table A4 Virtual amygdala ERP parameter values	66
Table A5 Virtual ACC ERP parameter values	67

1. Introduction

1.1. Emotion and Parkinson's Disease

Survival of an organism depends on its ability to recognize and act upon challenges and opportunities in the environment. Key to understanding the neural basis underlying these abilities in humans is the total identification of the ‘survival circuits’ (LeDoux, 2012) in the central nervous system that process the appraisal of external stimuli, their associated approach or avoidance responses, and reinforcement learning mechanisms. There is evidence that some of these circuits are conserved across vertebrates (Butler and Hodos, 2005; Swanson, 2002). Emotional processes like stimulus appraisal are encoded in circuits which receive input from sensory brain areas and send output to motor areas (Sander, Grandjean, & Scherer, 2005; Scherer et al., 2001), but such patterns of connectivity can be disrupted in the diseased brain (Argaud et al., 2018). Indeed, patients with Parkinson’s Disease (PD), a neurodegenerative disorder primarily associated with motor impairments, may experience hypomimia (Bologna et al., 2016), a condition characterized by an attenuation of gestural responses, despite the presence of a feeling like fear or joy. With non-motor symptoms of PD such as cognitive impairment and autonomic dysfunction having reached the status of clinical relevance (Khoo et al., 2013; Duncan et al., 2014), a number of studies on affective impairments in PD have emerged in the last decade (Blonder & Slevin, 2011; Susuki et al., 2006; den Brok et al., 2015; Kawamura & Kobayakawa, 2009; Dissanayaka et al., 2014; McIntosh et al., 2015; Lin et al., 2016), which suggests that the nuclei of the basal ganglia, or the modulation they exert via connections to other brain structures, may play a role in affective processing within limbic or ‘survival’ circuits. Interestingly, PD patients show a diminished late positive potential compared to healthy controls when observing images with unpleasant content, which may be due to defense circuits being compromised in PD (Dietz et al., 2013).

1.2. Parkinson’s Disease and its Neuropathology

PD is the second most common neurodegenerative disorder, after Alzheimer’s disease (Dorsey et al., 2007; Alzheimer’s Association, 2014). While progressive death of dopaminer-

gic neurons in the substantia nigra *pars compact* (SNpc) is considered the hallmark pathological feature of PD, abnormalities in other non-dopaminergic neurotransmitters also give rise to symptoms of PD (Kalia et al., 2013; Yarnall et al., 2011). PD patients suffer from disabling and progressive motor impairments which include bradykinesia (slowness of movement initiation and decreased speed and amplitude of movement), an essential diagnostic criterion, as well as rigidity, postural instability, and tremor (Kalia & Lang, 2015). Due to a heterogeneous symptomatology, subtypes have been proposed (Marras & Lang, 2013), although the most common division remains between tremor-dominant and non-tremor-dominant (also known as akinetic-rigid) symptoms. Age is the primary risk factor (Pringsheim et al., 2014), with incidence rates rising sharply at 60 and peaking at around 80 years (Driver et al., 2009). PD is more prevalent in men than in women (3:2 ratio, De Lau & Breteler, 2006), and incidence is greater in Europe and North and South America than in Africa, Asia, and Arabic countries (Kalia & Lang 2015).

Pharmacological treatments are highly effective at ameliorating motor impairments even if they do not change the evolving course of PD. In dopamine replacement therapy (DRT), patients are most commonly administered the dopamine precursor levodopa and dopamine agonists, which are most effective at reducing bradykinesia and rigidity (Fox et al., 2011; Connolly & Lang., 2014). DTR may generate disabling motor side-effects in patients, particularly at advanced stages of the disease, such as dyskinesia (Obeso et al., 2007) and fluctuations (motor and non-motor; Kikuchi, 2007). In particular, dopamine agonists can lead to impulse control disorders such as gambling (Santangelo et al., 2013) and hypersexuality (Klos et al., 2005; Codling et al., 2015). In recent years, non-motor adverse effects of dopaminergic drugs have gained increasing attention and are consistent with the known role of dopamine in the reward system. Patients may exhibit hyperappetitive behaviors ranging from increased creativity and hobbyism to severe impulse control disorders including pathological gambling (Santangelo et al., 2013), hypersexuality (Klos et al., 2005), binge eating, impulsive shopping and reckless driving in addition to stereotypic behavior called punding (Markovik et al., 2017), D2/D3 dopamine agonists have a higher risk of causing these abnormal behaviors compared to levodopa (Codling et al., 2015).

1.3. The Basal Ganglia

The basal ganglia (BG) are subcortical nuclei that are highly interconnected and are thought to contribute to action selection, procedural learning, and motivational processes. The principal input structure is the dorsal striatum, with projections deriving from motor, sensory, cognitive, and limbic cortices (Kemp and Powell, 1970; McFarland and Haber, 2000). The striatum is composed of the caudate and the putamen and receives massive cortical and thalamic excitatory glutamatergic afferents (Mathai & Smith, 2011) in a functionally segregated fashion: projections stemming from motor cortices terminate at the matrix compartment and those from prefrontal or limbic area at the striosome (Albin et al., 1989). In addition, the striatum receives dopaminergic afferents from the substantia nigra pars compacta (SNpc). Primary output structures in primates are the internal globus pallidus (GPi) and the substantia nigra pars reticulata (SNpr).

The striatum is primarily constituted by two types of medium spiny neurons (MSN), which differ in dopamine receptor expression and their projections' targets (Gerfen et al., 1990; Smith et al., 1998). D1-receptor MSNs are G_s -coupled (i.e., output-promoting) and project to GABAergic neurons in the SNpr and the internal GPi, whereas D2-receptor MSNs are G_i -coupled (i.e., output-inhibiting) and project to the external globus pallidus (GPe). Dopamine has thus opposite effects on D1- and D2-class MSNs, though the nature of the classical BG pathways leads to both ultimately promoting movement (Albin et al., 1989). The direct pathway starts with D1-receptor striatal neurons projecting inhibitory GABAergic axons onto the GPi, which contains GABAergic neurons and projects to the SNpr and the thalamus. The indirect pathway involves D2-receptor striatal forming inhibitory synapses onto the GPe, which in turn directs GABAergic axons onto the STN and the GPi. The STN is the only BG structure in these pathways that sends excitatory glutamatergic projections to other structures, namely the GPe (thus establishing a reciprocal connection; Loucif et al., 2005) and the GPi.

What role do these pathways play? The BG, in particular the dorsal striatum, have been observed to be involved in action selection and initiation during decision making (Balleine et al., 2007), where reward probability modulates the activity of striatal neurons (Kawagoe et

al., 1998) and dopamine-mediated changes in plasticity at the striatum are likely to underlie goal-directed learning (Kreitzer and Malenka, 2008). Specifically, a study using optogenetics to manipulate receptors D1 and D2 activation in mice during operant and place-preference tasks (Kravitz et al., 2012) found that activation of MSNs in the direct pathway is conducive to long-lasting reinforcement, whereas activation of indirect pathway, D2-receptor MSNs to short-lived punishment. In line with this, PD patients exhibit learning struggles when probabilistic stimuli relating action to outcome are used (Poldrack et al., 2001), but are unimpaired when there is no such action-outcome contingency (Shohamy et al., 2004).

1.4. The Subthalamic Nucleus

Among the nuclei of the basal ganglia lies the subthalamic nucleus (STN), a biconvex lens-shaped structure (Yelnik and Percheron, 1979) located ventral to the thalamus, dorsal to the substantia nigra and the cerebral peduncle, lateral to the red nucleus and the posterior lateral hypothalamic area, and medial to the GPe (Hamani et al., 2004). The STN-to-brain volume relationship is proportional in humans and non-human primates (Carpenter, 1982) and STN in cat, monkey, and human are densely populated by Golgi type 1 glutamatergic projection neurons (Yelnik and Percheron, 1979). GABAergic interneurons in the STN populate its medial ventrocaudal region (Levesque and Parent, 2005). The human STN receives inhibitory afferents from the GPe through the subthalamic fasciculus, excitatory projections from the cortex via the hyperdirect pathway (Nambu et al., 2002) and from the thalamus, and modulating dopaminergic innervation from the substantia nigra (Hamani et al., 2004). STN efferents are glutamatergic and primarily arborize the GPe and GPi, although it sends projections onto both compartments of the substantia nigra, particularly pars reticulata, and to a lesser extent to the striatum (Hamani et al., 2004).

The determination of functional subdivisions in the STN has been based on two inferential approaches. The earlier approach (Parent and Hazrati, 1995; Shink et al., 1996) relied on the parallel pathways model of the BG (Alexander et al., 1986), where motor, associative, and limbic corticostriatal afferents are followed by contiguous projections along the classical BG pathways that innervate virtually separate zones in the GPe, GPi, and STN. This tripartite

functional model divides in thirds the rostrocaudal and mediolateral axes. The limbic zone occupies the medial third within the rostral two thirds (hence ‘rostromedial’), the motor zone the dorsolateral portion of the two rostral thirds as well as the caudal third, and the associative zone the ventrolateral aspect of the two rostral thirds and a small ventromedial portion of the caudal third. The later approach appeals to cortical innervation of the STN via the hyper-direct pathway by employing diffusion weighted imaging (Lambert et al., 2012) and anterograde tracers (Haynes & Haber, 2013). The limbic STN receives afferents in its medial zone from the anterior cingulate cortex (ACC), the ventromedial prefrontal cortex, the orbitofrontal cortex, and the amygdala. Overall, these two approaches’ results are comparable. Yet, evidence against an absolute functional segregation in the STN has accrued from histological, connectivity, and stimulation studies. Dendrites extend along the rostrocaudal axis of the STN and may cover two thirds of the nucleus’ volume (Yelnik & Percheron, 1979), thus potentially receiving innervation from different functional domains. Pallidosubthalamic projections are not entirely functionally segregated, for a portion of associative pallidal fibers also innervate STN motor aspects (Hamani et al., 2004). Fibers from the OFC, vmPFC, and ACC converge at the medial tip, while dorsal prefrontal cortex (DPFC) terminals overlap with those from area 6 (a motor region; Haynes & Haber, 2013). Finally, direct electrical stimulation at the anteromedial STN of two PD patients both ameliorated motor impairments and caused a hypomanic state (Mallet et al., 2007). Thus, the STN might be a site of functional integration that can influence BG output structures with richer signals.

In addition, cortico-subthalamic input, known to be faster than the polysynaptic direct and indirect pathways (Nambu et al., 2002), may filter out the proportion of suboptimal or inappropriate behavioral programs that are transmitted on the direct pathway (Haynes & Haber, 2013). Beyond motor programs, other cortical areas, such as the rostral DPFC, which is involved in perceptual decision making, may influence BG output via the STN (Bogacz & Larsen, 2011). Thus, the STN might belong to a response inhibition network (Zavala et al., 2015), in which the medial PFC induces the elevation of decision thresholds (Frank et al., 2015) in the STN when this prefrontal structures detects conflict that demands the gathering of more information before making a choice. The conflict can occur when two or more pre-motor programs are released (Taylor et al., 2007), upon which prefrontal excitation of the

STN leads to the STN enhancing GPi inhibition of the thalamus, thus preventing movement until a corticostriatal signal is strong enough to effectively inhibit the GPi (Aron et al., 2016). Such a ‘pause’ function may come into play during other forms of cognitive processing, such as upon receiving a surprising stimulus. Indeed, unexpected stimuli do not only activate a cortical stopping system, as observed during a tone-paired imperative stimuli paradigm (Wessel & Aron, 2013), but they can also be accompanied by an increase in local field potential (LFP) synchronization at the STN during a working memory task (Wessel et al., 2016).

1.5. The STN and Oscillations

The study of LFPs in the STN has contributed significantly to our understanding of STN function, largely due to high temporal resolution, which allows better tracking of cognitive processes. The denomination ‘local field potential’ refers to a measurement via a metal or glass electrode of the extracellular electric potential V that arises from the superimposed electric current contributions of a plethora of sources, with synaptic transmembrane currents, also known as postsynaptic potentials (PSP), being the most significant contribution (Búzsaiki et al., 2012). Electroencephalography (EEG) is the superficial measurement of the same electric potential V that can be recorded at the scalp (Búzsaiki et al., 2012). Both excitatory and inhibitory PSPs contribute to the measured LFP and the amplitude of the source is inversely proportional to the distance from the recording electrode (Búzsaiki et al., 2012). A PSP is caused when a neurotransmitter binds to its corresponding receptor at the postsynaptic membrane and leads to ionic currents from the extracellular into the intracellular space. An excitatory PSP increases the probability of an action potential, while an inhibitory PSP decreases it (Purves et al., 2001). Ionic currents at the membrane generate ‘sinks’ and ‘sources’. Conventionally, the area where positive charges enter the cell body is a sink, whereas where they leave into extracellular space is a source (with opposite nomenclature for negative charges). Together, sinks and sources form dipoles. The geometry of a neuron as well as the spatial alignment of neighboring neurons determines the amplitude of their contribution to the LFP. Specifically, long dendrites and parallel alignment between neurons, which is the case of pyramidal neurons, create the conditions for high ionic flow, which in turn significantly alters the extracellular electric field (Búzsaiki et al., 2012). If an assembly of such neurons have

membranes that fluctuate synchronously, their overlapping PSP will summate (Buzsaki et al., 2012). Such rhythmic activity has been linked to cognitive processes such as attention, perception, and memory (Jones et al., 2010; Sacchet et al., 2015; Kopell, Gritton, Whittington, Kramer, 2014). For instance, cortical and subcortical synchronous or rhythmic activity in the theta (about 3.5–7.5 Hz) and alpha (about 7.5–12.5 Hz) bands has been correlated to information encoding and retrieval, respectively (Klimesch, 1999), while cortical beta desynchronization is observed during static motor control (Engel & Fries, 2010).

An array of studies have grappled with the question as to whether the changes in extracellular current produced by these summations have causal or epiphenomenal significance. Evidence for the former comes from modeling studies showing a monotonic relationship between synchrony and mean neuronal activity (i.e., synchrony leads to synaptic gain; Chawla et al., 1999) as well as ephaptic coupling, which occurs when the extracellular field modifies a neuron's transmembrane potential (i.e., its excitability), thus impacting spike timing (Anastassiou et al., 2010). Integration of information from different sources can occur through synchronous input onto the target of a functional network, as in predictive coding (Rao & Ballard, 1999; Friston et al., 2015). Synchronous input takes place either due to oscillatory synchrony or changes in plasticity, i.e. strengthening synapses, but the former is the more cost-effective alternative (Buzsaki & Draguhn, 2004). Indeed, oscillations can promote plasticity that depends on spike-timing (Buzsaki & Draguhn, 2004).

Thus rhythmic neural activity can serve physiological processes, yet synchrony may also impair normal brain function, such as loss of consciousness during epileptic seizures or under anesthesia (Steriade, 2001). Cortical and subcortical rhythms that are detrimental for cognition can be both high-frequency spiking activity (as in temporal lobe epilepsy, Yaari and Beck, 2002) or low-frequency, such as thalamic delta (about 0.5–3.5 Hz) and cortical theta (about 3.5–7 Hz) interensemble synchrony as in anesthesia (Sheeba, Stefanovska, & McClintock, 2008). In the STN, pathological oscillations are thought to be responsible for bradykinesia in PD (Engel & Fries, 2010). In particular, exaggerated synchrony in the beta band (about 13–30 Hz) may limit the diversity of processes in the STN, that is, it may oversaturate coding space in a maladaptive fashion (Brittain & Brown, 2014). Excessive STN beta arises

most likely due to cortical entrainment via the hyperdirect pathway in the higher beta band (20–30 Hz), which not only entrains an STN that in the dopamine-deficient state is uninhibited by the suppressed GPe, but also leads to dopamine-dependent non-linear correlations between low (13–20 Hz) and high beta rhythms (Marceglia et al., 2006; Brittain & Brown, 2014). More moderate beta synchrony is, however, arguably physiological, since it could enable the blocking of multiple inappropriate motor programs that emerge in a given context (Kühn et al., 2004), and therefore STN beta synchrony may be best conceptualized as an ‘immutability promoting rhythm’ (Brittain & Brown, 2014). Other faster physiological STN rhythms such as gamma oscillations (about 40–90 Hz) have been considered ‘mutability promoting’ by Brittain and Brown (2014) and ‘attention-related early stimulus encoding’ by Huebl and colleagues (2014), though slower STN rhythms in the alpha range have also been reported and may be associated with active retrieval of semantic memory (Klimesch, 1999). Alpha desynchronization during 1 to 2 seconds after the presentation of a picture has been observed to be higher for pictures with pleasant than with unpleasant content in PD patients in the medication state ON. Interestingly, the pattern is reversed in patients with low depression scores and in the medication OFF state (Huebl et al., 2014; Kühn et al., 2005; Brücke et al., 2007; Huebl et al., 2011). Such an enhancement of appetitive affective processing in the ON state (i.e., an approximation to the physiological state) could potentially play a role in BG-mediated positive reinforcement learning.

Inter-hemispheric STN synchrony (or functional coupling, see see Varela, Lachaux, Rodriguez, & Martinerie, 2001) has been reported in the alpha (Darvas & Hebb, 2014) and beta (de Solages, Hill, Koop, Henderson, & Bronte-Stewart, 2010) bands. While it has been associated to the resting state (Little et al, 2013), its functional role has not been demonstrated. Inter-STN connectivity probably arises from both nuclei being entrained by a common cortical input (Litvak et al., 2011). Indeed, inter-nuclei coupling (as indexed by alpha coherence) decreases during movement (Talakoub et al., 2016). Inconsistencies with regards to correlations with motor scores or dependence on dopaminergic medication states (Little et al., 2013; West et al., 2016) leave open the question as to whether left-right STN coupling might be physiological, pathological, or just epiphenomenal.

1.6. Deep Brain Stimulation

Deep brain stimulation (DBS) is a well-established treatment for motor disorders pioneered by Alim Louis Benabid in 1987 (Benabid, Pollak, Louveau, Henry, & de Rougemont, 1987) which delivers direct electrical current into an appropriate target in the brain. Targets are identified through combined use of stereotactic coordinates and pre-operative magnetic resonance imaging. The electrical stimulation occurs after setting patient-personalized parameters such as frequency, voltage, and pulsewidth and is delivered via an electrode implanted by neurosurgeons, which in turn is connected through a lead to an impulse generator. The neurostimulator, which houses the battery source is implanted in the chest below the clavicle (Okun, 2014). Treatment is chronic (Kalia et al., 2013). DBS surgery is indicated for patients who experience drug-induced dyskinesia and disabling ‘off time’ (a period of time during the day when symptoms are not ameliorated despite drug treatment), but who nevertheless continue to respond to levodopa (Okun, 2012). Targets of stimulation vary by disorder, but for PD, the STN (Limousin et al., 1995) and the globus pallidus *internus* (Odekerken et al., 2013; Volkmann et al., 2001) have shown successful clinical outcomes with regards to improving UPDRS (Unified Parkinson's disease rating scale) motor scores (Okun, 2012) and quality of life (as quantified using the Parkinson's Disease Questionnaire; Jenkinson et al., 1997). DBS is also being explored for the treatment of non-motor disorders such as major depression (Lozano et al. 2012), obsessive-compulsive disorder (Mallet et al., 2008), and treatment-refractory anorexia (Lipsman et al., 2013).

While the mechanisms that lead to positive clinical outcomes of DBS are still a matter of investigation, changes in plasticity, alterations of local and long-range electrophysiological and neurochemical states, and even neurogenesis and neuroprotection have been proposed (Herrington et al., 2016). Changes in plasticity may relieve interconnected brain regions within functional circuits from abnormal neuronal input, which could cause malfunctioning of the entire circuit. A PET study showed metabolic reductions in brain areas that are connected to the site of stimulation is modulated in ways that correlate with clinical response (Asanuma et al., 2006), and thus monitoring M1 and premotor areas MEG activity (Oswal et al., 2016) may improve success rates (Horn, 2017). As for affective side-effects of DBS, although there

are inconsistent results on effects on arousal and subjective feeling (Péron et al., 2013), deficits in recognition of emotional facial expressions (Biseul et al., 2005; Péron et al., 2010b;) and emotional prosody (Péron et al., 2010a) have been reported. The long-term effects of DBS remain to be understood, but there is evidence that it stimulates plasticity of, among others, limbic and motor functional networks (van Hartevelt et al., 2016). In addition to being a highly effective therapy, DBS affords scientists the opportunity to directly study the role of deep brain nuclei in human behavior by modulating the activity of the target nuclei in stimulation experiments or by recording neuronal activity from the implanted nuclei. This has led to new findings beyond motor neuroscience, such as causal evidence that the STN intervenes in the adjustment of decision thresholds (Cavanagh et al., 2011; Herz et al., 2018) as well as evidence for dopamine-dependent limbic processing across sensory modalities (Brücke et al., 2007; Huebl et al., 2014; Kühn et al., 2005; Péron et al., 2015) in addition to the lateralization of limbic processing in the right ventral STN (Eitan et al., 2013).

1.7. Emotion Circuits in the Brain

What is the neurobiological substrate of emotion? Scientists have posited different answers since the publication of Darwin's "The Expression of the Emotions in Man and Animals" in 1872. A unitary or 'one system for all emotions' framework dominated for most of the first half of the XXth century. Walter Cannon and Philip Bard identified the hypothalamus as the center of emotion, modulated only by the inhibitory control of the neocortex (Cannon, 1927; Cannon, 1931; Bard, 1928; Bard & Rioch, 1937). A fully fleshed-out affective circuit was proposed by James Papez, who centered the thalamus as giving origin to two pathways, the 'upstream' (towards sensory cortices, for 'thought') and the 'downstream' (to the mammillary bodies, for 'feeling') pathways (Papez, 1937). While some of the pathways in the Paper circuit do exist, some of its structures, like the hippocampus, do not seem to play an important role in emotion processing (Dalgleish, 2004). In 1949, Paul MacLean introduced a system that most closely resembles the current use of the term 'limbic system'. He built on his predecessors' ideas and recent work by Kluver and Bucy on the affective implications of temporal lobe removal in monkeys (Kluver & Bucy, 1937). MacLean's system was a 'triune architecture' (MacLean, 1970) composed of three evolutionarily successive tiers: the reptilian (BG

and striatum), the ‘old’ mammalian (prefrontal cortex (PFC), amygdala , and other Papez circuit structures), and the ‘new’ mammalian (neocortex) brains. However, while by and large a central contribution to affective neuroscience, some elements of MacLean’s system (anterior thalamus, hippocampus) have failed to garner evidence for their place in an emotion circuit.

The common thread among these limbic system models is that different putatively basic emotions (fear, surprise, anger, sadness, happiness, and disgust, to use the influential canon outlined in Ekman et al., 1983) share a common set of brain structures specialized for affect processing. This unified model of affect has come under attack in light of the ample evidence for distinct circuits for different affective processes (LeDoux, 1996; Calder, 2001). Furthermore, whether there are basic emotions (and thus basic emotion neural circuits) has been questioned (Barrett, 2006; Barrett, 2007, LeDoux, 2012) due to the lack of convergence between different theories on the number of emotions and the difficulties in matching emotions in animals to human emotions. In order to overcome semantic issues that lead to methodological problems, LeDoux proposed referring instead to ‘survival circuits’ which must be shared across phylogeny and serve mechanisms of “defense, maintenance of energy and nutritional supplies, fluid balance, thermoregulation, and reproduction” (LeDoux, 2012). Thus, instead of a ‘fear system’, there are different defense circuits for, e.g., responses to unconditioned (Pagani & Rosen, 2009) and conditioned (Johansen et al, 2001; Maren, 2001) stimuli.

Hemispheric specialization neatly exemplifies the idea of distinct specialized affective circuits. Although sensory and motor processing were long known to involve lateralization, the different roles for each hemisphere in emotional processing only became the subject of study after Guido Gainotti proposed the ‘right hemisphere hypothesis’ based on differential effects of lateralized brain damage, where lesions in the right hemisphere lead to ‘unemotionality’ or indifference, whereas injuries sustained in the left hemisphere were associated with anxiety and depression (Gainotti 1969, 1972). More recently, the right hemisphere has been linked to activation of autonomic responses (Spence, Shapiro, & Zaidel, 1996), facial emotional communication (Borod, Haywood, & Koff, 1997), and subconscious processing of emotion (Gainotti, 2012). A common approach to probe brain lateralization involves delivering visual stimuli to different visual hemifields. Using this method, Hung and colleagues (2010) argue

that the right amygdala receives rapid and slow (feedback) signals containing information about fearful stimuli via separate subcortical and cortical circuits, respectively (Hung et al., 2010). Little is known about the possible hemispheric specialization of the STN for affective processing, although evidence from Granger causality analysis between the subthalamic nuclei showed a dominance of information flow from the right to the left STN during cued movement (Darvas & Hebb, 2014).

What is the empirical evidence on STN connectivity with other structures involved in emotion processing? Haynes & Haber (2013) employed anterograde tracers by injecting them in multiple cortices known to be linked to the hyperdirect pathway in macaque monkeys. The 3D renderings of the projection fields showed fibers from the dorsal anterior cingulate cortex (dACC) accessing the STN at the rostral pole and terminating at the rostromedial pole of the STN; a comparatively small proportion of the ventromedial PFC (vmPFC) and orbitofrontal fibers also terminated at the medial tip, while most ended at the adjacent lateral hypothalamus, a structure cytoarchitecturally similar to the STN. Functional connectivity between the STN and ACC has been reported in an MRI study investigating compulsivity (Morris, Baek, & Voon, 2017). In another study, diffusion tensor imaging revealed a network connecting the STN to basolateral amygdala (Lambert et al, 2012). Further evidence for STN connectivity with OFC and the amygdala comes from a study combining psychophysiological interaction (PPI) analysis of fMRI and diffusion tensor imaging during an emotional prosody decoding paradigm (Péron, Frühholz, Ceravolo, & Grandjean, 2016). Finally, the STN is known to have reciprocal connection to the ventral pallidum (in rodents, Perkins & Stone, 1980; in non-human primates, Karachi et al., 2005), which is identified as a significant output of the limbic circuit (Temel et al., 2005).

1.8 Understanding the Limbic Brain through Affective Pictures

At the most basic level, for an organism to survive it must be able to approach or withdraw from an external agent which may respectively support or threaten its existence. The neural circuitry underpinning our responses to aversive and appetitive cues has evolved from more

primitive forms and is shared across mammalian species (Lang, 2010). Early detection of cues relevant to survival can trigger feedback mechanisms which cause more attentional resources to be allocated to sensory processing of subsets of relevant features, for example via re-entrant projections into the primary visual cortex (Keil et al., 2009). A two-dimensional framework (Russell, 1980) to study affect processing in the brain parses emotional information into two axes, namely arousal (from high to low, representing stimulus intensity and is thus directly related to motivation per se) and valence (consisting of pleasant, unpleasant, and neutral, where each is associated to a mode of behavioral response, such as approach, withdrawal, or no response). The Center for the Study of Attention and Emotion constructed a set of pictures (Lang, Bradley, Cuthbert, 2008) depicting scenes capable of eliciting a wide range of emotional reactions, from non-arousing (e.g. a glass) through mildly arousing (e.g. scared faces or babies) to highly arousing (e.g. erotic or violent scenes). Each picture is associated to standardized arousal and valence scores based on ratings by cohorts of American college students. It is thought that the images can activate motivational circuits in the brain that would be responsive to actually rewarding or threatening stimuli (Lang, 2010). Scalp potentials elicited by this stimulus set covary with autonomic responses such as skin conductance and heart rate (Cuthbert, Schupp, Bradley, Birbaumer, & Lang, 2000).

A vast literature demonstrates that emotional pictures elicit brain electrophysiological responses such as short (100–200 ms), middle (200–300 ms), and long (>300 ms) latency event-related potentials (ERP; see review in Olofsson, Nordin, Sequeira, & Polich, 2008) and oscillatory activity in all the canonical frequency bands (see review in Güntekin & Başar, 2014) as measured via EEG. Based on the previously discussed hyperdirect projections onto the STN originating in limbic structures and single-unit (Sieger et al., 2015) and LFP (Buot et al., 2013; Huebl et al., 2014) evidence of STN processing of emotional pictures, an investigation of the place of the STN within affect brain circuitry in PD was undertaken. First we attempted to reproduce other groups' results using ERP and time-frequency analysis on invasive STN recordings obtained from PD patients during a passive picture presentation task. Patients participated both in the dopaminergic medication state OFF (after overnight withdrawal) and ON (after administration of levodopa). Accordingly, we expected both higher ERP amplitudes and alpha synchronization in response to negative stimuli compared to neu-

tral in the OFF state and higher ERP amplitude and alpha synchronization for pleasant pictures compared to negative pictures in the ON state. Moreover, the right STN was hypothesized to exhibit shorter latencies than the left STN for emotional pictures (and not for neutral stimuli) possibly through amygdala-STN connectivity. The second part of the analysis was devoted to STN connectivity with its hemispheric counterpart and with the amygdala and the ACC. To this end, EEG recordings were obtained at the same time as the STN recordings from the DBS electrodes and bilateral virtual amygdala and ACC channels were created by means of source reconstruction techniques. As mentioned above, these two structures are known to be involved in affect processing and their activation during paradigms employing emotional pictures set has previously been investigated (Sabatinelli, Lang, Bradley, Costa, & Keil, 2009; Sabatinelli, Keil, Frank, & Lang, 2013; Albert, López-Martín, Tapia, Montoya, & Carretié, 2012). Based on evidence from motor studies cortical entrainment of the STN in the high beta range, a corresponding coupling between the STN and the reconstructed limbic sources, with the expectation that such connectivity takes place at lower (alpha or low beta) frequencies due to these slower rhythms' reported valence sensitivity (Huebl et al., 2014). Amygdala volume is reduced in PD (Harding, Stimson, Henderson, & Halliday, 2002) and its activation is modulated by dopamine in PD (Tessitore et al., 2002), thus impaired emotional discrimination as indexed by synchrony and connectivity measures was expected, particularly in the OFF state.

2. Methods

2.1. Data Collection

8 patients with PD who had been referred for DBS were recruited for the implantation of the ACTIVA PC+S (Medtronic) device at the University Hospital Würzburg, JMU Würzburg, Würzburg, Germany. The ACTIVA PC+S device not only delivers controlled electrical pulses at the STN like the ACTIVA PC stimulation device, but is additionally capable of recording and storing electrophysiological activity from the STN which can then be telemetrically downloaded into a tablet for offline processing. Details concerning the functional stereotactic surgical procedure are explained elsewhere (Steigerwald et al., 2008). Time elapsed since implantation date was 3.5 ± 0.2 months and recordings for the experiment presented by this thesis were obtained between April and November of 2016. Dopamine replacement therapy was suspended overnight for at least 12 hours prior to the experiment. Specifically, levodopa was withdrawn overnight and the administration of dopamine agonists was halted about two days before the experiments. All participants were right-handed and gave their informed written consent for the study. Patients had normal or corrected-to-normal vision. More detailed patient information is presented on Table A1 in the appendix. The project was approved by the local ethical committee and was conducted in accordance to the Declaration of Helsinki.

2.2. Recordings and Paradigm

For each medication state, two sessions were ran for a duration of ~15min each, due to storage constraints in the ACTIVA PC+S® device (Medtronic, PLC, Dublin, Ireland). Subjects simply sat passively on a comfortable chair in front of a table wearing a set of video glasses (Cinemizer OLED, Zeiss), whose prescription acuity settings were adapted to the individual subject's needs by using two sample images that were not part of the stimulus set. These glasses create the impression of looking at a screen (105 cm diagonal) at a distance of 2 meters. The video glasses were connected via an HDMI cable to a portable computer which ran Presentation® (Version 18.2, Neurobehavioral Systems, Inc., Berkeley, CA, USA, [15](http://www.neu-</p></div><div data-bbox=)

robs.com), a software specialized for stimulus presentation. The screen refresh rate was 60 Hz. 33 pictures per valence (pleasant, unpleasant, neutral) were chosen from the International Affective Picture System (IAPS; Lang, Bradley, & Cuthbert, 2008)¹. Brightness was normalized with MATLAB and the Wavelet Toolbox (release 2016b, The MathWorks, Inc, Natick, MA, USA) by reading each image into an RGB variable, computing the mean and standard deviation for each color (red, green, blue), and, for each value of each of the three colors, subtracting the corresponding mean and dividing by the corresponding standard deviation. All values were subsequently multiplied by 60 and added 100 for images to be visible. Spatial frequency (Delplanque, N'diaye, Scherer, & Grandjean, 2007) did not significantly differ between valence groups (all three pairwise comparisons $p > .05$). The stimulus set was partitioned into two sessions with 16 or 17 items per valence. See Table 2.1 for mean arousal and

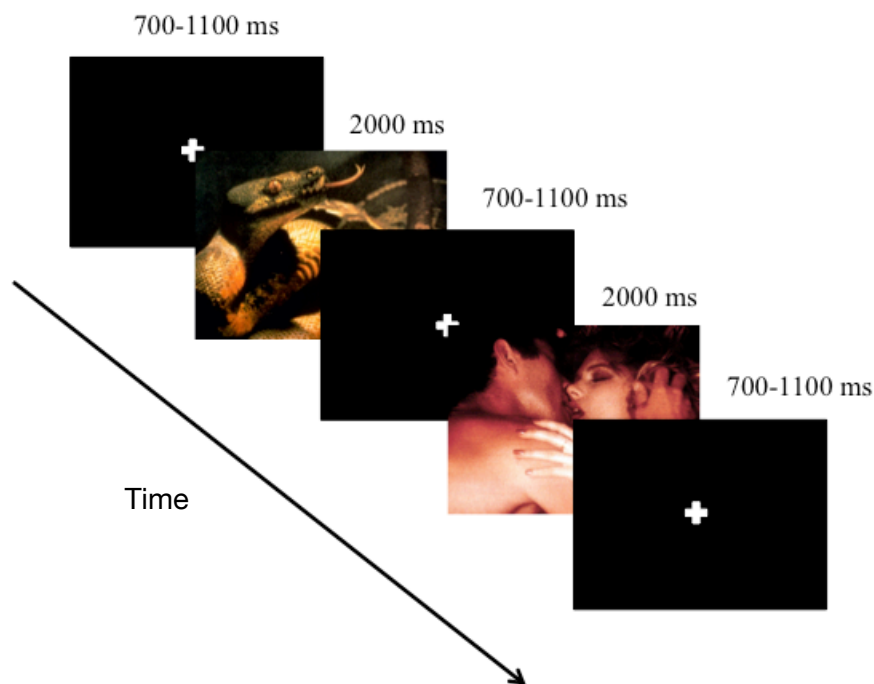


Fig. 2.1 | **Schematic of picture presentation paradigm.** Pictures from the IAPS set were presented for 2000 ms. The length of the inter-stimulus intervals was pseudorandom within the range 700–1100 ms and consisted of a fixation cross.

¹ The selected pictures' codes were: 1022, 1303, 1390, 1411, 1540, 1600, 1630, 1722, 1726, 1811, 1945, 2102, 2332, 2352.1, 2372, 2383, 2393, 2493, 2598, 2730, 2770, 2800, 2900.1, 2981, 3005.1, 3017, 3051, 3063, 3080, 3100, 3102, 3110, 3300, 3310, 3400, 4000, 4605, 4608, 4610, 4623, 4626, 4631, 4659, 4664.1, 4670, 5199, 5210, 5471, 5531, 5534, 5621, 5740, 6230, 6250.1, 6263, 6311, 6510, 6540, 6550, 6900, 7006, 7030, 7032, 7035, 7137, 7175, 7224, 7248, 7260, 7490, 7570, 7595, 8030, 8060, 8080, 8120, 8185, 8186, 8210, 8370, 8400, 8470, 8490, 8492, 8497, 9000, 9040, 9265, 9290, 9320, 9331, 9340, 9342, 9402, 9415, 9561, 9611, and 9630.

valence scores. Arousal differed significantly between emotional and non-emotional pictures ($p < .001$) but not between pleasant and unpleasant stimuli ($p = .70$). Each picture was presented 6 times for 2 s with a randomly variable interstimulus interval within the range 0.7 to 1.1 s (Fig. 2.1). During this interval a black screen with a white fixation cross was displayed. Stimulus order was pseudorandomized such that no picture appeared twice consecutively. To control for attention, a separate 'test' item (image 7490) was included in each session to randomly occur 3 times, and subjects were instructed to say 'blau' upon its appearance. At the end of the second session, subjects were administered their individual levodopa equivalent dose and waited 1 hour before starting the first session of the medication "ON" phase.

Table 2.1 | **Normative ratings of IAPS stimuli used in this study.** Scale for both valence and arousal is 1–9, SD in parentheses.

	Valence	Arousal
Pleasant	7.32 (0.31)	4.10 (1.26)
Neutral	4.85 (0.38)	5.63 (1.11)
Unpleasant	2.37 (0.48)	5.75 (1.03)

STN-LFPs were bilaterally recorded at a nominal sampling frequency of 422 Hz from the electrode contact pairs (bipolar configuration) that were identified as being the most clinically effective during stimulation and where at least one contact lay within the STN, as observed on post-operative MRIs. STN-LFP recordings were amplified by a factor of 1000. EEG recordings were acquired by means of the EEG BrainAmp System (Brain Products, <https://www.brainproducts.com/>) at a sampling frequency of 1000 Hz using a separate computer running BrainVision. The amplifier's input impedance was 10 M Ω and the A/D converter's resolution 0.1 μ V per bit. We used EEG caps with 128 Ag/AgCl sensors (EASYCAP GmbH, Germany) whose placement corresponded to the 5–10 System (Oostenveld & Praamstra, 2001). FCz was used the reference electrode. EEG recordings were amplified by 1000. Picture presentation timing was fed from the computer running Presentation to the computer running BrainVision by connecting the ExpressCard port in the former to the parallel port in the latter. To synchronize STN-LFPs and the Presentation log file, a TENS (transcutaneous electrical nerve stimulation) impulse was delivered at the scalp over the ACTIVA PC+S® wire and an EEG electrode and on the neck, ~30s after the beginning and before the end of

every session. EEG and STN-LFP signals were synchronized offline using MATLAB, as explained in Canessa et al., 2016. Three EEG electrodes were removed from the cap in order to record electrocardiograms (ECG; F4 for subject wue06, FFC4h for wue03, FCC1h for the rest) and electrooculograms (EOG; FT8 and FT9, each placed bilaterally over the zygomatic bone area) for offline rhythmic heart beat and eye-movement artifact removal.

2.3. Preprocessing

Signals were preprocessed and analyzed offline on MATLAB using functions from the Fieldtrip Toolbox (Oostenveld, Fries, Maris, & Schoffelen, 2011; <http://www.ru.nl/neuroimaging/fieldtrip>) and custom scripts. STN recordings were downsampled to 400 Hz during the synchronization process. Trials were visually inspected for artifacts and abnormal activity. Subsequent preprocessing is detailed separately for each type of analysis.

2.4. STN Event-Related Potentials

Before segmentation into epochs, each continuous recording was highpass-filtered at 0.1 Hz with using an infinite impulse response (IIR) Butterworth filter of 4th order in a forward and reverse pass fashion to avoid phase delays. Epochs in the range $[-0.7, 2.6]$ s relative to each stimulus presentation were extracted for analysis. The four datasets (two datasets for each medication state) were merged, and epochs were time-locked averaged by valence for each medication state and for each hemisphere. Due to the varying positions of the electrode contacts within the STN relative to the locus of stimulus-locked activity, deflections of both polarities within overlapping periods can be observed on the cross-condition averages² of the time-locked STN-LFP data (Fig. 3.1). Indeed, Buot and colleagues (2013) observed that not only the amplitude but also the polarity of STN potentials evoked by emotional pictures change as the electrode contact pairs descend, thus implying the generation of changes in potential is localized at the STN itself (Buot et al., 2013). Based on the putative localization of a ERP generator in the STN, the fact that amplitude would be quantified using signed area (see

² In this thesis, 'cross-condition average' refers to the average across valence and dopaminergic medication states.

below), and the almost mirror-like behavior across the time axis of left and right STN time-locked average waveforms for 3 subjects (Fig. 3.1, Table 2.2), time-locked average waveforms whose first large deflection was negative were reflected (‘flipped’) across the time axis for ERP analysis by multiplying waveforms by -1 (Fig. 3.1, 3.2). In order to define the measurement windows (MW), the inter-hemispheric cross-condition grand average was computed and then smoothed using a moving average filter with window length of 5 data points (corresponding to 12.5 ms) to identify zero-crossings delimiting the two major deflections. Then the time points t_i at which the signed area under each deflection can be divided into halves were identified. Finally, MWs were set at $t_i \pm 150$ ms. Selecting MWs based on the grand average waveform across patients is an unbiased method to avoid circular inference since the grand average is orthogonal to any contrast (i.e., condition comparisons) involved in the hypotheses tested in this study (Cohen, 2014).

Subject	wue03	wue04	wue06	wue07	wue09	wue11
R	no change	flip	flip	no change	no change	no change
L	flip	flip	no change	flip	flip	no change

Table 2.2 | **Patient ERP (‘flipping’)**. Reflection (‘flipping’) across the time-axis of time-locked averages such that first large deflection is ‘up’ (positive) and the second ‘down’ (negative) in order to meaningfully perform group analysis. L = left STN, R = right STN.

To quantify ERPs, amplitude and latency parameters were computed as follows. Signed area amplitude (SAM, Luck, 2014) was computed to measure amplitude, where positively and negatively signed areas were computed for the first and second measurement windows, respectively. Midpoint latency (ML) was estimated via 50% fractional area latency (Luck, 2014), where we selected the time-point at which the signed area within the measurement window reaches a given fraction of that area, in this case 50%. ML was chosen over peak latency due to the former’s lower sensitivity to noise and the latter’s equivalence to the mode of the distribution of single-trials, which is not normally used to estimate central tendency (Luck, 2014). Moreover, computer simulations ran in Kiesel, Miller, Jolicœur, & Brisson, 2008, showed ML to be the most accurate way of measuring how onset latency changes between conditions or groups, compared to traditional methods. Since STN recording locations

varied across subjects and hemispheres, the SAM of each subject, hemisphere, and measurement window were normalized by the corresponding cross-condition average SAM. Normalization aids in preventing disproportionate influence of measurements from an individual subject or subject's hemisphere.

All factorial analyses was carried out using R 3.5 (R Core Team, Vienna, Austria). For ERPs, three non-parametric 2×3 repeated-measures factorial analyses were performed on the amplitude and latency measures. To investigate dopamine and valence effects on STN-ERP, mean parameter values (amplitude and latency) of the same measurement windows were used. First, we collapsed the data via simple averaging across hemispheres to test dopaminergic medication state (DOP, with levels OFF and ON) and valence (VAL, with levels UNPLEASANT, PLEASANT, and NEUTRAL). To test $SIDE \times VAL$, where $SIDE$ has levels RIGHT and LEFT, data was collapsed across dopaminergic medication states. Finally, to test $DD \times VAL$, where DD stands for dopaminergic denervation and contains levels MOST DD vs LEAST DD, data was collapsed across dopaminergic medication states. In order to overcome issues of sample size and non-normality (Shapiro-Wilk normality test, $p > .05$), the ARTool package for R (Wobbrock, Findlater, Gergle, & Higgins, 2011) was used to transform the data prior to performing 2×3 ANOVAs. ARTool facilitates nonparametric multifactorial analyses of repeated measures, unlike the Friedman test, which can only handle nonparametric tests with one factor. Alignment requires bringing observations sharing the same levels, i.e. a block, in alignment by averaging the mean response of the block and subtracting this mean from each response in order to obtain an estimated effect (Hodges & Lehmann, 1962). The effect estimate is added to its corresponding residual and subsequently ranked.

2.5. STN Power Analysis

For time-frequency analysis, each continuous recording was high-pass filtered at a 0.1 Hz cutoff with an IIR Butterworth filter of 4th order using a forward and a reverse pass. Epochs of $[-.75, 2.6]$ s relative to stimulus presentation were then extracted and low-pass filtered at 128 Hz with an IIR Butterworth filter of 4th order using a forward and a reverse pass, then each trial waveform was baseline-corrected by subtracting the mean baseline ($[-0.5, -0.2]$ s)

value. Power was extracted by convolving the epochs with the hanning window using 0.5 s windows in 0.05 s steps.

For statistical analysis, different approaches were used, namely a non-parametric permutation method to investigate power changes due to stimulus presentation relative to baseline and non-parametric factorial analyses to investigate effects of the factors mentioned in the previous section.

Changes in power due to picture presentation, across all dopamine and valence conditions, were investigated via a permutation test comparing baseline (−0.5 to −0.2 ms) to activation (0 to 2000 ms) across subjects for each hemisphere as well as after collapsing data across hemispheres over the frequency range 3–45 Hz. This test was run on MATLAB and proceeds as follows (Cohen, 2014). For each condition an observed test statistic was obtained according to the following steps. Each subject’s cross-condition average time-frequency map was smoothed using a 2-D Gaussian kernel with $\sigma = 2$. We first computed the observed, baseline-corrected mean map by obtaining the decibel change from baseline of the subject-average time-frequency maps. A distribution of time-frequency maps is then created by randomly cutting, shifting, and baseline-correcting the subject-average map 1000 times. A z-map is subsequently computed by subtracting the mean of the distribution from the observed mean map and dividing by the standard deviation of the distribution. In order to define clusters of significant z-scores, a threshold of $p = .01$ was set to exclude z-scores from the z-map whose absolute value fell under 2.33 (the inverse of the normal cumulative distribution at $p = 1 - 0.01$). We applied cluster-correction methods to correct for multiple comparisons. For this, we created a distribution of maximum cluster sizes by selecting the cluster with the highest number of pixels from thresholded z-maps obtained from each permutation created above. A minimum cluster size threshold corresponding to a p -value of .05 from the cluster size distribution is then selected to identify which clusters ‘survive’ the correction.

Three non-parametric 2×3 repeated-measures factorial analyses were performed on the mean power values of regions of interest (ROI) identified by looking at the significant clusters obtained through the permutation test of the bilateral cross-condition average spectro-

gram (which excluded wue03 due to highly artifactual left hemisphere recordings). As mentioned above, this unbiased method avoids the circular inference involved in selecting an ROI based on maximum difference between conditions that are then to be tested. The same factorial configurations were used as for STN-ERP analysis. Data was collapsed as in STN-ERP analysis for the different factorial setups. Simple subtraction was subsequently used for baseline correction, which involves subtracting for each frequency bin its mean power within the baseline period. This subtraction method has been shown to avoid introducing a positive bias, as with a percentage change approach, where event-related synchronization (ERS) and desynchronization (ERD) tend to be over- and underestimated, respectively (Hu, Xiao, Zhang, Mouraux, & Iannetti, 2014).

2.6. Inter-STN Coupling

Connectivity between the left and right STN was quantified by computing wavelet coherence. A wavelet is a function $\psi \in L^2(\mathbb{R})$ with zero mean, norm equal to 1, and centered around $t = 0$ (Mallat, 2009). The first requirement, being a member of the set of square-integrable functions, implies that the dot product with other functions from the same set is valid. Wavelets can be discrete or continuous, real- or complex-valued. As in Fourier analysis, a time series $g(t)$ can be convolved with a wavelet to obtain a different representation that permits time-frequency localization, i.e. to identify which frequency components dominate at a given time interval, also known as frequency decomposition. This operation is called a wavelet transform and is expressed as (Daubechies, I., 1992)

$$Wf(u, s) := \int_{\mathbb{R}} f(t) \frac{1}{\sqrt{s}} \psi^* \left(\frac{t - u}{s} \right) dt,$$

where the asterisk superscript denotes the complex conjugate, s represents ‘scaling’ (reciprocal of frequency) and u time. Let the cross-spectrum (a measure of spectral cross-correlation) of $f(t)$ and $g(t)$ be $Wfg := WfW^*g$ and cross-wavelet power $|Wfg|$ (Grinsted, Moore, & Jevrejeva, 2004). The phase covariance between two time-series can then be examined by looking at their squared cross-spectrum normalized by their squared auto-spectra in what is known as wavelet coherence (WC; Grinsted, A. et al., 2004):

$$WC_{fg}^2(u, s) = \frac{|W^*fg(u, s)|^2}{|Wff(u, s)|^2 \cdot |Wgg(u, s)|^2}$$

Thus WC is a measure of linear dependence between two signals that is a function of both time and frequency and is determined by their amplitude and phase. In practice, the numerical computation of WC requires the cross-spectra to be smoothed (Torrence & Compo, 1998). As in Fourier coherence, a WC value of 0 for the frequencies of interest means that the two time-series are wholly independent, whereas a value of 1 would indicate a perfect linear dependence, i.e., one signal's patterns can be predicted from the other's. In this study, we used the complex-valued Morlet wavelet,

$$\psi_0(t) = \pi^{-1/4} e^{i\omega_0 t} e^{-t^2/2},$$

where ω_0 stands for dimensionless frequency (Torrence & Compo, 1998), is widely used in wavelet spectral analysis of electrophysiological signals (Klein, Sauer, Jedynak, & Skrandies, 2006; Li, Yao, Fox, & Jefferys., 2007) due to its complex (which allows to investigate phase) and Gaussian (which gives a relatively smooth spectrum) terms. As with conventional coherence, WC does not require the underlying time-series to be stationary (i.e., mean, variance, and other statistical properties do not change over time), a property that electrophysiological signals by and large lack. Coherence measures are extensively used to quantify statistical dependence between two sources of activity, also known as functional connectivity (Friston, 2011). Unlike effective connectivity, however, functional connectivity does not explain the source of the correlation. WC was computed using the *wcoherence* function (with $\omega_0 = 6$) in the Wavelet Toolbox of MATLAB.

For statistical analysis, different approaches were used, namely a non-parametric permutation method to investigate changes in coupling due to stimulus presentation relative to baseline and non-parametric factorial analyses to investigate effects of dopaminergic medication state and valence. Changes in connectivity between STN due to picture presentation, across all dopamine and valence conditions, were investigated via a permutation test comparing base-

line to activation. DOP \times VAL repeated-measures tests were performed on the mean coherence values of regions of interest (ROI), which were chosen based on the significant clusters obtained from a permutation test comparing baseline with period of stimulus presentation (see above), using the cross-condition average coherograms (coherence map) of each patient, except wue03 due to highly artifactual left hemisphere recordings.

2.7. Source Reconstruction

In order to investigate how external emotional visual stimuli modulate connectivity patterns between the STN and other brain structures involved in affect processing, LFP signals from such locations are required. To estimate the location and strength of electromagnetic activity in the brain that is reflected in EEG recordings, the forward and inverse solutions must be computed. Source reconstruction was performed using Fieldtrip functions. A solution to the forward problem is a matrix called the leadfield which is used to calculate scalp potentials at each EEG channel given a dipole moment at a given location in the brain. The computation of the leadfield requires a volume conductor model, a grid representing positions of dipoles in the brain, and EEG electrode positions. An anatomical atlas (AAL, Tzourio-Mazoyer et al., 2002) was used while creating the source grid to assign brain anatomical areas to subsets of grid locations. Electrode positions were manually realigned with the patient's scalp surface using Fieldtrip's interactive tools. The volume conductor model, or head model, can be computed using the boundary element method (BEM), which assigns volume conductor properties to three head compartments (brain, skull, and scalp) by assuming that the conductivity in each compartment is isotropic (i.e., for each point, equal in all directions) and homogenous. The surfaces of each compartment are represented by closed meshes of triangles (surfaces) and each compartment is assigned a different conductivity (.33, .0042, .33 S/m, respectively). Compartment dimensions and segmentation are extracted from each subject's MR scans. To obtain the electric potential at a scalp electrode caused by a dipole moment in the brain, it suffices to first compute its corresponding potential on the skin mesh and then project the electrode position onto the closest triangle of the skin surface/mesh to linearly interpolate the electric potential values of the three triangle nodes (Fuchs, Kastner, Wagner, Hawes, & Ebersole, 2002).

The inverse solution allows us to estimate the sources of activity that cause a pattern of electric potentials as observed in the EEG channels. These sources are modeled as dipoles or multipoles (Baillet, Mosher, & Leahy, 2001). The inverse problem arises from the infinite possibilities of inner dipole which could produce the same scalp potential, i.e., there is no unique solution, and thus constraints are necessary. Spatial filtering, or beamforming, was used to attenuate electrical activity from some brain locations and pass activity from other positions using the linearly constrained minimum variance approach (LCMV, see Van Veen, van Dronkelen, Yuchtman, & Suzuki, 1997). Reconstructed signals were then reduced by deriving the coordinates of the locations corresponding to the parcels of interest, in this case the ACC and amygdala. Though there is evidence for separate representation in the brain of pleasant and unpleasant components in mixed odor samples (Grabenhorst, Rolls, Margot, da Silva, & Velazco, 2007), the amygdala and the ACC are known to discriminate valence and motivational value, respectively (Britton, Taylor, Sudheimer, & Liberzon, 2006; Janak & Tye, 2015). The chosen limbic structures were included in the AAL atlas used for parcellation and have been identified in MRI studies employing a comparable paradigm (Sabatinelli et al., 2009, 2013; Albert et al., 2012). Moreover, as previously discussed, structural connectivity between the STN and the ACC (Lambert et al., 2012) and the STN and the amygdala (Péron et al., 2016) have been reported.

Since the exact coordinates of each structure varies across subjects, individual MRI were normalized to a template anatomical MRI in order to convert MNI coordinates into individual coordinates. A source model can then be derived for the particular locations in order to compute the filters for the EEG data required to extract so-called virtual sensors for each structure of interest.

Preprocessing of EEG signals was as follows. Continuous recordings were high-pass filtered at 0.1 Hz with (IIR) Butterworth filter of 4th order with forward and reverse passes, then epochs of $[-0.75, 2.6]$ s relative to stimulus presentation were extracted. Cardiac and oculomotor artifacts were removed from EEG recordings by means of Independent Component Analysis as implemented in the Fieldtrip Toolbox. Visually identified bad trials were rejected.

Rejected bad channels were interpolated using the average of neighbors. Neighbor channels were identified through a triangulation method, which is based on a two-dimensional projection of the sensor position. EEG recordings were further downsampled to 256 Hz to ease computation. An average of 83 ± 25 trials were rejected per subject.. Epochs from reconstructed signals were then baseline corrected using $[-200, 0]$ ms relative to stimulus as a baseline. Data was re-referenced to the common average. Unlike for the STN, the measurement windows were based only on the maximum absolute peak values ± 150 ms of the cross-condition grand average waveforms for the reconstructed amygdala and ACC channels.

2.8. Event-Related Potentials with Reconstructed Sources

For each subject, condition, and reconstructed source, trials were time-locked averaged and amplitude and latency were quantified as for STN-LFPs. The measurement window of 194–494 ms was derived from the cross-condition grand averages for the virtual amygdala and ACC sources, where the range consisting of minimum of the downward deflection ± 150 ms was chosen for ERP analysis (Fig. 3.7).

For virtual amygdala and virtual ACC, three non-parametric 2×3 repeated-measures factorial analyses were performed on the amplitude and latency measures. To investigate dopamine and valence effects, mean parameter values (amplitude and latency) of the same measurement windows were used. Data was collapsed as for STN ERPs to carry out factorial analyses $DOP \times VAL$, $SIDE \times VAL$, and $DD \times VAL$, for each virtual brain structure.

2.9. Power Analysis with Reconstructed Sources

Power values was computed and statistically evaluated following the protocol used with STN-LFP data for the reconstructed amygdala and ACC channels. ROIs derived from permutation method to be used for factorial analysis were ‘alpha’ (7–12 Hz, 50–300 ms) and ‘high beta’ (23–31 Hz, 400–750 ms) for the amygdala and ‘alpha’ (7–12 Hz, 50–300 ms) for ACC.

2.10. Coherence with STN-LFPs and Reconstructed Sources

Coherence was calculated for left STN-amygdala, left STN-ACC, right STN-amygdala, and right STN-ACC using Fieldtrip's *ft_connectivityanalysis* function, which employs Fourier power and cross-spectra to compute the coherence at successive time bins, thus allowing for time localization. ROIs based on surviving clusters ($p < .05$) from a permutation test involving cross-condition averages for each subject were used, thus setting as ROIs 'low beta' (12–17 Hz, 1800–2000 ms) and 'high beta' (20–27 Hz, 200–400 ms) for the amygdala and 'alpha' (7–11 Hz, 700–900 ms) and 'low beta' (14–21 Hz, 1650–1850 ms) for ACC. Statistical evaluation was carried out as for inter-STN coupling.

3. Results

3.1. Event-Related Potentials in the STN

Based on 50% area latency, the first and second measurement windows were observed at *mean* (M) = .39 s, *standard deviation* (SD) = .04 s and $M = .85$ s, $SD = .03$ s, respectively. The corresponding signed area amplitudes before normalization were $M = .10$ μV s, $SD = .06$ and $M = -.06$ μV s, $SD = .02$, respectively. None of the group level datasets for each component and parameter passed Shapiro-Wilk normality tests ($p < .05$). For non-parametric repeated measures 2×3 factorial analyses, subject wue03 was excluded in the DOP \times VAL analysis of variance since no recordings in the dopaminergic ON state could take place. Wue03 was also excluded from SIDE \times VAL and DD \times VAL tests due to noise in left STN recordings. An alpha level of .05 was used for all statistical tests.

The DOP \times VAL test yielded no significant effects on either amplitude or MW. The SIDE \times VAL analysis of variance showed that the effect of valence (Figure 3.3) on the midpoint latency within the second measurement window was significant ($F(2, 24) = 4.46$, $p = .049$), with post-hoc pairwise comparisons indicating that the latency of unpleasant stimuli ($M = .87$ s, $SD = .05$) was longer than that of pleasant ($M = .83$ s, $SD = .03$, $p = .049$). Tukey correction was applied on all post hoc tests. Latencies for measurement window 1 were $M = .38$ s, $SD = .04$ s and $M = .40$ s, $SD = .06$ s for the right and left hemisphere, respectively. For measurement window 2, right: $M = .85$ s, $SD = .05$; left: $M = .85$ s, $SD = .03$. The SIDE effect was not significant for the latency of the first ($F(1, 24) = .16$, $p > .05$) and second ($F(1, 24) = .28$, $p > .05$) components. This test did not yield any significant effects for amplitude of either component or the latency of the first component (see tables A2 and A3 in Appendix for descriptive statistics of all condition combinations).

Latency in the STN of the hemisphere with higher DD was shorter than in the hemisphere with lower DD for the first measurement window ($M = .38$ s, $SD = .06$ vs $M = .40$ s, $SD = .03$, $p > .05$) and for the second ($M = .84$ s, $SD = .04$ vs $M = .86$ s, $SD = .04$, $p > .05$), but not

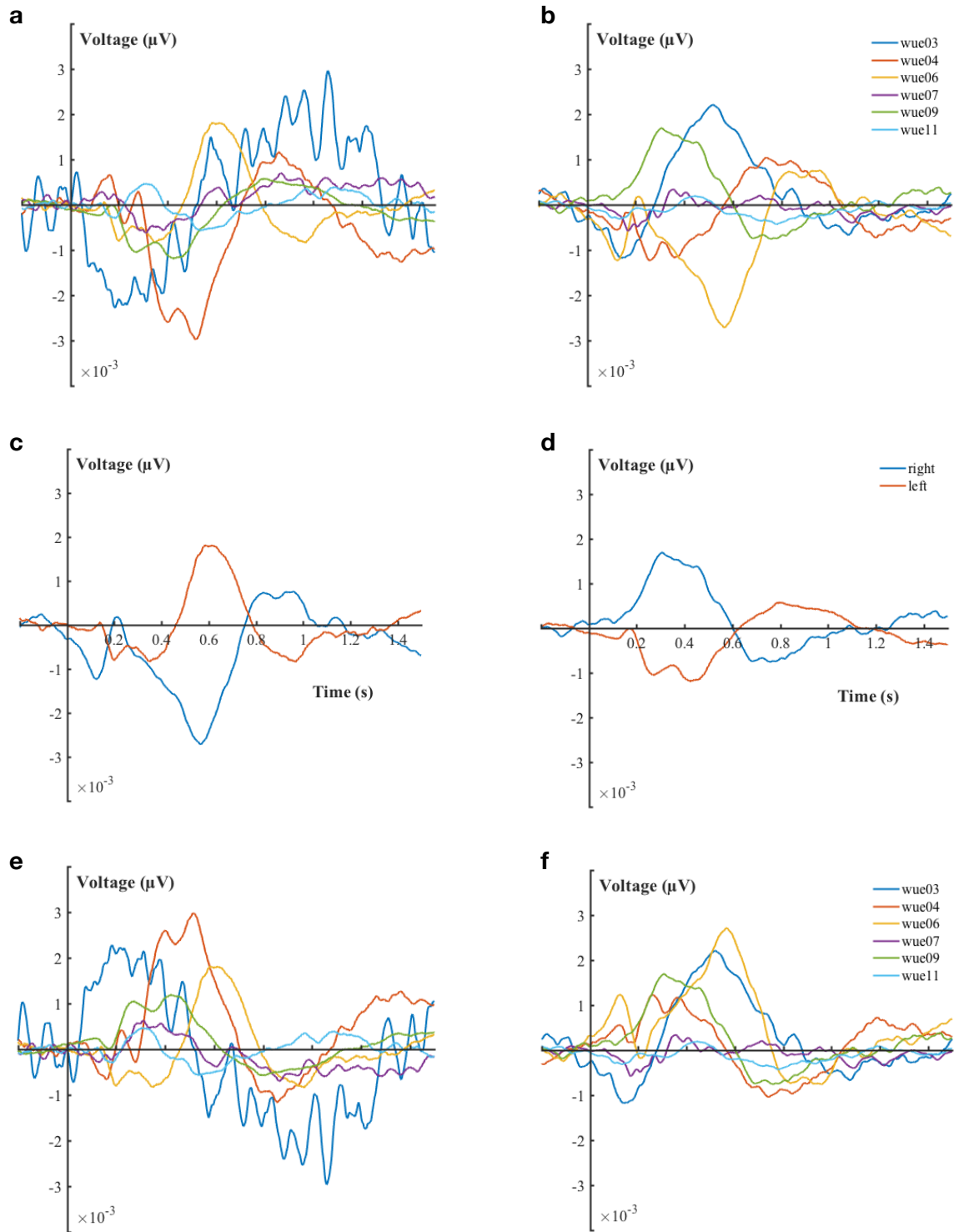


Fig. 3.1 | **STN waveforms.** **a, b** | Superpositions of time-locked cross-condition patient average waveforms for the left and right STN, respectively. **c, d** | Left vs right comparison of STN time-locked average waveforms from subjects wue06 and wue09, respectively, displaying mirror-like time-courses. **e, f** | Same as **a** and **b** after 'flipping' waveforms across time axis to ensure first large deflection is up, i.e. positive. Despite smoothing, it is clear that wue03's left STN recordings are highly noisy. $t = 0$ indicates stimulus presentation. Color figures can be found on the electronic version of this thesis on OPUS (<https://opus.bibliothek.uni-wuerzburg.de/home>).

significantly so. The DD and interaction effects on amplitude or latency were significant for neither measurement window per this test.

3.2. Power Analysis in the STN

Group permutation tests showed significant clusters ($p < .05$) for the cross-condition average power maps comparing post-onset activity against baseline activity. Subject wue03 was excluded from the left STN permutation test due to the abnormal oscillatory behavior of the subject's left STN recordings. A significant ERS cluster spanning the low and high beta bands (within about 13–25 Hz, 0–500 ms) in the right STN, whereas ERD clusters in the the low beta (within about 12–19 Hz, 400–800 ms) and high beta (within about 28–40 Hz, 900–1250 ms) bands were obtained in the left STN permutation tests. Moreover, an ERD high beta clus-

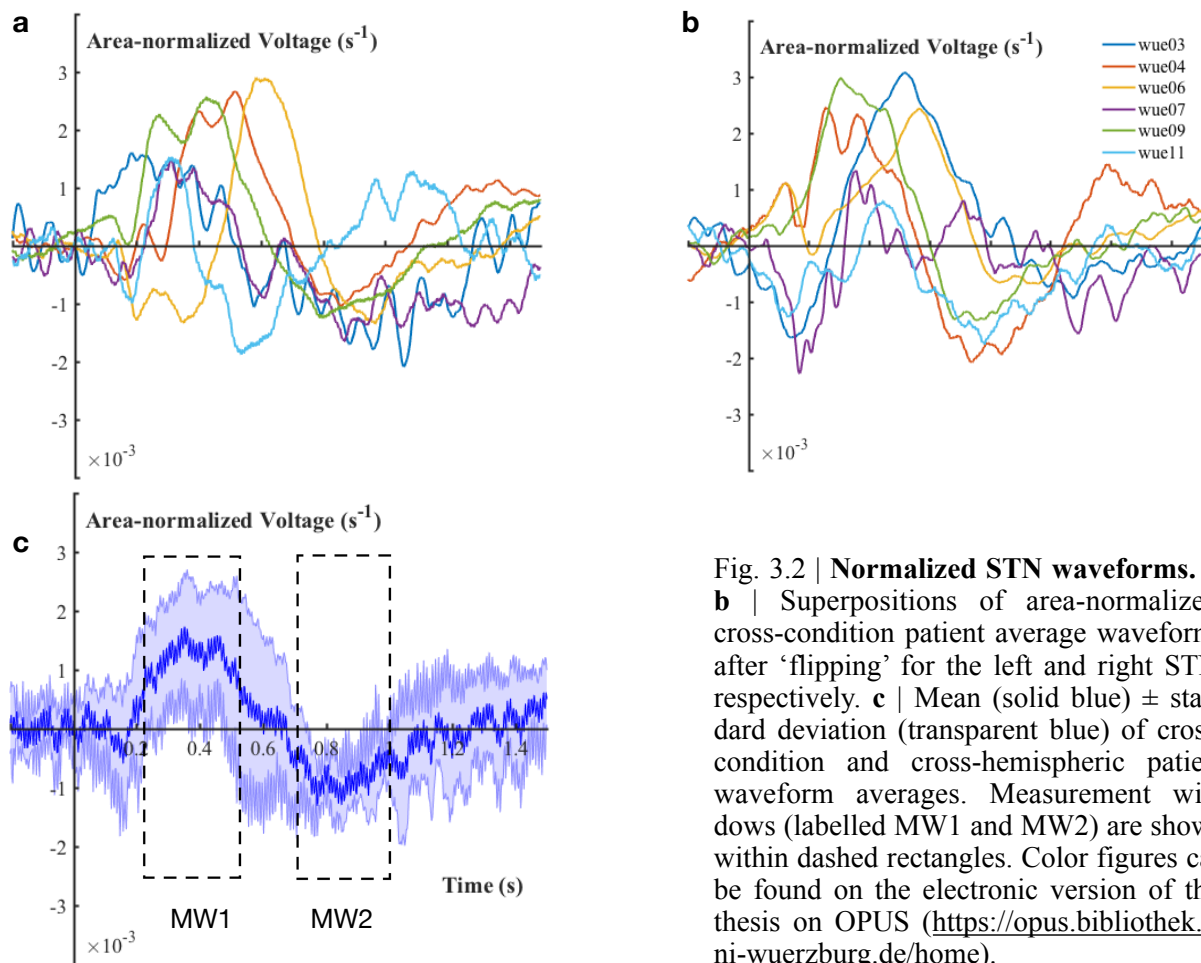


Fig. 3.2 | **Normalized STN waveforms.** **a**, **b** | Superpositions of area-normalized, cross-condition patient average waveforms after ‘flipping’ for the left and right STN, respectively. **c** | Mean (solid blue) \pm standard deviation (transparent blue) of cross-condition and cross-hemispheric patient waveform averages. Measurement windows (labelled MW1 and MW2) are shown within dashed rectangles. Color figures can be found on the electronic version of this thesis on OPUS (<https://opus.bibliothek.uni-wuerzburg.de/home>).

ter (within about 28–40 Hz, 800–1200 ms) was statistically significant when collapsing STN spectrograms across lateralities (Figure 3.4).

None of the group level datasets for each measurement window and parameter passed Shapiro-Wilk normality tests ($p < .05$). As explained above, subject wue03 was excluded from analyses of variance. DOP \times VAL and DD \times VAL factorial analyses did not yield any significant effects. The SIDE \times VAL analysis of variance yielded a significant SIDE effect ($F(1, 24) = 11.94, p = .026$) for ‘high beta’ ERD (Figure 3.5). Subsequent post-hoc pairwise comparisons indicated stronger ‘high beta’ ERD in the left STN (Tuckey, $p = .026$). The VAL effect was not significant ($F(2, 24) = .08, p > .05$).

3.3. STN-STN Coupling

Group permutation tests showed significant clusters ($p < .05$) for the cross-condition average coherence map comparing post-onset activity against baseline activity. Subject wue03 was excluded from the STN permutation test due to the abnormal oscillatory behavior of the sub-

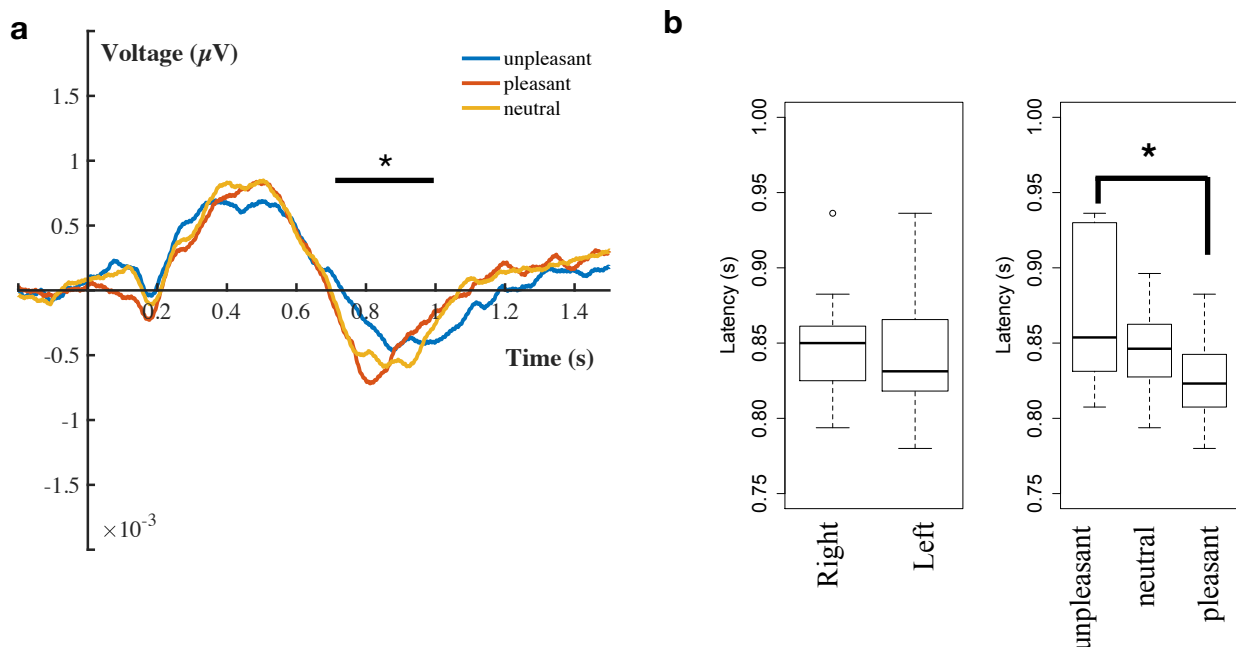


Fig. 3.3 | **STN-ERP and valence.** **a** | Time-locked averages across medication states and hemispheres. The thick back covers the second measurement window. **b** | Box-plots for SIDE \times VAL test on latency within measurement window 2. One star represents $p < .05$. Color figures can be found on the electronic version of this thesis on OPUS (<https://opus.bibliothek.uni-wuerzburg.de/home>).

ject's left STN recordings. A significant cluster showing early alpha (7–14 Hz, 300–600 ms) event-related coupling was observed (Figure 3.6).

None of the group level datasets for each measurement window and parameter passed Shapiro-Wilk normality tests ($p < .05$). The DOP \times VAL factorial analysis did not yield significant DOP ($F(1, 24) = .17, p > .05$) or VAL ($F(2, 24) = 1.42, p > .05$) effects.

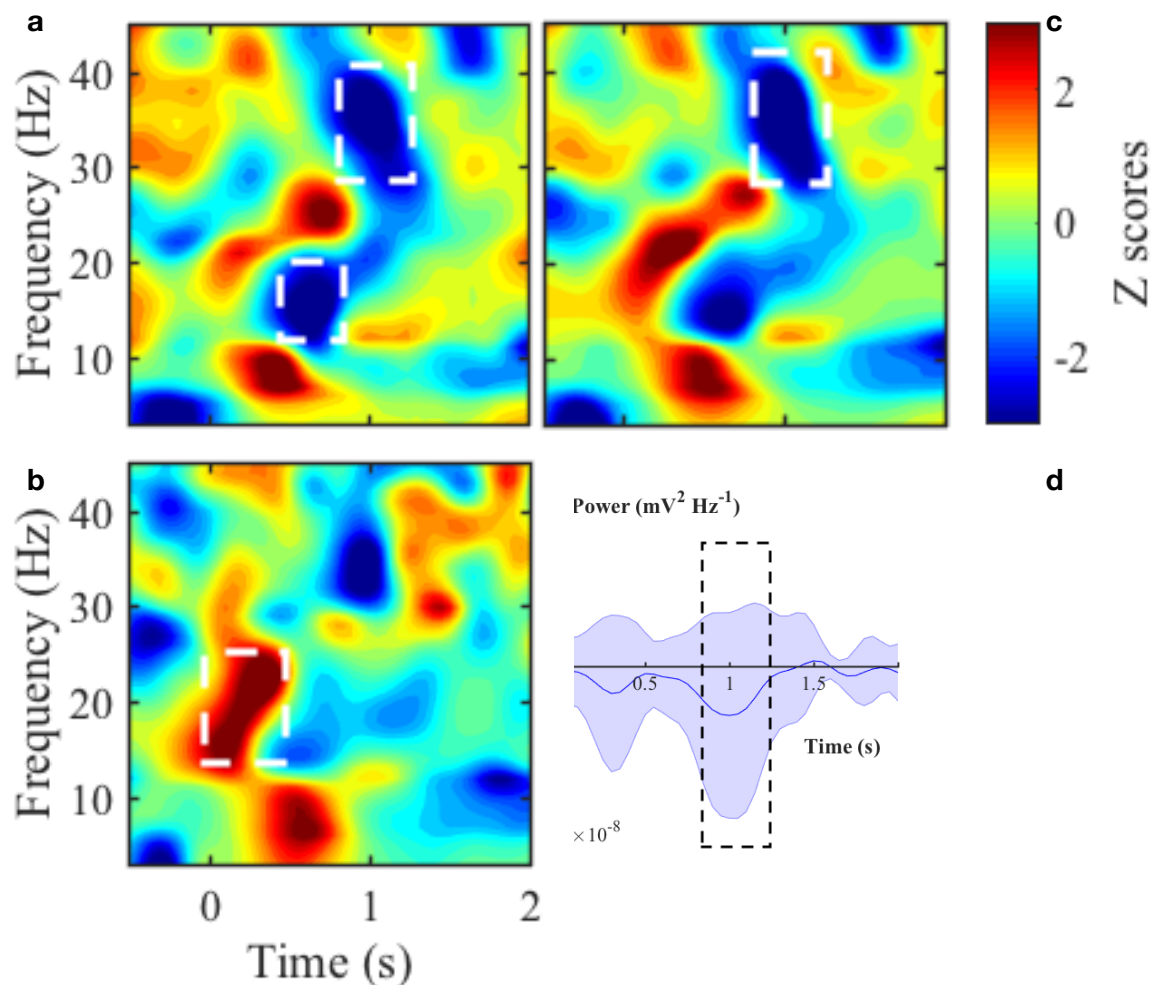


Fig. 3.4 | **STN time-frequency analysis.** **a, b** | Unthresholded z-maps obtained by subtracting mean values of the permutation set from the mean of the cross-condition patient average power values and then dividing by the standard deviation values of the permutation set. The maps correspond to left (**a**) and right (**b**) STN activity. Significant clusters are highlighted within white dashed rectangles. **c** | Unthresholded z-map computed after collapsing across hemispheres. **d** | Baseline-corrected mean \pm sd time-course of high beta (28–40 Hz) activity across patients. Time range (800–1200 ms) corresponding to ROI is highlighted within

3.4. Event-Related Potentials in Reconstructed Sources

The maximum absolute peaks for both sources were observed at $M = .344$ s, $SD = .15$. Thus, we analyzed the measurement window 194–494 ms for both reconstructed sources (Figure 3.7). 50% fractional latencies for the reconstructed amygdala and ACC channels were $M = .34$ s, $SD = .04$ s and $M = .35$ s, $SD = .03$ s, respectively. For non-parametric repeated measures 2×3 factorial analyses, subject wue03 was excluded in the $DOP \times VAL$ analysis of variance since no recordings in the dopaminergic ON state could take place.

None of the group level datasets for each measurement window and parameter passed Shapiro-Wilk normality tests ($p < .05$). The $DOP \times VAL$ analysis of variance yielded a significant DOP effect for amygdala ERP latency ($F(1, 24) = 8.59$, $p = .042$) and subsequent post-hoc tests showed that the latency in the medication OFF condition ($M = .31$ s, $SD = .03$ s) was significantly shorter than in the ON condition ($M = .36$ s, $SD = .04$ s) (Figure 3.8). The

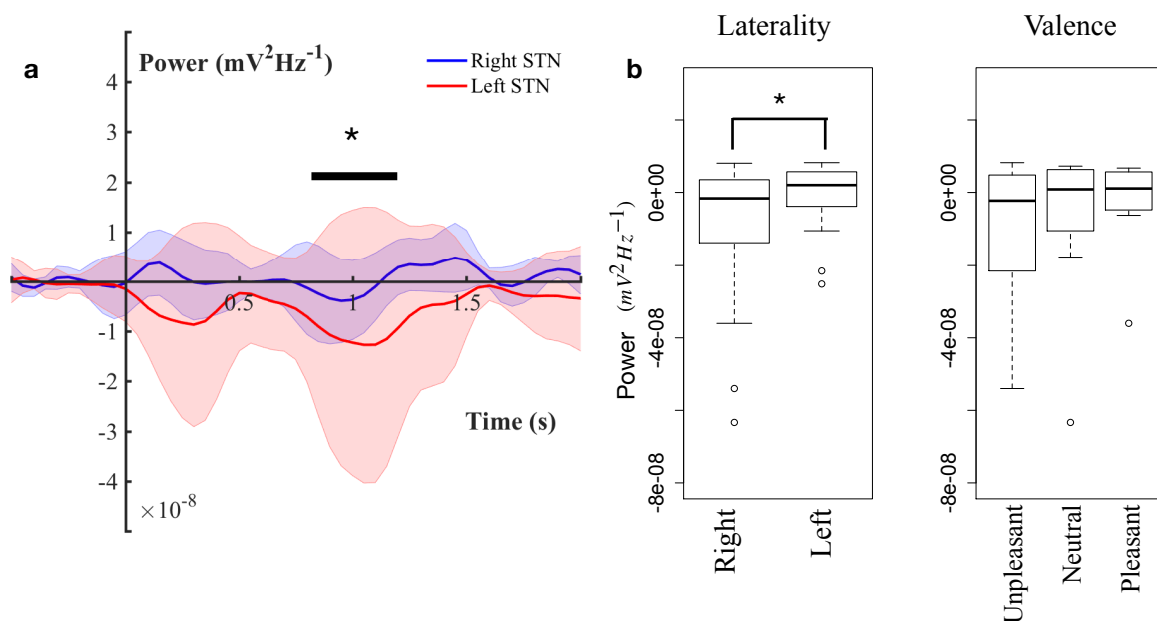


Fig. 3.5 | **Laterality effect on low beta ERD in STN.** **a** | Display of average STN waveforms of both hemispheres (hard lines) and standard deviation (transparent coloring) highlighting measurement window where a significant laterality effect was obtained. **b** | Box-plots representation of laterality and valence statistics for low beta oscillations. Color figures can be found on the electronic version of this thesis on OPUS (<https://opus.bibliothek.uni-wuerzburg.de/home>).

VAL ($F(2, 24) = 8.59, p = .042$) and DOP \times VAL interaction ($F(2, 24) = 8.59, p = .042$) effects were not significant.

In addition, the SIDE \times VAL factorial analysis showed a significant SIDE effect for ACC signed area amplitude ($F(1, 30) = 29.05, p = .006$), with Tukey-corrected post-hoc tests ($p = .006$) revealing larger mean area amplitude in the right virtual ACC ($M = 1.01 \mu\text{V s}, SD = .81 \mu\text{V s}$) than in the left virtual ACC ($M = .71 \mu\text{V s}, SD = .62 \mu\text{V s}$) (Figure 3.8).

The DD effect in the DD \times VAL analysis of variance was not significant for both sources and parameters. See tables A4 and A5 in Appendix for descriptive statistics of all condition combinations.

3.5. Power Analysis for Reconstructed Sources

Group permutation tests showed significant clusters ($p < .05$) for the cross-condition average power maps comparing post-onset activity against baseline activity. A significant ERS cluster spanning the ‘alpha’ and ‘beta’ bands (within about 7–23 Hz, 50–300 ms) and an ERD cluster in the ‘high beta’ band (within about 24–31 Hz, 400–700 ms) were obtained in the amygdala

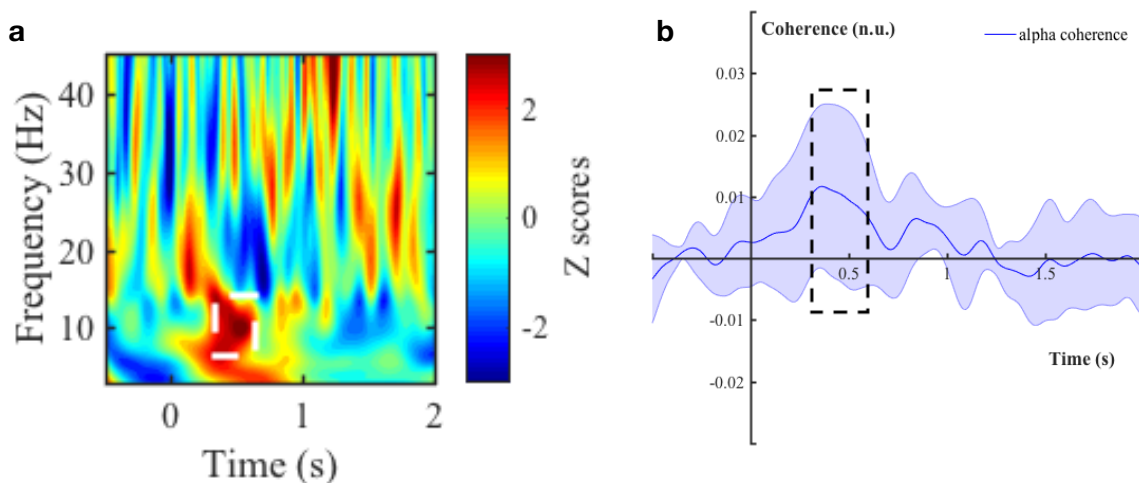


Fig. 3.6 | **Inter-hemispheric STN coherence.** **a** | Unthresholded z-map obtained by subtracting mean values of the permutation set from the mean of the cross-condition patient average wavelet coherence values and then dividing by the standard deviation values of the permutation set. A significant cluster is highlighted by a white dashed rectangle. **b** | Baseline-corrected mean \pm standard deviation time-course of alpha (7–14 Hz) coherence across patients. Time range (300–600 ms) corresponding to ROI is highlighted within black dashed rectangle. Color figures can be found on the electronic version of this thesis on OPUS (<https://opus.bibliothek.uni-wuerzburg.de/home>).

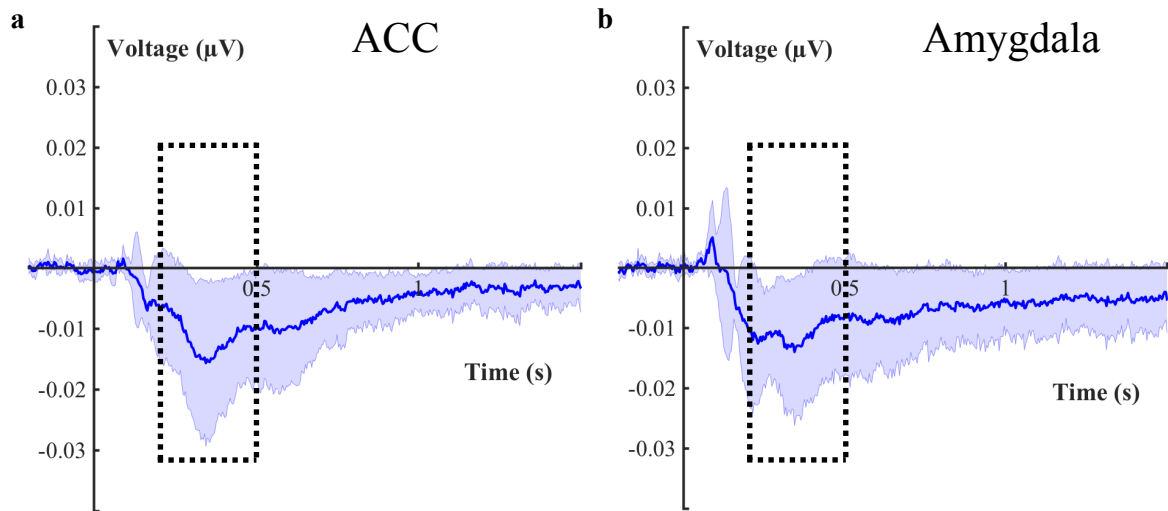


Fig 3.7 | **Waveforms of reconstructed sources.** a, b | Mean (hard blue) \pm standard deviation (transparent blue) waveforms corresponding to ACC and amygdala, respectively.

permutation test after collapsing across hemispheres. Moreover, an ERS ‘alpha’ cluster (with- in about 7–12 Hz, 50–300 ms) was statistically significant when collapsing ACC spectro- grams across sides. These clusters defined the ROI for subsequent analyses of variance (Fig- ure 3.9).

None of the group level datasets for each component and parameter passed Shapiro-Wilk normality tests ($p < .05$). The DOP \times VAL did not yield any significant effects for either structure. For laterality, factorial analysis showed ‘alpha-beta’ ERS in the amygdala ($F(1, 30) = 6.7, p = .048$) and ‘alpha’ ERS in the ACC ($F(1, 30) = 11.22, p = .02$) to be significantly higher in the right hemisphere.

The DD and VAL effects in the DD \times VAL analysis of variance were not significant for both sources and all frequency bands. A significant DD \times VAL interaction for ‘alpha’ activity in the ACC ($F(2,30) = 4.87, p = .033$) was followed by non-significant post-hoc Wilcoxon signed-rank tests after a Holm correction ($p > .05$).

3.6. STN-Reconstructed Sources Coherence

Group permutation tests showed significant clusters ($p < .05$) for the cross-condition average power maps comparing post-onset activity against baseline activity. Subject wue03 was excluded for the above mentioned reasons. We saw a significant STN-virtual amygdala coupling cluster spanning the ‘high beta’ band (within about 20–25 Hz, 200–400 ms) as well as a significant late STN-virtual amygdala coupling cluster in the ‘low beta’ band (within about 12–17 Hz, 1800–2000 ms). We also obtained a significant STN-virtual ACC coupling cluster in the ‘alpha’ range (within about 7–11 Hz, 700–900 ms) and a significant uncoupling cluster in the ‘low beta’ range (within about 14–21 Hz, 1650–1850 ms). These clusters defined the

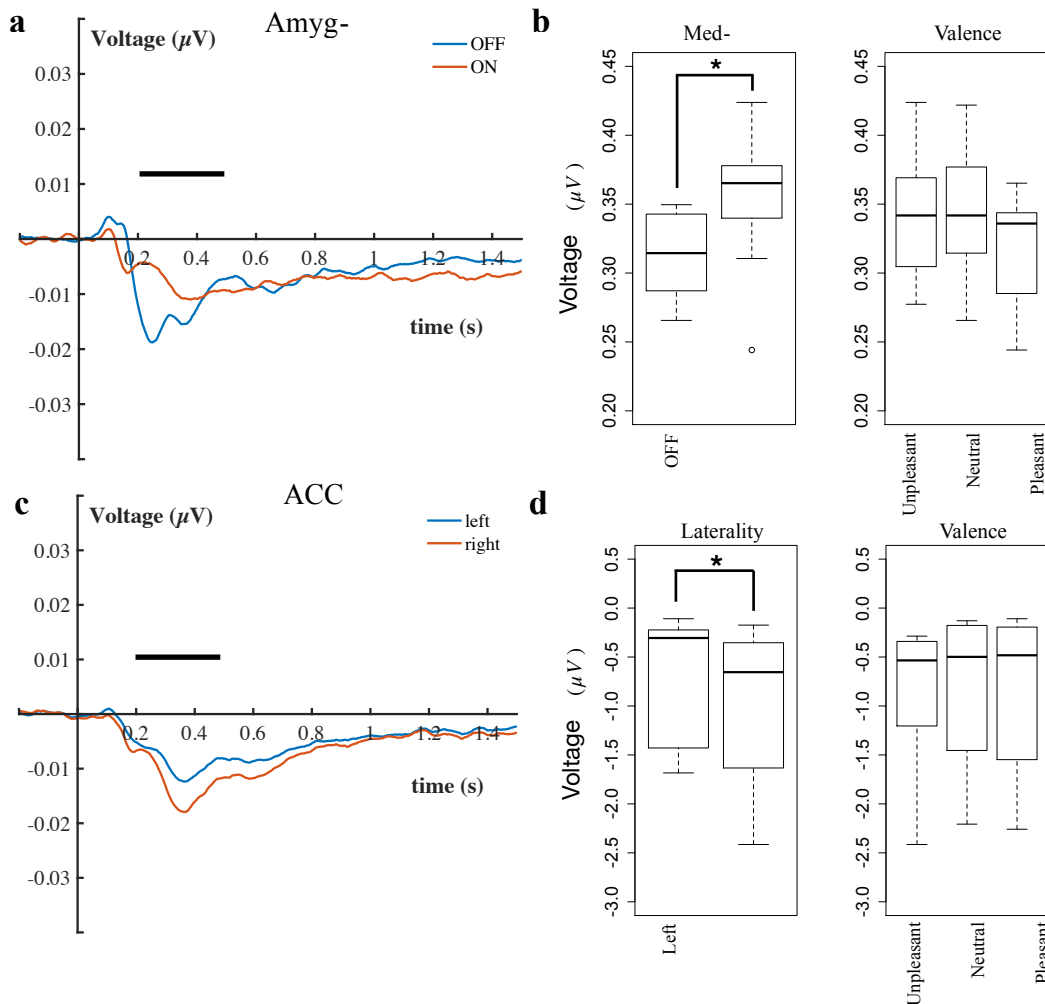


Fig. 3.8 | **Dopamine and laterality effects in ERP analysis of reconstructed sources.** **a** | Grand average amygdala waveforms in the OFF and ON medication states. **c** | Grand average ACC waveforms in left and right hemispheres. **b, d** | Box-plot displays of statistics corresponding to **a** and **c**, respectively.

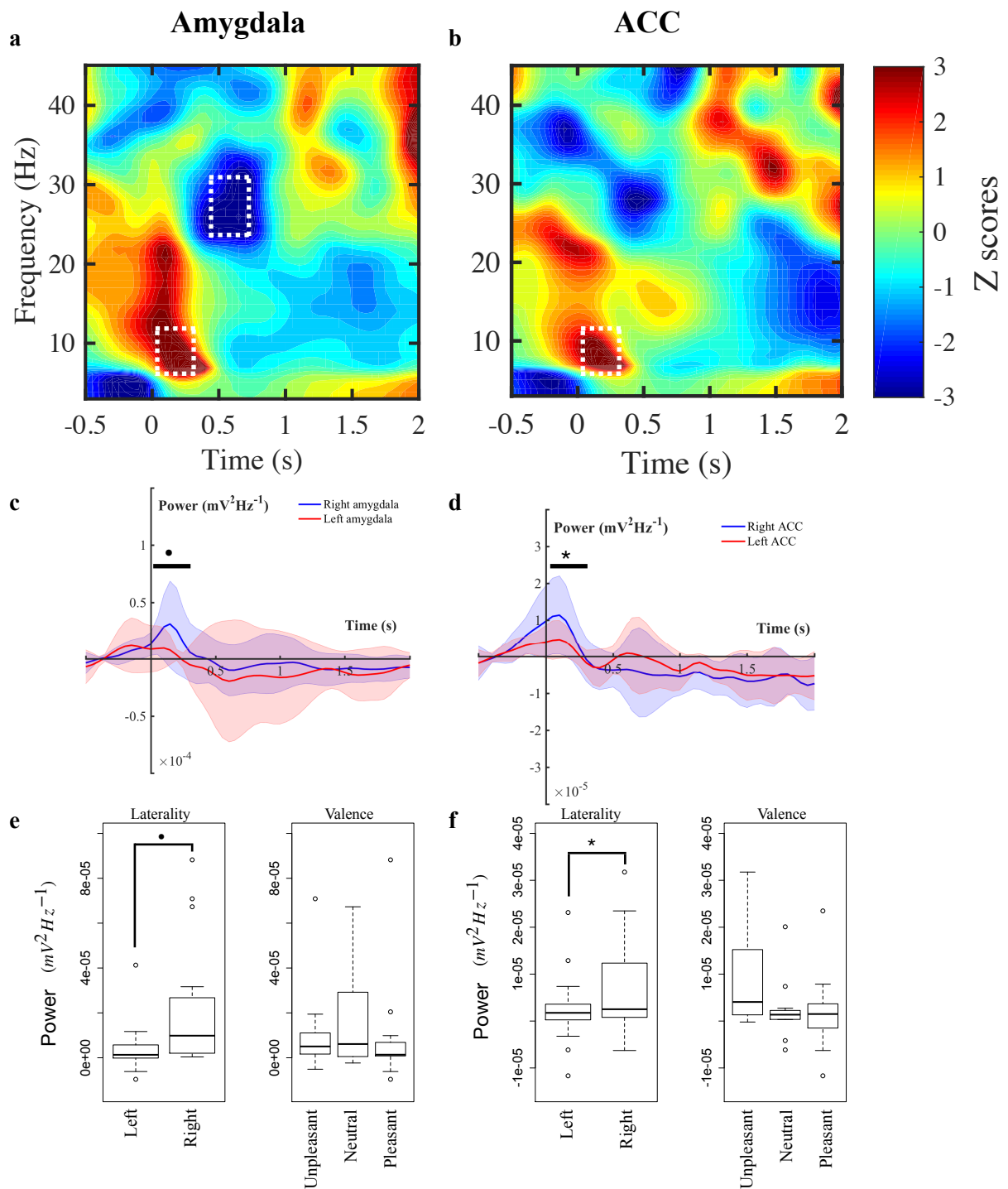


Fig. 3.9 | Laterality in time-frequency analysis of reconstructed sources. a, b | Unthresholded z-maps of power values of the reconstructed amygdala (a) and ACC (b) signals. ROI based on significant clusters are highlighted by white dashed rectangles. **c, d** | Mean (hard lines) \pm standard deviation (transparent coloring) waveforms from the right and left hemisphere, highlighting a trend (\bullet) and a significant laterality effect (*). **e, f** | Box-plot display of statistics corresponding to c and d, respectively. Color figures can be found on the electronic version of this thesis on OPUS (<https://opus.bibliothek.uni-wuerzburg.de/home>).

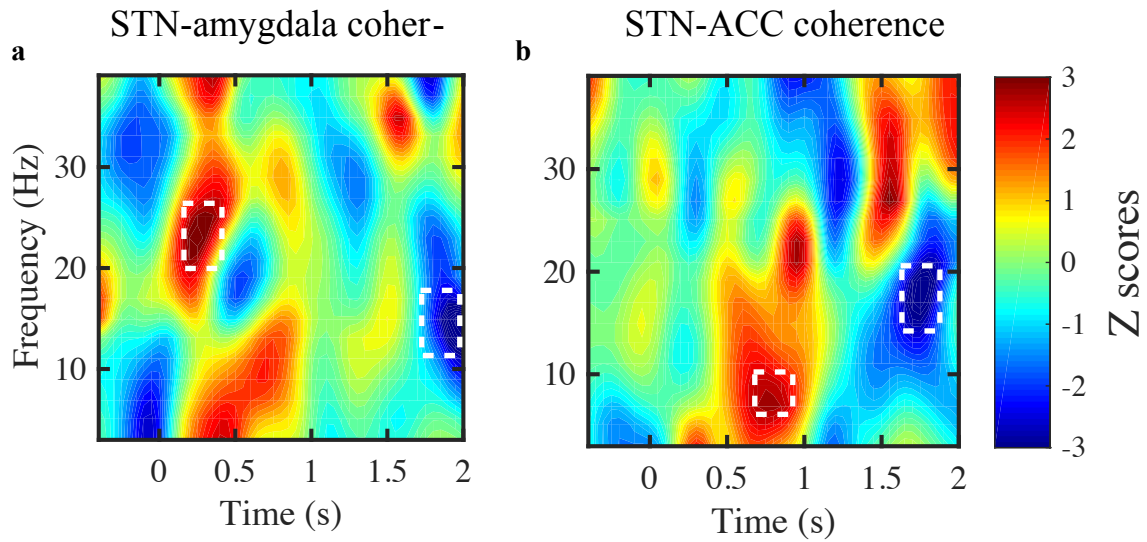


Fig. 3.10 | **Functional connectivity between the STN and reconstructed sources.** **a, b** | Un-thresholded z-maps of coherence values of the reconstructed amygdala (**a**) and ACC (**b**) signals. ROI based on the location of significant clusters are highlighted within white dashed rectangles.

ROI for subsequent analyses of variance (Figure 3.10).

No significant effects for either structure were revealed by the $DOP \times VAL$, $SIDE \times VAL$, or the $DD \times VAL$ analyses of variance.

4. Discussion

This study used ERP, power, and coherence analysis to assess the effect of dopaminergic medication state, stimulus valence, laterality, and striatal dopaminergic denervation on visuo-affective processing in the STN in PD subjects. In addition, STN functional connectivity to the amygdala and the ACC during visuo-affective processing was estimated by means of source reconstruction.

4.1. STN ERP Analysis

Two measurement windows (250–650 ms and 750–1250 ms post-onset) were selected for ERP analysis based on prominent post-stimulus presentation deflections observed on the cross-condition grand average waveforms. The first measurement window overlaps with the only ERP reported in Buot et al., 2013 (onset: 168 ± 74 ms, maximum: 363 ± 125 ms; $n = 13$ subjects for medication state OFF and $n = 7$ for ON). These discrepancies could be due to both studies relying on a small sample size, however Buot and colleagues averaged STN measurements from different depths along the dorsoventral axis, while the recordings in this thesis were obtained largely from dorsal STN regions, and thus the waveforms in Buot et al., 2013 may be more representative of ventral (i.e., limbic) STN processing. Nevertheless, the ERP onset reported in Buot et al., 2013 appears rather premature, since it indicates some of their measured ERPs begin at $168 - (2 \times 74) = 20$ ms after stimulus onset, and thus their results may reflect differences in perceptual processing due to physical properties not controlled for such as contrast (Keil et al., 2014). As for the source of the observed ERPs, Buot and colleagues report changes in amplitude and polarity reversal between recordings from adjacent channels arguing that this confirms the STN as the local source for the observed ERPs (Buot et al., 2013). Although our recordings do not allow for a comparison across the dorsoventral axis, mirror images of average waveforms across the time axis in both hemispheres appear in line with the polarity reversal observed in Buot et al., 2013.

Interestingly, both deflections are observable regardless of stimulus valence, including neu-

tral, which suggests that either physical properties or higher-order properties may be represented in STN activity within those time periods. The presentation of an image could be processed as an event that is potentially relevant for a decision, which is in line with the STN's role in setting up decision thresholds (Cavanagh et al., 2011, Frank et al., 2015). Moreover, the observed ERPs may indicate that the presentation of an image elicits temporally distinct STN responses. Indeed, EEG studies in both PD patients and controls consistently report early (Wieser et al., 2006) and late (Dietz et al., 2013) stimulus-evoked potentials in occipital and centroparietal cortical areas, respectively. Further, evidence from Huebl et al, 2014, who analysed event-related synchronization in the STN using a comparable paradigm, observed valence and arousal modulation of synchronous activity (alpha ERD during 1000–2000 ms and gamma ERS during 375–725 ms post onset) that is thought to represent different processes (sensory information processing and arousal-dependent attention, respectively).

The main finding from the ERP part of the analysis was the longer midpoint latency associated with threatening pictures compared to appetitive and neutral pictures in the DOP \times VAL and DD \times VAL analyses of variance. This contrasts with the “negativity bias” framework (Cacioppo, Bertson, & Gardner, 1999; Carretié, Martín-Loeches, Hinojosa, & Mercado, 2001), according to which aversive information in the environment is rapidly processed by the amygdala in order to preferentially allocate attentional resources towards processing of threatening over appetitive or neutral stimuli. Although such framework predicts shorter latency and higher amplitude for ERPs elicited by negative stimuli compared to positive or neutral, inconsistent results in the literature do not confirm this (Olofsson et al., 2008). In addition, there is consensus in ERP studies that stimulus valence does not modulate latency of a component as observed via scalp recordings (Olofsson et al., 2008). Two possible scenarios could explain the contradiction between the relative late latency of threatening stimuli reported here and the “negativity bias” framework and the lack of evidence for valence-modulation of latency. If processing of aversive stimuli in the STN in parkinsonian patients is impaired, then an approximation to a comparison between physiological and pathological functioning of the basal ganglia is achievable by comparing ERPs in the medication ON and OFF states. Such an impairment may underlie the affected neural networks responsible for the blunted emotional reactivity observed in PD patients (Tessitore et al., 2002). Specifically, responses

obtained with BOLD fMRI were seen bilaterally in the amygdala upon presentation of emotional face images in healthy controls but were absent in parkinsonian subjects in the hypodopaminergic state and partially restored in medication state ON (Tessitore et al., 2002). Thus, an impaired, amygdala-mediated, fast orienting of attention towards processing of negative stimuli could lead to the relative delay of the second ERP compared to appetitive and neutral stimuli. Though lack of a significant dopamine effect in the DOP \times VAL test is compatible with an insufficient amygdala activation even after dopamine repletion, the fact that this analysis of variance did not yield a significant valence effect suggests that the small sample size ($n = 5$) is to blame for the absence of an significant effect otherwise obtained in the other two analyses of variance ($n = 6$). Importantly, the notion of the amygdala as a nucleus specialized in aversive processing has been superseded by studies demonstrating left amygdala activity evoked by pleasant faces (Fitzgerald, Angstadt, Jelsone, Nathan, & Phan, 2006), indicating a more general role for the primate amygdala, namely processing of salient social information (Adolphs, 2003). Therefore, amygdala impairment could in principle affect processing of both pleasant and unpleasant stimuli. To overcome this impasse, replication studies with larger sample sizes probing the effect of dopamine should be conducted. If such an effect fails to prove significant, then the STN might be a brain region uniquely unbiased towards negative stimuli, underlining a role for the STN and the basal ganglia at large in positive reinforcement learning. The shorter latency of appetitive images compared to neutral images of the first ERP of this study falls in line with this picture, even though early components are associated with perceptual processing, and indeed, the DD \times VAL interaction effect being in the trend zone ($F(2,30)$, $p = .063$) and the non-significant post-hoc pairwise comparisons (Holm, $p > 0.05$) cast doubt on such an interpretation.

4.2. STN Power Analysis

We investigated changes in neural synchrony as indexed by power magnitude to probe the effect of emotional pictures on STN oscillatory activity across all conditions, as well as under each individual valence and medication state conditions, collapsing recordings from both hemispheres as well as analyzing right and left STN separately. As we expected, picture presentation elicited a late desynchronization in the high beta band, however, the permutation

test also showed an early significant cluster for beta ERS in the right STN. Beta synchronization has been interpreted as antikinetic (Brown, 2003), relevant for maintenance of the status quo (Engel & Fries, 2010), and as an immutability promoting rhythm (Brittain & Brown, 2014). Moreover, high beta in the STN is known to be entrained by the motor cortex (Litvak et al., 2012). Hence, beta synchronization followed by desynchronization could reflect an initial response inhibition during sensory processing, followed by a mutability-promoting desynchronization wherein beta information channels become unsaturated and pathway segregation is restored (Middleton & Strick, 2002; Pessiglione et al., 2005).

The difference in significant clusters in the left and right STN cross-condition average permutation tests suggests that STN limbic processing is lateralized, and the $SIDE \times VAL$ analysis of variance supported this conclusion. While only observed in the right STN permutation test, early theta and alpha ERS are consistent with previous studies (Huebl et al., 2014). The observed stronger high beta ERD in the left STN contradicts the lateralization effect found by Eitan and colleagues (2013), where stronger low beta ERD and in the right STN was elicited by emotive auditory stimuli (Eitan et al., 2013). However, our results concern high beta ERD and our signals were not recorded directly at the ventral STN, as were those by Eitan and colleagues. This could be explained by the fact that the more dorsal the site of recording, the likelier it is that the recordings will capture high beta cortically-entrained rhythms. STN theta ERS has been associated with high-conflict processing (Rappel et al., 2018), where theta rhythms entrain STN spiking activity to hinder impulsive decisions (Zavala et al., 2017). Alpha oscillations on the other hand are thought to index sensory information processing (Klimesch, Fellinger, & Freunberger, 2011), and specifically, STN activity in the dopaminergic ON state has been observed to desynchronize in the alpha band more strongly upon presentation of pleasant than unpleasant images, with a reversed pattern in the OFF state (Huebl et al., 2014). Thus, late alpha ERD permits approach-related processing (Huebl et al., 2014) by inhibiting inappropriate or irrelevant neural mechanisms (Klimesch et al., 2011). This study only found significant early alpha ERS in the right STN, most likely involved in early sensory processing as observed cortically during comparable paradigms (for a review, see Güntekin & Başar, 2014). Late alpha ERD, though not significant, is observable on the thresholded z-map where cross-condition averages of both STN are collapsed, and thus the

disparity between this study and that by Huebl and colleagues (Huebl et al., 2014), is likely due to low statistical power. Overall, STN rhythmic activity comprises multiple processes segregated in the frequency domain which may enable the orientation of attention towards processing of salient stimuli in the environment.

4.3. STN Coherence Analysis

We investigated the question of bilateral basal ganglia networks by looking at the wavelet coherence between the left and right STN. Consistent with the majority of recent literature on inter-hemispheric STN coupling at rest or during a motor task (Darvas & Hebb, 2014; Kato et al., 2015; Talakoub et al., 2016; West et al., 2016), we found an increase in alpha coupling after stimulus presentation using the cross-condition average permutation test. In contrast, other studies have reported not alpha, but beta left-right STN coupling (de Solages et al., 2010; Little et al., 2013; Hohlefeld et al., 2014). At any rate, this is the first time, to the best of our knowledge, that inter-STN coherence has been observed during an affective task. Moreover, left-right STN coupling was shown to be unmodulated by dopaminergic medication state or stimulus valence. Inconsistent results exist in the literature regarding dopamine modulation of inter-hemispheric STN functional connectivity (a significant dopamine effect was found in Little et al., 2013; Hohlefeld et al., 2014; but not in West et al., 2016).

Two brain structures are connected either mono- or poly-synaptically. DBS stimulation of one nucleus has been shown to elicit activity in the contralateral STN (Walker et al., 2011; Brun et al., 2012), but there is no known direct anatomical connection between both STN in primates (Carpenter & Strominger, 1967; Carpenter, Carleton, Keller, & Conte, 1981) and the effects of stimulation occur at a longer latency than the phase lag reported in bilateral STN coherence (Little et al., 2013). Alternatively, the bilateral nuclei can be coupled by simultaneous entrainment through a common input from a third structure such as a cortical area via a corticostriatal or hyperdirect pathway (Little et al., 2013) or the thalamus (Talakoub et al., 2016), the latter of which generates and modulates alpha rhythms (Schreckenberger et al., 2004), projects afferents to the monkey STN via the centromedian-parafascicular complex of

the posterior thalamus (Parent & Hazrati, 1995), and has been shown to be linked to the STN with structural and functional connectivity methods (Brunenberg et al., 2012).

The functional role of interhemispheric STN coherence in the alpha band is unclear. Synchrony between the nuclei could help coordinate the inhibition of irrelevant neural mechanisms (Klimesch et al., 2011) bilaterally in order to direct attention towards behaviorally salient stimuli. In motor studies, alpha inter-STN coherence is interpreted as maintenance of the status quo or idling state (Talakoub et al., 2016).

4.4. Analysis of Reconstructed Sources

In order to investigate how dopamine, stimulus valence, laterality, and dopaminergic denervation modulate functional connectivity between the STN and limbic structures such as the amygdala and the ACC in PD patients during the presentation of emotional visual stimuli, coherence was computed and ROI were statistically evaluated with non-parametric analysis of variance. Moreover, in order to corroborate that the effects seen using coherence were mirrored by reconstructed local activity in the virtual channels, ERP and time-frequency analyses were performed on both the virtual amygdala and ACC channels. We found that emotional pictures elicited changes of middle (about 700–900 ms) and late (about 1650–1850 ms) latency in functional connectivity between the STN and the reconstructed ACC, where the first change, a coupling, was stronger in the left hemisphere, while the second change, an uncoupling, was of higher magnitude in the right hemisphere. Connectivity between the virtual amygdala and the STN was found to begin earlier (200–400 ms), though a later uncoupling (1800–2000 ms) in the ‘low beta’ range was observed too. Although dopaminergic medication state and laterality had an effect on local time-frequency and ERP analyses, these were not mirrored by the STN-virtual amygdala functional connectivity analysis.

Long known for rapid processing of threatening stimuli thanks to subcortical circuits, the amygdala receives additional, though slower, cortical input, thus engaging in both rapid and reflexive processing and is sensitive to both aversive and appetitive cues (Hung et al., 2010).

An MEG source reconstruction ERP study using emotional faces found two peaks at ~100 ms and ~170 after stimulus presentation (Hung et al., 2010). Early high beta coupling with the STN (200–400 ms) would in this line follow the integration of both rapid subcortical processing and cortical feedback in the amygdalae. In the motor domain, high beta coupling between then STN and premotor cortex is mainly driven by the cortex via the hyperdirect pathway (Litvak et al., 2011; Hirschmann et al., 2011). Thus amygdala afferents onto the STN might contribute early to STN beta synchrony, which has been interpreted as an immutability-promoting rhythm (Brittain & Brown, 2014) that allows the brain more time to gather further information before the STN can desynchronize in the beta range and thus desaturate information channels of the subthalamic-cortical fibers, which in turn may permit that a motor program be effectuated, if behaviorally relevant.

Emotional discrimination of visual stimuli at the amygdala has been reported to occur at a latency of 1 s shorter than at the extrastriate occipital cortex (and roughly 3 s after stimulus presentation) based on hemodynamic response amplitudes (Sabatinelli et al., 2009). However, a temporally more sensitive MEG study found early (130–170 ms) discrimination between unpleasant and neutral stimuli as indexed by peak amplitude of reconstructed amygdala trials (Dumas et al., 2013). Thus, it is surprising that we did not find a valence effect in connectivity, synchrony, or ERP analysis of the reconstructed amygdala LFP activity, since pictures were presented for 2 s. In terms of synchronization, higher alpha-beta synchrony (50–300 ms) in the right amygdala may correspond to ERP findings which associate the right amygdala with more rapid, coarsely tuned processing and the left amygdala with a finely-tuned, cortical-feedback-dependent response (Hung et al., 2010; Hardee, Thompson, & Puce, 2008; Gläscher & Adolphs, 2003). We observed a dopamine effect on synchronization, where ‘alpha-beta’ ERS was stronger in the ON state, consistent with PD literature documenting PD amygdala activation closer to that of healthy controls after a levodopa challenge upon seeing fearful stimuli (Tessitore et al., 2002). The unexpected lack of dopamine effect on ‘alpha’ ERS might indicate that a levodopa challenge may be insufficient to restore normal amygdala activity in PD. Nevertheless, a dopamine effect with no significant interaction on ERP latency might shed light on how the spread of extranigral pathology in PD alters emotional processing. Compared to healthy controls, amygdalae in PD can undergo a loss of volume of ~20%

(~30% in corticomedial complex) and Lewy bodies can be found throughout its subcomponent structures (Harding et al, 2002). Moreover, grey matter density is more reduced in the right hemisphere without further progression after mild PD stages (Li, Xing, Schwarz, & Auer, 2017). Thus, the shorter ERP latency in the OFF state may reflect a precipitated response in the compromised amygdala, which may no longer efficiently discriminate between salient and non-salient stimuli (Yoshimura et al., 2005; Hrybouski et al., 2016). Finally, the fact that the experiments were always conducted in the same sequence (first in dopaminergic medication OFF, then in ON state) represents a limitation due to the possible ‘order effect’, where issues like fatigue and potentially discomfort from sitting might influence how attentional resources are allocated to emotional processing.

Among the various higher order cognitive functions performed by the ACC, determining the motivational relevance of a stimulus (Albert et al., 2012) may be a prerequisite computation before establishing ‘alpha’ STN-ACC functional connectivity. The prominence of relatively late (700–900 ms) ‘alpha’ coupling is difficult to interpret in the absence of conflict, but may reflect cortical entrainment of the STN for the purpose of blocking emotional motor responses until the motivational relevance of the picture is computed. Early (50–300 ms) alpha ERS and higher ERP area amplitude (194–494 ms) in the right ACC would in turn reflect more schematic processing of simple emotions (Gainotti, 2012), potentially due to amygdalic-ACC connectivity, where bottom-up appraisal by the amygdala is followed by top-down conflict resolution, if there is any (Comte et al., 2016). Another interpretation of ACC activity elicited by emotional pictures comes from the studies showing ACC involvement in updating the internal model of the environment (Kolling, Behrens, Wittmann, & Rushworth, 2016), although whether the ACC distinguishes between the motivational value of real and represented (i.e. pictures of) aversive/appetitive cues remains to be investigated.

In this study we reconstructed the activity of the amygdala in one ‘channel’, although the amygdaloid complex is composed of substructures such as the basolateral complex (BLA) and the central nucleus (CeA), which are in turn associated with distinct roles in affective processes (Janak & Tye, 2015). For instance, fear and appetitive conditioning by the amygdala requires parallel and serial processing incorporating different circuits involving both the

BLA and CeA. Value representation (appetitive or aversive) of a given stimulus or action requires the ability to update current value as a function of outcome value (computed within BLA, which contains valence-tuned neuronal populations, see Belova, Paton, Morrison, & Salzman, 2007 and Paton, Belova, Morrison, & Salzman, 2006 for evidence in primates) as well as information regarding motivational significance, as observed in CeA (Balleine & Killcross, 2006; Janak & Tye, 2015). In addition, though EEG measures are sensitive to electrical sources in the cortex, sensitivity to structures such as the amygdala, buried down in the temporal lobe, is more limited than for the ACC (Keil et al., 2009). Likewise, the ACC is composed of a pregenual (pgACC) and a subgenual (sgACC) component, which in turn form separate parallel circuits with other structures, such as the amygdala (Marusak et al., 2016). The functional specialization of the ACC subcomponent connections with the amygdala is suggested by differential symptomatology associated with their disruption (Marusak et al., 2016). Hence, although this study used a passive viewing task, either more granular reconstruction methods or invasive electrode recordings as well as concomitant behavioral tasks are necessary to obtain a more detailed mechanistic view of how the value and motivational significance of emotional pictures are represented in the amygdaloid and ACC complexes.

5. Concluding Remarks

It is important to note that the results presented here represent emotional processing in the PD brain, and thus caution should be exercised in extrapolating these findings to the healthy brain. Indeed, even in the medication ON state (typically described as an approximation to the healthy physiological state), PD patients may experience impaired evaluation of risk and impulsive behaviors after receiving a levodopa challenge (Zhang et al., 2014). Furthermore, long-term dopaminergic therapy has been shown to induce changes in plasticity in the primary motor cortex as well as in connectivity between the dorsal premotor and the motor cortices (Suppa et al., 2010). Yet, a number of recent studies employing diffusion tensor imaging and fMRI techniques have also shown that DBS may have restorative effects on brain connectivity (van Hartevelt, 2014; Mueller et al., 2018).

This study showed that stimulus valence, dopaminergic medication state, and laterality affect visuo-affective processing in the brain. It is important for survival that visual information with emotional content can be met with the appropriate approach or withdrawal response by relaying coarse visual information to brain areas that can typify stimulus valence, which in turn should activate motor cortices to produce adaptive behavior. Evidence for the relation between emotion and motor processing comes from multiple studies which show that emotional priming (i.e., preconditioning brain processing by briefly presenting an emotional stimulus) modulates reaction time (for a meta-analysis, see Phaf, Mohr, Rotteveel, & Wicherts, 2014), voluntary motor response inhibition (Kalanthoff, Cohen, & Henik, 2013; Verbruggen & De Houwer, 2007), and force output (particularly with erotic stimuli, see Coombes, Gamble, Cauraugh, & Janelle, 2008). Indeed, Grèzes and colleagues (2014) demonstrated structural connectivity between the amygdala and multiple motor cortices (Grèzes, Valabrègue, Gholipour, Chevallier, 2014). The role of the STN in the context of affect processing could be akin to its functional role during motor processing. Cortical input onto the STN via the hyperdirect pathway is thought to mediate increases in STN synchrony, whose immutability promoting effects (Brittain & Brown, 2014) may allow time for enough information to be accumulated before the appropriate motor program is released. This has been exemplified by a

multimodal PPI study in HC where reward uncertainty was indexed by an increase in hemodynamic response amplitude in the supplementary motor area (SMA) and the STN during a decision-making task (Frank et al., 2015). Furthermore, the STN is entrained in the theta range by the medial frontal cortex during conflict as shown using granger causality (Zavala et al., 2014). Thus, a picture emerges (Fig. X) where affective visual information coarsely processed by the visual cortex is relayed via the dorsal stream to the frontal cortex and via the ventral stream to the amygdala, which in turn entrain the STN via the hyperdirect pathway

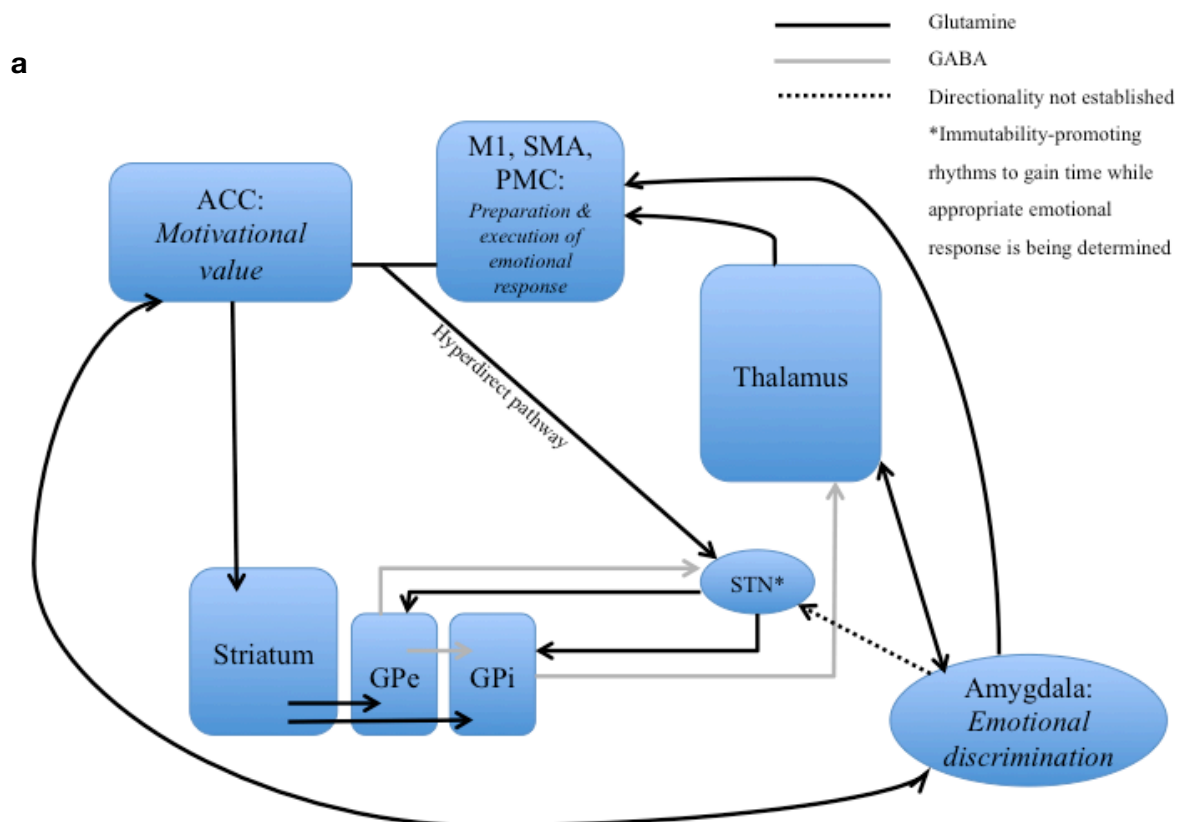


Fig. 5.1 | **Motor-affective information processing schematic.** a | Representation of the place of the STN within limbic and motor circuits highlighting major cortical and subcortical anatomical connections.

and, in the case of the amygdala, via the striatum (Cho, Ernst, & Fudge, 2013; Seymour & Dolan, 2008) or possibly via a direct connection (Lambert et al., 2012; Péron et al., 2016) to inhibit competing emotional responses until the adequate response is selected by parallel BG processing along the direct and indirect pathways. Once the STN desynchronizes, the uninhibited GPi can send the chosen emotional motor program to the ventral anterior and ventral

lateral nuclei of the thalamus before reaching the premotor cortex.

6. Future Directions

The study presented in this thesis involved a passive picture viewing paradigm. The mere perception of affective stimuli is an important first step in mapping affect circuits in the brain, yet with this experimental setup one may not conclude that other brain functions such as emotional motor or autonomic responses are related to the patterns of synchrony and coupling observed here. Thus more complex designs are necessary to further elucidate the role of the STN in processing emotional data within the context of behavioral responses and decision-making. For example, simultaneous intracranial STN and electrocortical recordings and tasks involving priming with emotional and non-emotional pictures during a GO/NOGO task in particular could afford the temporal resolution to reveal the differential implication of frontal cortices in behavioral inhibition as indexed by the evolution of cortico-STN functional connectivity.

The quantification of oscillatory activity by means of measures of Fourier power has recently come under criticism since such measure tends to be falsely interpreted as indexing only rhythmic activity (Jones, 2016). In fact, the electrical signatures of the brain are composed of rhythmic and transient activity. The latter occurs irregularly (i.e. not rhythmically) at high amplitudes yet trials with transient activity can greatly distort the representation of oscillatory activity in grand average spectrograms (Jones, 2016). Lagged coherence has been proposed to quantify rhythmicity, interpreted as the degree of repeatability in successive time windows (Fransen, van Ede, & Maris, 2015). Lagged coherence is not confounded by amplitude and has been shown to better identify top-down attentional modulations cortical rhythms (Fransen, van Ede, & Maris, 2015). In addition, information-theoretical tools have been adapted for the analysis of dependence between sources of oscillatory activity. Mutual information between two signals tells us how much bits of information are shared between them. Thus, mutual information could enable the identification of the cortical area most responsible for STN entrainment during complex sensory-cognitive tasks.

Finally, it is worth noting that the downloading time of the ACTIVA PC+S® device (essentially the same duration of the recording itself) will be significantly shortened with the development of new stimulating devices with recording capabilities. This, together with increases in memory storage will enable shorter experiments that in turn may prevent a fatigue effect during the last recording sessions.

7. References

- Adolphs, R. (n.d.). Is the Human Amygdala Specialized for Processing Social Information? *Annals of the New York Academy of Sciences*, 985(1), 326–340. <https://doi.org/10.1111/j.1749-6632.2003.tb07091.x>
- Albert, J., López-Martín, S., Tapia, M., Montoya, D., & Carretié, L. (2012). The role of the anterior cingulate cortex in emotional response inhibition. *Human Brain Mapping*, 33(9), 2147–2160. <https://doi.org/10.1002/hbm.21347>
- Albin, R. L., Young, A. B., & Penney, J. B. (1989). The functional anatomy of basal ganglia disorders. *Trends in Neurosciences*, 12(10), 366–375.
- Alexander, G. E., DeLong, M. R., & Strick, P. L. (1986). Parallel organization of functionally segregated circuits linking basal ganglia and cortex. *Annual Review of Neuroscience*, 9, 357–381. <https://doi.org/10.1146/annurev.ne.09.030186.002041>
- Alzheimer's Association. (2014). 2014 Alzheimer's disease facts and figures. *Alzheimer's & Dementia: The Journal of the Alzheimer's Association*, 10(2), e47-92.
- Anastassiou, C. A., Montgomery, S. M., Barahona, M., Buzsáki, G., & Koch, C. (2010). The effect of spatially inhomogeneous extracellular electric fields on neurons. *The Journal of Neuroscience: The Official Journal of the Society for Neuroscience*, 30(5), 1925–1936. <https://doi.org/10.1523/JNEUROSCI.3635-09.2010>
- Argaud, S., Vérin, M., Sauleau, P., & Grandjean, D. (2018). Facial emotion recognition in Parkinson's disease: A review and new hypotheses. *Movement Disorders*, 33(4), 554–567. <https://doi.org/10.1002/mds.27305>
- Aron, A. R., Herz, D. M., Brown, P., Forstmann, B. U., & Zaghoul, K. (2016). Frontosubthalamic Circuits for Control of Action and Cognition. *The Journal of Neuroscience: The Official Journal of the Society for Neuroscience*, 36(45), 11489–11495. <https://doi.org/10.1523/JNEUROSCI.2348-16.2016>
- Asanuma, K., Tang, C., Ma, Y., Dhawan, V., Mattis, P., Edwards, C., ... Eidelberg, D. (2006). Network modulation in the treatment of Parkinson's disease. *Brain: A Journal of Neurology*, 129(Pt 10), 2667–2678. <https://doi.org/10.1093/brain/awl162>
- Baillet, S., Mosher, J. C., & Leahy, R. M. (2001). Electromagnetic brain mapping. *IEEE Signal Processing Magazine*, 18(6), 14–30. <https://doi.org/10.1109/79.962275>
- Balleine, B. W., Delgado, M. R., & Hikosaka, O. (2007). The role of the dorsal striatum in reward and decision-making. *The Journal of Neuroscience: The Official Journal of the Society for Neuroscience*, 27(31), 8161–8165. <https://doi.org/10.1523/JNEUROSCI.1554-07.2007>
- Balleine, B. W., & Killcross, S. (2006). Parallel incentive processing: an integrated view of amygdala function. *Trends in Neurosciences*, 29(5), 272–279. <https://doi.org/10.1016/j.tins.2006.03.002>
- Bard, P. A. (1928). A diencephalic mechanism for the expression of rage with special reference to the central nervous system. *Am. J. Physiol.* 84, 490–513
- Bard, P. A. & Rich, D. M. (1937). A study of four cats deprived of neocortex and additional portions of the forebrain. *John Hopkins Med. J.* 60, 73–153
- Barrett, L. F. (2006). Are Emotions Natural Kinds? *Perspectives on Psychological Science*, 1(1), 28–58. <https://doi.org/10.1111/j.1745-6916.2006.00003.x>
- Barrett, L. F., Lindquist, K. A., Bliss-Moreau, E., Duncan, S., Gendron, M., Mize, J., & Brennan, L. (2007). Of Mice and Men: Natural Kinds of Emotions in the Mammalian Brain? A Response to Panksepp and Izard. *Perspectives on Psychological Science: A Journal of the Association for Psychological Science*, 2(3), 297–312. <https://doi.org/10.1111/j.1745-6916.2007.00046.x>
- Belova, M. A., Paton, J. J., Morrison, S. E., & Salzman, C. D. (2007). Expectation modulates neural responses to pleasant and aversive stimuli in primate amygdala. *Neuron*, 55(6), 970–984. <https://doi.org/10.1016/j.neuron.2007.08.004>
- Benabid, A. L., Pollak, P., Louveau, A., Henry, S., & de Rougemont, J. (1987). Combined (thalamotomy and stimulation) stereotactic surgery of the VIM thalamic nucleus for bilateral Parkinson disease. *Applied Neurophysiology*, 50(1–6), 344–346.

- Biseul, I., Sauleau, P., Haegelen, C., Trebon, P., Drapier, D., Raoul, S., ... Verin, M. (2005). Fear recognition is impaired by subthalamic nucleus stimulation in Parkinson's disease. *Neuropsychologia*, 43(7), 1054–1059. <https://doi.org/10.1016/j.neuropsychologia.2004.10.006>
- Blonder, L. X., & Slevin, J. T. (2011). Emotional Dysfunction in Parkinson's Disease. *Behavioural Neurology*, 24(3), 201–217. <https://doi.org/10.3233/BEN-2011-0329>
- Bogacz, R., & Larsen, T. (2011). Integration of reinforcement learning and optimal decision-making theories of the basal ganglia. *Neural Computation*, 23(4), 817–851. https://doi.org/10.1162/NECO_a_00103
- Bologna, M., Berardelli, I., Paparella, G., Marsili, L., Ricciardi, L., Fabbrini, G., & Berardelli, A. (2016). Altered Kinematics of Facial Emotion Expression and Emotion Recognition Deficits Are Unrelated in Parkinson's Disease. *Frontiers in Neurology*, 7. <https://doi.org/10.3389/fneur.2016.00230>
- Borod, J. C., Haywood, C. S., & Koff, E. (1997). Neuropsychological aspects of facial asymmetry during emotional expression: a review of the normal adult literature. *Neuropsychology Review*, 7(1), 41–60.
- Brittain, J.-S., & Brown, P. (2014). Oscillations and the basal ganglia: motor control and beyond. *NeuroImage*, 85 Pt 2, 637–647. <https://doi.org/10.1016/j.neuroimage.2013.05.084>
- Britton, J. C., Taylor, S. F., Sudheimer, K. D., & Liberzon, I. (2006). Facial expressions and complex IAPS pictures: common and differential networks. *NeuroImage*, 31(2), 906–919. <https://doi.org/10.1016/j.neuroimage.2005.12.050>
- Brok, M. G. H. E. den, Dalen, J. W. van, Gool, W. A. van, Charante, E. P. M. van, Bie, R. M. A. de, & Richard, E. (n.d.). Apathy in Parkinson's disease: A systematic review and meta-analysis. *Movement Disorders*, 30(6), 759–769. <https://doi.org/10.1002/mds.26208>
- Brown, P. (2003). Oscillatory nature of human basal ganglia activity: relationship to the pathophysiology of Parkinson's disease. *Movement Disorders: Official Journal of the Movement Disorder Society*, 18(4), 357–363. <https://doi.org/10.1002/mds.10358>
- Brücke, C., Kupsch, A., Schneider, G.-H., Hariz, M. I., Nuttin, B., Kopp, U., ... Kühn, A. A. (2007). The subthalamic region is activated during valence-related emotional processing in patients with Parkinson's disease. *The European Journal of Neuroscience*, 26(3), 767–774. <https://doi.org/10.1111/j.1460-9568.2007.05683.x>
- Brun, Y., Karachi, C., Fernandez-Vidal, S., Jodoin, N., Grabli, D., Bardinet, E., ... Welter, M.-L. (2012). Does unilateral basal ganglia activity functionally influence the contralateral side? What we can learn from STN stimulation in patients with Parkinson's disease. *Journal of Neurophysiology*, 108(6), 1575–1583. <https://doi.org/10.1152/jn.00254.2012>
- Brunenberg, E. J. L., Moeskops, P., Backes, W. H., Pollo, C., Cammoun, L., Vilanova, A., ... Platel, B. (2012). Structural and resting state functional connectivity of the subthalamic nucleus: identification of motor STN parts and the hyperdirect pathway. *PloS One*, 7(6), e39061. <https://doi.org/10.1371/journal.pone.0039061>
- Buot, A., Welter, M.-L., Karachi, C., Pochon, J.-B., Bardinet, E., Yelnik, J., & Mallet, L. (2013). Processing of emotional information in the human subthalamic nucleus. *J Neurol Neurosurg Psychiatry*, 84(12), 1331–1339. <https://doi.org/10.1136/jnnp-2011-302158>
- Butler, A. B., & Hodos, W. (1996). *Comparative vertebrate neuroanatomy: Evolution and adaptation*. New York, NY, US: Wiley-Liss.
- Buzsáki, G., Anastassiou, C. A., & Koch, C. (2012). The origin of extracellular fields and currents--EEG, ECoG, LFP and spikes. *Nature Reviews. Neuroscience*, 13(6), 407–420. <https://doi.org/10.1038/nrn3241>
- Buzsáki, G., & Draguhn, A. (2004). Neuronal oscillations in cortical networks. *Science (New York, N.Y.)*, 304(5679), 1926–1929. <https://doi.org/10.1126/science.1099745>
- Cacioppo, J. T., Gardner, W. L., & Berntson, G. G. (1999). The affect system has parallel and integrative processing components: Form follows function. *Journal of Personality and Social Psychology*, 76(5), 839–855. <https://doi.org/10.1037/0022-3514.76.5.839>
- Calder, A. J., Lawrence, A. D., & Young, A. W. (2001). Neuropsychology of fear and loathing. *Nature Reviews. Neuroscience*, 2(5), 352–363. <https://doi.org/10.1038/35072584>
- Canessa, A., Pozzi, N. G., Arnulfo, G., Brumberg, J., Reich, M. M., Pezzoli, G., ... Isaias, I. U. (2016). Striatal Dopaminergic Innervation Regulates Subthalamic Beta-Oscillations and Cortical-Subcortical Coupling during Movements: Preliminary Evidence in Subjects with Parkinson's Disease. *Frontiers in Human Neuroscience*, 10. <https://doi.org/10.3389/fnhum.2016.00611>

- Cannon, W. B. (1927). The James-Lange Theory of Emotions: A Critical Examination and an Alternative Theory. *The American Journal of Psychology*, 39(1/4), 106–124. <https://doi.org/10.2307/1415404>
- Cannon, W. B. (1931). Again the James-Lange and the thalamic theories of emotion. *Psychological Review*, 38(4), 281–295. <https://doi.org/10.1037/h0072957>
- Carpenter, M. B., Carleton, S. C., Keller, J. T., & Conte, P. (1981). Connections of the subthalamic nucleus in the monkey. *Brain Research*, 224(1), 1–29.
- Carpenter, M. B. (1982). Anatomy and physiology of the basal ganglia. In: Schaltenbrand G, Walker AE, editors. *Stereotaxy of the human brain. Anatomical, physiological, and clinical applications*. 2nd ed. Stuttgart: Thieme; 1982: p. 233–68.
- Carpenter, M. B., & Strominger, N. L. (1967). Efferent fibers of the subthalamic nucleus in the monkey. A comparison of the efferent projections of the subthalamic nucleus, substantia nigra and globus pallidus. *The American Journal of Anatomy*, 121(1), 41–72. <https://doi.org/10.1002/aja.1001210105>
- Carretié, L., Martín-loeches, M., Hinojosa, J. A., & Mercado, F. (2001). Emotion and Attention Interaction Studied Through Event-Related Potentials. *J. Cognitive Neuroscience*, 13(8), 1109–1128. <https://doi.org/10.1162/089892901753294400>
- Cavanagh, J. F., Wiecki, T. V., Cohen, M. X., Figueroa, C. M., Samanta, J., Sherman, S. J., & Frank, M. J. (2011). Subthalamic nucleus stimulation reverses mediofrontal influence over decision threshold. *Nature Neuroscience*, 14(11), 1462–1467. <https://doi.org/10.1038/nn.2925>
- Chawla, D., Lumer, E. D., & Friston, K. J. (1999). The relationship between synchronization among neuronal populations and their mean activity levels. *Neural Computation*, 11(6), 1389–1411.
- Cho, Y. T., Ernst, M., & Fudge, J. L. (2013). Cortico-amygdala-striatal circuits are organized as hierarchical subsystems through the primate amygdala. *The Journal of Neuroscience: The Official Journal of the Society for Neuroscience*, 33(35), 14017–14030. <https://doi.org/10.1523/JNEUROSCI.0170-13.2013>
- Codling, D., Shaw, P., & David, A. S. (n.d.). Hypersexuality in Parkinson’s Disease: Systematic Review and Report of 7 New Cases. *Movement Disorders Clinical Practice*, 2(2), 116–126. <https://doi.org/10.1002/mdc3.12155>
- Cohen, M. X. (2014). *Analyzing neural time series data : theory and practice*. The MIT Press (Cambridge, Massachusetts).
- Comte, M., Schön, D., Coull, J. T., Reynaud, E., Khalfa, S., Belzeaux, R., ... Fakra, E. (2016). Dissociating Bottom-Up and Top-Down Mechanisms in the Cortico-Limbic System during Emotion Processing. *Cerebral Cortex (New York, N.Y.: 1991)*, 26(1), 144–155. <https://doi.org/10.1093/cercor/bhu185>
- Connolly, B. S., & Lang, A. E. (2014). Pharmacological treatment of Parkinson disease: a review. *JAMA*, 311(16), 1670–1683. <https://doi.org/10.1001/jama.2014.3654>
- Coombes, S. A., Gamble, K. M., Cauraugh, J. H., & Janelle, C. M. (2008). Emotional states alter force control during a feedback occluded motor task. *Emotion (Washington, D.C.)*, 8(1), 104–113. <https://doi.org/10.1037/1528-3542.8.1.104>
- Cuthbert, B. N., Schupp, H. T., Bradley, M. M., Birbaumer, N., & Lang, P. J. (2000). Brain potentials in affective picture processing: covariation with autonomic arousal and affective report. *Biological Psychology*, 52(2), 95–111.
- Dalgleish, T. (2004). The emotional brain. *Nature Reviews. Neuroscience*, 5(7), 583–589. <https://doi.org/10.1038/nrn1432>
- Darvas, F., & Hebb, A. O. (2014). Task specific inter-hemispheric coupling in human subthalamic nuclei. *Frontiers in Human Neuroscience*, 8, 701. <https://doi.org/10.3389/fnhum.2014.00701>
- Daubechies, I. (1992). *Ten Lectures on Wavelets*. Society for Industrial and Applied Mathematics. <https://doi.org/10.1137/1.9781611970104>
- de Lau, L. M. L., & Breteler, M. M. B. (2006). Epidemiology of Parkinson’s disease. *The Lancet. Neurology*, 5(6), 525–535. [https://doi.org/10.1016/S1474-4422\(06\)70471-9](https://doi.org/10.1016/S1474-4422(06)70471-9)
- de Solages, C., Hill, B. C., Koop, M. M., Henderson, J. M., & Bronte-Stewart, H. (2010). Bilateral symmetry and coherence of subthalamic nuclei beta band activity in Parkinson’s disease. *Experimental Neurology*, 221(1), 260–266. <https://doi.org/10.1016/j.expneurol.2009.11.012>
- Delplanque, S., N’diaye, K., Scherer, K., & Grandjean, D. (2007). Spatial frequencies or emotional effects? A systematic measure of spatial frequencies for IAPS pictures by a discrete wavelet analysis. *Journal of Neuroscience Methods*, 165(1), 144–150. <https://doi.org/10.1016/j.jneumeth.2007.05.030>

- Dietz, J., Bradley, M. M., Jones, J., Okun, M. S., Perlstein, W. M., & Bowers, D. (2013). The late positive potential, emotion and apathy in Parkinson's disease. *Neuropsychologia*, 51(5), 960–966. <https://doi.org/10.1016/j.neuropsychologia.2013.01.001>
- Dissanayaka, N. N. N. W., White, E., O'Sullivan, J. D., Marsh, R., Pachana, N. A., & Byrne, G. J. (2014). The clinical spectrum of anxiety in Parkinson's disease. *Movement Disorders: Official Journal of the Movement Disorder Society*, 29(8), 967–975. <https://doi.org/10.1002/mds.25937>
- Dorsey, E. R., Constantinescu, R., Thompson, J. P., Biglan, K. M., Holloway, R. G., Kieburtz, K., ... Tanner, C. M. (2007). Projected number of people with Parkinson disease in the most populous nations, 2005 through 2030. *Neurology*, 68(5), 384–386. <https://doi.org/10.1212/01.wnl.0000247740.47667.03>
- Driver, J. A., Logroscino, G., Gaziano, J. M., & Kurth, T. (2009). Incidence and remaining lifetime risk of Parkinson disease in advanced age. *Neurology*, 72(5), 432–438. <https://doi.org/10.1212/01.wnl.0000341769.50075.bb>
- Dumas, T., Dubal, S., Attal, Y., Chupin, M., Jouvent, R., Morel, S., & George, N. (2013). MEG Evidence for Dynamic Amygdala Modulations by Gaze and Facial Emotions. *PLOS ONE*, 8(9), e74145. <https://doi.org/10.1371/journal.pone.0074145>
- Duncan, G. W., Khoo, T. K., Yarnall, A. J., O'Brien, J. T., Coleman, S. Y., Brooks, D. J., ... Burn, D. J. (2014). Health-related quality of life in early Parkinson's disease: the impact of nonmotor symptoms. *Movement Disorders: Official Journal of the Movement Disorder Society*, 29(2), 195–202. <https://doi.org/10.1002/mds.25664>
- Eitan, R., Shamir, R. R., Linetsky, E., Rosenbluh, O., Moshel, S., Ben-Hur, T., ... Israel, Z. (2013). Asymmetric right/left encoding of emotions in the human subthalamic nucleus. *Frontiers in Systems Neuroscience*, 7, 69. <https://doi.org/10.3389/fnsys.2013.00069>
- Ekman, P., Levenson, R. W., & Friesen, W. V. (1983). Autonomic nervous system activity distinguishes among emotions. *Science (New York, N.Y.)*, 221(4616), 1208–1210.
- Engel, A. K., & Fries, P. (2010). Beta-band oscillations—signalling the status quo? *Current Opinion in Neurobiology*, 20(2), 156–165. <https://doi.org/10.1016/j.conb.2010.02.015>
- Fitzgerald, D. A., Angstadt, M., Jelsone, L. M., Nathan, P. J., & Phan, K. L. (2006). Beyond threat: Amygdala reactivity across multiple expressions of facial affect. *NeuroImage*, 30(4), 1441–1448. <https://doi.org/10.1016/j.neuroimage.2005.11.003>
- Fox, S. H., Katzenschlager, R., Lim, S.-Y., Ravina, B., Seppi, K., Coelho, M., ... Sampaio, C. (2011). The Movement Disorder Society Evidence-Based Medicine Review Update: Treatments for the motor symptoms of Parkinson's disease. *Movement Disorders: Official Journal of the Movement Disorder Society*, 26 Suppl 3, S2-41. <https://doi.org/10.1002/mds.23829>
- Frank, M. J., Gagne, C., Nyhus, E., Masters, S., Wiecki, T. V., Cavanagh, J. F., & Badre, D. (2015). fMRI and EEG predictors of dynamic decision parameters during human reinforcement learning. *The Journal of Neuroscience: The Official Journal of the Society for Neuroscience*, 35(2), 485–494. <https://doi.org/10.1523/JNEUROSCI.2036-14.2015>
- Fransen, A. M. M., van Ede, F., & Maris, E. (2015). Identifying neuronal oscillations using rhythmicity. *NeuroImage*, 118, 256–267. <https://doi.org/10.1016/j.neuroimage.2015.06.003>
- Friston, K. J. (2011). Functional and effective connectivity: a review. *Brain Connectivity*, 1(1), 13–36. <https://doi.org/10.1089/brain.2011.0008>
- Friston, K. J., Bastos, A. M., Pinotsis, D., & Litvak, V. (2015). LFP and oscillations-what do they tell us? *Current Opinion in Neurobiology*, 31, 1–6. <https://doi.org/10.1016/j.conb.2014.05.004>
- Fuchs, M., Kastner, J., Wagner, M., Hawes, S., & Ebersole, J. S. (2002). A standardized boundary element method volume conductor model. *Clinical Neurophysiology: Official Journal of the International Federation of Clinical Neurophysiology*, 113(5), 702–712.
- Gainotti, G. (1969). Reactions “catastrophiques” et manifestations d'indifférence au cours des atteintes cérébrales. *Neuropsychologia*, 7(2), 195–204. [https://doi.org/10.1016/0028-3932\(69\)90017-7](https://doi.org/10.1016/0028-3932(69)90017-7)
- Gainotti, G. (1972). Emotional Behavior and Hemispheric Side of the Lesion. *Cortex*, 8(1), 41–55. [https://doi.org/10.1016/S0010-9452\(72\)80026-1](https://doi.org/10.1016/S0010-9452(72)80026-1)
- Gainotti, G. (2012). Unconscious processing of emotions and the right hemisphere. *Neuropsychologia*, 50(2), 205–218. <https://doi.org/10.1016/j.neuropsychologia.2011.12.005>
- Gerfen, C. R., Engber, T. M., Mahan, L. C., Susel, Z., Chase, T. N., Monsma, F. J., & Sibley, D. R. (1990). D1 and D2 dopamine receptor-regulated gene expression of striatonigral and striatopallidal neurons. *Science (New York, N.Y.)*, 250(4986), 1429–1432.

- Gläscher, J., & Adolphs, R. (2003). Processing of the arousal of subliminal and supraliminal emotional stimuli by the human amygdala. *The Journal of Neuroscience: The Official Journal of the Society for Neuroscience*, 23(32), 10274–10282.
- Grabenhorst, F., Rolls, E. T., Margot, C., da Silva, M. A. A. P., & Velazco, M. I. (2007). How pleasant and unpleasant stimuli combine in different brain regions: odor mixtures. *The Journal of Neuroscience: The Official Journal of the Society for Neuroscience*, 27(49), 13532–13540. <https://doi.org/10.1523/JNEUROSCI.3337-07.2007>
- Grèzes, J., Valabrègue, R., Gholipour, B., & Chevallier, C. (2014). A direct amygdala-motor pathway for emotional displays to influence action: A diffusion tensor imaging study. *Human Brain Mapping*, 35(12), 5974–5983. <https://doi.org/10.1002/hbm.22598>
- Grinsted, A., Moore, J. C., & Jevrejeva, S. (2004). Application of the cross wavelet transform and wavelet coherence to geophysical time series. *Nonlin. Processes Geophys.*, 11(5/6), 561–566. <https://doi.org/10.5194/npg-11-561-2004>
- Güntekin, B., & Başar, E. (2014). A review of brain oscillations in perception of faces and emotional pictures. *Neuropsychologia*, 58, 33–51. <https://doi.org/10.1016/j.neuropsychologia.2014.03.014>
- Hamani, C., Saint-Cyr, J. A., Fraser, J., Kaplitt, M., & Lozano, A. M. (2004). The subthalamic nucleus in the context of movement disorders. *Brain: A Journal of Neurology*, 127(Pt 1), 4–20. <https://doi.org/10.1093/brain/awh029>
- Hardee, J. E., Thompson, J. C., & Puce, A. (2008). The left amygdala knows fear: laterality in the amygdala response to fearful eyes. *Social Cognitive and Affective Neuroscience*, 3(1), 47–54. <https://doi.org/10.1093/scan/nsn001>
- Harding, A. J., Stimson, E., Henderson, J. M., & Halliday, G. M. (2002). Clinical correlates of selective pathology in the amygdala of patients with Parkinson's disease. *Brain: A Journal of Neurology*, 125(Pt 11), 2431–2445.
- Haynes, W. I. A., & Haber, S. N. (2013). The organization of prefrontal-subthalamic inputs in primates provides an anatomical substrate for both functional specificity and integration: implications for Basal Ganglia models and deep brain stimulation. *The Journal of Neuroscience: The Official Journal of the Society for Neuroscience*, 33(11), 4804–4814. <https://doi.org/10.1523/JNEUROSCI.4674-12.2013>
- Herrington, T. M., Cheng, J. J., & Eskandar, E. N. (2016). Mechanisms of deep brain stimulation. *Journal of Neurophysiology*, 115(1), 19–38. <https://doi.org/10.1152/jn.00281.2015>
- Herz, D. M., Little, S., Pedrosa, D. J., Tinkhauser, G., Cheeran, B., Foltynie, T., ... Brown, P. (2018). Mechanisms Underlying Decision-Making as Revealed by Deep-Brain Stimulation in Patients with Parkinson's Disease. *Current Biology: CB*, 28(8), 1169–1178.e6. <https://doi.org/10.1016/j.cub.2018.02.057>
- Hirschmann, J., Özkurt, T. E., Butz, M., Homburger, M., Elben, S., Hartmann, C. J., ... Schnitzler, A. (2011). Distinct oscillatory STN-cortical loops revealed by simultaneous MEG and local field potential recordings in patients with Parkinson's disease. *NeuroImage*, 55(3), 1159–1168. <https://doi.org/10.1016/j.neuroimage.2010.11.063>
- Hodges, J. L., & Lehmann, E. L. (1962). Rank Methods for Combination of Independent Experiments in Analysis of Variance. *The Annals of Mathematical Statistics*, 33(2), 482–497. Retrieved from <http://www.jstor.org/stable/2237528>
- Hohlefeld, F. U., Huchzermeyer, C., Huebl, J., Schneider, G.-H., Brücke, C., Schönecker, T., ... Nikulin, V. V. (2014). Interhemispheric functional interactions between the subthalamic nuclei of patients with Parkinson's disease. *The European Journal of Neuroscience*, 40(8), 3273–3283. <https://doi.org/10.1111/ejn.12686>
- Horn, A., Reich, M., Vorwerk, J., Li, N., Wenzel, G., Fang, Q., ... Fox, M. D. (2017). Connectivity Predicts deep brain stimulation outcome in Parkinson disease. *Annals of Neurology*, 82(1), 67–78. <https://doi.org/10.1002/ana.24974>
- Hrybouski, S., Aghamohammadi-Sereshki, A., Madan, C. R., Shafer, A. T., Baron, C. A., Seres, P., ... Malykhin, N. V. (2016). Amygdala subnuclei response and connectivity during emotional processing. *NeuroImage*, 133, 98–110. <https://doi.org/10.1016/j.neuroimage.2016.02.056>
- Huebl, J., Schoenecker, T., Siegert, S., Brücke, C., Schneider, G.-H., Kupsch, A., ... Kühn, A. A. (2011). Modulation of subthalamic alpha activity to emotional stimuli correlates with depressive symptoms in Parkinson's disease. *Movement Disorders: Official Journal of the Movement Disorder Society*, 26(3), 477–483. <https://doi.org/10.1002/mds.23515>

- Huebl, J., Spitzer, B., Brücke, C., Schönecker, T., Kupsch, A., Alesch, F., ... Kühn, A. A. (2014). Oscillatory subthalamic nucleus activity is modulated by dopamine during emotional processing in Parkinson's disease. *Cortex; a Journal Devoted to the Study of the Nervous System and Behavior*, 60, 69–81. <https://doi.org/10.1016/j.cortex.2014.02.019>
- Hung, Y., Smith, M. L., Bayle, D. J., Mills, T., Cheyne, D., & Taylor, M. J. (2010). Unattended emotional faces elicit early lateralized amygdala-frontal and fusiform activations. *NeuroImage*, 50(2), 727–733. <https://doi.org/10.1016/j.neuroimage.2009.12.093>
- Janak, P. H., & Tye, K. M. (2015). From circuits to behaviour in the amygdala. *Nature*, 517(7534), 284–292. <https://doi.org/10.1038/nature14188>
- Jenkinson, C., Fitzpatrick, R., Peto, V., Greenhall, R., & Hyman, N. (1997). The Parkinson's Disease Questionnaire (PDQ-39): development and validation of a Parkinson's disease summary index score. *Age and Ageing*, 26(5), 353–357.
- Johansen, J. P., Cain, C. K., Ostroff, L. E., & LeDoux, J. E. (2011). Molecular mechanisms of fear learning and memory. *Cell*, 147(3), 509–524. <https://doi.org/10.1016/j.cell.2011.10.009>
- Jones, S. R. (2016). When brain rhythms aren't "rhythmic": implication for their mechanisms and meaning. *Current Opinion in Neurobiology*, 40, 72–80. <https://doi.org/10.1016/j.conb.2016.06.010>
- Jones, S. R., Kerr, C. E., Wan, Q., Pritchett, D. L., Hämäläinen, M., & Moore, C. I. (2010). Cued Spatial Attention Drives Functionally Relevant Modulation of the Mu Rhythm in Primary Somatosensory Cortex. *Journal of Neuroscience*, 30(41), 13760–13765. <https://doi.org/10.1523/JNEUROSCI.2969-10.2010>
- Kalanthroff, E., Cohen, N., & Henik, A. (2013). Stop feeling: inhibition of emotional interference following stop-signal trials. *Frontiers in Human Neuroscience*, 7, 78. <https://doi.org/10.3389/fnhum.2013.00078>
- Kalia, L. V., & Lang, A. E. (2015). Parkinson's disease. *The Lancet*, 386(9996), 896–912. [https://doi.org/10.1016/S0140-6736\(14\)61393-3](https://doi.org/10.1016/S0140-6736(14)61393-3)
- Kalia, S. K., Sankar, T., & Lozano, A. M. (2013). Deep brain stimulation for Parkinson's disease and other movement disorders. *Current Opinion in Neurology*, 26(4), 374–380. <https://doi.org/10.1097/WCO.0b013e3283632d08>
- Karachi, C., Yelnik, J., Tandé, D., Tremblay, L., Hirsch, E. C., & François, C. (2005). The pallidum-subthalamic projection: an anatomical substrate for nonmotor functions of the subthalamic nucleus in primates. *Movement Disorders: Official Journal of the Movement Disorder Society*, 20(2), 172–180. <https://doi.org/10.1002/mds.20302>
- Kato, K., Yokochi, F., Taniguchi, M., Okiyama, R., Kawasaki, T., Kimura, K., & Ushiba, J. (2015). Bilateral coherence between motor cortices and subthalamic nuclei in patients with Parkinson's disease. *Clinical Neurophysiology: Official Journal of the International Federation of Clinical Neurophysiology*, 126(10), 1941–1950. <https://doi.org/10.1016/j.clinph.2014.12.007>
- Kawagoe, R., Takikawa, Y., & Hikosaka, O. (1998). Expectation of reward modulates cognitive signals in the basal ganglia. *Nature Neuroscience*, 1(5), 411–416. <https://doi.org/10.1038/1625>
- Kawamura, M., & Kobayakawa, M. (2009). Emotional impairment in Parkinson's disease. *Parkinsonism & Related Disorders*, 15 Suppl 1, S47–52. [https://doi.org/10.1016/S1353-8020\(09\)70013-6](https://doi.org/10.1016/S1353-8020(09)70013-6)
- Keil, A., Debener, S., Gratton, G., Junghöfer, M., Kappenman, E. S., Luck, S. J., ... Yee, C. M. (2014). Committee report: publication guidelines and recommendations for studies using electroencephalography and magnetoencephalography. *Psychophysiology*, 51(1), 1–21. <https://doi.org/10.1111/psyp.12147>
- Kemp, J. M., & Powell, T. P. (1970). The cortico-striate projection in the monkey. *Brain: A Journal of Neurology*, 93(3), 525–546.
- Khoo, T. K., Yarnall, A. J., Duncan, G. W., Coleman, S., O'Brien, J. T., Brooks, D. J., ... Burn, D. J. (2013). The spectrum of nonmotor symptoms in early Parkinson disease. *Neurology*, 80(3), 276–281. <https://doi.org/10.1212/WNL.0b013e32827deb74>
- Kiesel, A., Miller, J., Jolicoeur, P., & Brisson, B. (2008). Measurement of ERP latency differences: a comparison of single-participant and jackknife-based scoring methods. *Psychophysiology*, 45(2), 250–274. <https://doi.org/10.1111/j.1469-8986.2007.00618.x>
- Kikuchi, S. (2007). Motor fluctuations in Parkinson's disease. *Journal of Neurology*, 254(5), 32–40. <https://doi.org/10.1007/s00415-007-5006-6>
- Klein, A., Sauer, T., Jedynak, A., & Skrandies, W. (2006). Conventional and wavelet coherence applied to sensory-evoked electrical brain activity. *IEEE Transactions on Bio-Medical Engineering*, 53(2), 266–272. <https://doi.org/10.1109/TBME.2005.862535>

- Klimesch, W. (1999). EEG alpha and theta oscillations reflect cognitive and memory performance: a review and analysis. *Brain Research. Brain Research Reviews*, 29(2–3), 169–195.
- Klimesch, Wolfgang, Fellinger, R., & Freunberger, R. (2011). Alpha oscillations and early stages of visual encoding. *Frontiers in Psychology*, 2, 118. <https://doi.org/10.3389/fpsyg.2011.00118>
- Klos, K. J., Bower, J. H., Josephs, K. A., Matsumoto, J. Y., & Ahlskog, J. E. (2005). Pathological hypersexuality predominantly linked to adjuvant dopamine agonist therapy in Parkinson’s disease and multiple system atrophy. *Parkinsonism & Related Disorders*, 11(6), 381–386. <https://doi.org/10.1016/j.parkreldis.2005.06.005>
- Klüver, H., & Bucy, P. C. (1937). “Psychic blindness” and other symptoms following bilateral temporal lobectomy in Rhesus monkeys. *American Journal of Physiology*, 119, 352–353.
- Kolling, N., Behrens, T., Wittmann, M. K., & Rushworth, M. (2016). Multiple signals in anterior cingulate cortex. *Current Opinion in Neurobiology*, 37, 36–43. <https://doi.org/10.1016/j.conb.2015.12.007>
- Kopell, N. J., Gritton, H. J., Whittington, M. A., & Kramer, M. A. (2014). Beyond the Connectome: The Dynome. *Neuron*, 83(6), 1319–1328. <https://doi.org/10.1016/j.neuron.2014.08.016>
- Kravitz, A. V., Tye, L. D., & Kreitzer, A. C. (2012). Distinct roles for direct and indirect pathway striatal neurons in reinforcement. *Nature Neuroscience*, 15(6), 816–818. <https://doi.org/10.1038/nn.3100>
- Kreitzer, A. C., & Malenka, R. C. (2008). Striatal plasticity and basal ganglia circuit function. *Neuron*, 60(4), 543–554. <https://doi.org/10.1016/j.neuron.2008.11.005>
- Kühn, A. A., Hariz, M. I., Silberstein, P., Tisch, S., Kupsch, A., Schneider, G.-H., ... Brown, P. (2005). Activation of the subthalamic region during emotional processing in Parkinson disease. *Neurology*, 65(5), 707–713. <https://doi.org/10.1212/01.wnl.0000174438.78399.bc>
- Kühn, Andrea A., Williams, D., Kupsch, A., Limousin, P., Hariz, M., Schneider, G.-H., ... Brown, P. (2004). Event-related beta desynchronization in human subthalamic nucleus correlates with motor performance. *Brain: A Journal of Neurology*, 127(Pt 4), 735–746. <https://doi.org/10.1093/brain/awh106>
- Lambert, C., Zrinzo, L., Nagy, Z., Lutti, A., Hariz, M., Foltynie, T., ... Frackowiak, R. (2012). Confirmation of functional zones within the human subthalamic nucleus: patterns of connectivity and sub-parcellation using diffusion weighted imaging. *NeuroImage*, 60(1), 83–94. <https://doi.org/10.1016/j.neuroimage.2011.11.082>
- Lang, P. J. (2010). Emotion and Motivation: Toward Consensus Definitions and a Common Research Purpose. *Emotion and Motivation: Toward Consensus Definitions and a Common Research Purpose. Emotion Review*, 2(3), 229–233. <https://doi.org/10.1177/1754073910361984>
- Lang, P.J., Bradley, M.M., & Cuthbert, B.N. (2008). International affective picture system (IAPS): Affective ratings of pictures and instruction manual. Technical Report A-8. University of Florida, Gainesville, FL.
- LeDoux, J. (2012). Rethinking the emotional brain. *Neuron*, 73(4), 653–676. <https://doi.org/10.1016/j.neuron.2012.02.004>
- LeDoux, J. E. (1996). *The emotional brain: The mysterious underpinnings of emotional life*. New York, NY, US: Simon & Schuster.
- Lévesque, J.-C., & Parent, A. (2005). GABAergic interneurons in human subthalamic nucleus. *Movement Disorders: Official Journal of the Movement Disorder Society*, 20(5), 574–584. <https://doi.org/10.1002/mds.20374>
- Li, Xiaoli, Yao, X., Fox, J., & Jefferys, J. G. (2007). Interaction dynamics of neuronal oscillations analysed using wavelet transforms. *Journal of Neuroscience Methods*, 160(1), 178–185. <https://doi.org/10.1016/j.jneumeth.2006.08.006>
- Li, Xingfeng, Xing, Y., Schwarz, S. T., & Auer, D. P. (2017). Limbic grey matter changes in early Parkinson’s disease. *Human Brain Mapping*. <https://doi.org/10.1002/hbm.23610>
- Limousin, P., Pollak, P., Benazzouz, A., Hoffmann, D., Broussolle, E., Perret, J. E., & Benabid, A. L. (1995). Bilateral subthalamic nucleus stimulation for severe Parkinson’s disease. *Movement Disorders: Official Journal of the Movement Disorder Society*, 10(5), 672–674. <https://doi.org/10.1002/mds.870100523>
- Lin, C.-Y., Tien, Y.-M., Huang, J.-T., Tsai, C.-H., & Hsu, L.-C. (2016). Degraded Impairment of Emotion Recognition in Parkinson’s Disease Extends from Negative to Positive Emotions. *Behavioural Neurology*, 2016, 9287092. <https://doi.org/10.1155/2016/9287092>

- Lipsman, N., Woodside, D. B., Giacobbe, P., Hamani, C., Carter, J. C., Norwood, S. J., ... Lozano, A. M. (2013). Subcallosal cingulate deep brain stimulation for treatment-refractory anorexia nervosa: a phase 1 pilot trial. *Lancet (London, England)*, 381(9875), 1361–1370. [https://doi.org/10.1016/S0140-6736\(12\)62188-6](https://doi.org/10.1016/S0140-6736(12)62188-6)
- Little, S., Tan, H., Anzak, A., Pogosyan, A., Kühn, A., & Brown, P. (2013). Bilateral functional connectivity of the basal ganglia in patients with Parkinson's disease and its modulation by dopaminergic treatment. *PloS One*, 8(12), e82762. <https://doi.org/10.1371/journal.pone.0082762>
- Litvak, V., Eusebio, A., Jha, A., Oostenveld, R., Barnes, G., Foltynie, T., ... Brown, P. (2012). Movement-related changes in local and long-range synchronization in Parkinson's disease revealed by simultaneous magnetoencephalography and intracranial recordings. *The Journal of Neuroscience: The Official Journal of the Society for Neuroscience*, 32(31), 10541–10553. <https://doi.org/10.1523/JNEUROSCI.0767-12.2012>
- Litvak, V., Jha, A., Eusebio, A., Oostenveld, R., Foltynie, T., Limousin, P., ... Brown, P. (2011). Resting oscillatory cortico-subthalamic connectivity in patients with Parkinson's disease. *Brain: A Journal of Neurology*, 134(Pt 2), 359–374. <https://doi.org/10.1093/brain/awq332>
- Loucif, K., Wilson, C., Baig, R., Lacey, M., & Stanford, I. (2005). Functional interconnectivity between the globus pallidus and the subthalamic nucleus in the mouse brain slice. *The Journal of Physiology*, 567(Pt 3), 977–987. <https://doi.org/10.1113/jphysiol.2005.093807>
- Lozano, A. M., Giacobbe, P., Hamani, C., Rizvi, S. J., Kennedy, S. H., Kolivakis, T. T., ... Mayberg, H. S. (2012). A multicenter pilot study of subcallosal cingulate area deep brain stimulation for treatment-resistant depression. *Journal of Neurosurgery*, 116(2), 315–322. <https://doi.org/10.3171/2011.10.JNS102122>
- MacLean, P. D. (1970). in *The Neurosciences. Second Study Program* (ed. Schmidt, F. O.) 336–349 (Rockefeller Univ. Press, New York).
- Mallet, L., Polosan, M., Jaafari, N., Baup, N., Welter, M.-L., Fontaine, D., ... STOC Study Group. (2008). Subthalamic nucleus stimulation in severe obsessive-compulsive disorder. *The New England Journal of Medicine*, 359(20), 2121–2134. <https://doi.org/10.1056/NEJMoa0708514>
- Mallet, L., Schüpbach, M., N'Diaye, K., Remy, P., Bardin, E., Czernecki, V., ... Yelnik, J. (2007). Stimulation of subterritories of the subthalamic nucleus reveals its role in the integration of the emotional and motor aspects of behavior. *Proceedings of the National Academy of Sciences of the United States of America*, 104(25), 10661–10666. <https://doi.org/10.1073/pnas.0610849104>
- Marceglia, S., Foffani, G., Bianchi, A. M., Baselli, G., Tamma, F., Egorov, M., & Priori, A. (2006). Dopamine-dependent non-linear correlation between subthalamic rhythms in Parkinson's disease. *The Journal of Physiology*, 571(Pt 3), 579–591. <https://doi.org/10.1113/jphysiol.2005.100271>
- Markovic, V., Agosta, F., Canu, E., Inuggi, A., Petrovic, I., Stankovic, I., ... Filippi, M. (2017). Role of habenula and amygdala dysfunction in Parkinson disease patients with punding. *Neurology*, 88(23), 2207–2215. <https://doi.org/10.1212/WNL.0000000000004012>
- Maren, S. (2001). Neurobiology of Pavlovian fear conditioning. *Annual Review of Neuroscience*, 24, 897–931. <https://doi.org/10.1146/annurev.neuro.24.1.897>
- Marras, C., & Lang, A. (2013). Parkinson's disease subtypes: lost in translation? *Journal of Neurology, Neurosurgery, and Psychiatry*, 84(4), 409–415. <https://doi.org/10.1136/jnnp-2012-303455>
- Marusak, H. A., Thomason, M. E., Peters, C., Zundel, C., Elrahal, F., & Rabinak, C. A. (2016). You say “prefrontal cortex” and I say “anterior cingulate”: meta-analysis of spatial overlap in amygdala-to-prefrontal connectivity and internalizing symptomology. *Translational Psychiatry*, 6(11), e944. <https://doi.org/10.1038/tp.2016.218>
- Mathai, A., & Smith, Y. (2011). The corticostriatal and corticosubthalamic pathways: two entries, one target. So what? *Frontiers in Systems Neuroscience*, 5, 64. <https://doi.org/10.3389/fnsys.2011.00064>
- McFarland, N. R., & Haber, S. N. (2000). Convergent inputs from thalamic motor nuclei and frontal cortical areas to the dorsal striatum in the primate. *The Journal of Neuroscience: The Official Journal of the Society for Neuroscience*, 20(10), 3798–3813.
- McIntosh, L. G., Mannava, S., Camalier, C. R., Folley, B. S., Albritton, A., Konrad, P. E., ... Neimat, J. S. (2015). Emotion recognition in early Parkinson's disease patients undergoing deep brain stimulation or dopaminergic therapy: a comparison to healthy participants. *Frontiers in Aging Neuroscience*, 6. <https://doi.org/10.3389/fnagi.2014.00349>

- Middleton, F. A., & Strick, P. L. (2002). Basal-ganglia “projections” to the prefrontal cortex of the primate. *Cerebral Cortex* (New York, N.Y.: 1991), 12(9), 926–935.
- Moors, A., Ellsworth, P. C., Scherer, K. R., & Frijda, N. H. (2013). Appraisal Theories of Emotion: State of the Art and Future Development. *Emotion Review*, 5(2), 119–124. <https://doi.org/10.1177/1754073912468165>
- Morris, L. S., Baek, K., & Voon, V. (2017). Distinct cortico-striatal connections with subthalamic nucleus underlie facets of compulsivity. *Cortex; a Journal Devoted to the Study of the Nervous System and Behavior*, 88, 143–150. <https://doi.org/10.1016/j.cortex.2016.12.018>
- Mueller, K., Jech, R., Růžička, F., Holiga, Š., Ballarini, T., Bezdicek, O., ... Urgošik, D. (2018). Brain connectivity changes when comparing effects of subthalamic deep brain stimulation with levodopa treatment in Parkinson’s disease. *NeuroImage: Clinical*, 19, 1025–1035. <https://doi.org/10.1016/j.nicl.2018.05.006>
- Nambu, A., Tokuno, H., & Takada, M. (2002). Functional significance of the cortico-subthalamo-pallidal “hyperdirect” pathway. *Neuroscience Research*, 43(2), 111–117.
- Obeso, J. A., Merello, M., Rodríguez–Oroz, M. C., Marin, C., Guridi, J., & Alvarez, L. (2007). Levodopa–induced dyskinesias in Parkinson’s disease. In W. C. Koller & E. Melamed (Eds.), *Handbook of Clinical Neurology* (Vol. 84, pp. 185–218). Elsevier. [https://doi.org/10.1016/S0072-9752\(07\)84040-1](https://doi.org/10.1016/S0072-9752(07)84040-1)
- Odekerken, V. J. J., van Laar, T., Staal, M. J., Mosch, A., Hoffmann, C. F. E., Nijssen, P. C. G., ... de Bie, R. M. A. (2013). Subthalamic nucleus versus globus pallidus bilateral deep brain stimulation for advanced Parkinson’s disease (NSTAPS study): a randomised controlled trial. *The Lancet. Neurology*, 12(1), 37–44. [https://doi.org/10.1016/S1474-4422\(12\)70264-8](https://doi.org/10.1016/S1474-4422(12)70264-8)
- Okun, M. S. (2014). Deep-brain stimulation--entering the era of human neural-network modulation. *The New England Journal of Medicine*, 371(15), 1369–1373. <https://doi.org/10.1056/NEJM-p1408779>
- Olofsson, J. K., Nordin, S., Sequeira, H., & Polich, J. (2008). Affective picture processing: An integrative review of ERP findings. *Biological Psychology*, 77(3), 247–265. <https://doi.org/10.1016/j.biopsycho.2007.11.006>
- Oostenveld, R., & Praamstra, P. (2001). The five percent electrode system for high-resolution EEG and ERP measurements. *Clinical Neurophysiology: Official Journal of the International Federation of Clinical Neurophysiology*, 112(4), 713–719.
- Oostenveld, Robert, Fries, P., Maris, E., & Schoffelen, J.-M. (2011). FieldTrip: Open Source Software for Advanced Analysis of MEG, EEG, and Invasive Electrophysiological Data [Research article]. <https://doi.org/10.1155/2011/156869>
- Oswal, A., Jha, A., Neal, S., Reid, A., Bradbury, D., Aston, P., ... Litvak, V. (2016). Analysis of simultaneous MEG and intracranial LFP recordings during Deep Brain Stimulation: a protocol and experimental validation. *Journal of Neuroscience Methods*, 261, 29–46. <https://doi.org/10.1016/j.jneumeth.2015.11.029>
- Pagani, J. H., & Rosen, J. B. (2009). The medial hypothalamic defensive circuit and 2,5-dihydro-2,4,5-trimethylthiazoline (TMT) induced fear: comparison of electrolytic and neurotoxic lesions. *Brain Research*, 1286, 133–146. <https://doi.org/10.1016/j.brainres.2009.06.062>
- Papez, J. W. (1937). A PROPOSED MECHANISM OF EMOTION. *Archives of Neurology & Psychiatry*, 38(4), 725–743. <https://doi.org/10.1001/archneurpsyc.1937.02260220069003>
- Parent, A., & Hazrati, L. N. (1995). Functional anatomy of the basal ganglia. II. The place of subthalamic nucleus and external pallidum in basal ganglia circuitry. *Brain Research. Brain Research Reviews*, 20(1), 128–154.
- Paton, J. J., Belova, M. A., Morrison, S. E., & Salzman, C. D. (2006). The primate amygdala represents the positive and negative value of visual stimuli during learning. *Nature*, 439(7078), 865–870. <https://doi.org/10.1038/nature04490>
- Perkins, M. N., & Stone, T. W. (1980). Subthalamic projections to the globus pallidus: an electrophysiological study in the rat. *Experimental Neurology*, 68(3), 500–511.
- Péron, J., Biseul, I., Leray, E., Vicente, S., Le Jeune, F., Drapier, S., ... Vérin, M. (2010). Subthalamic nucleus stimulation affects fear and sadness recognition in Parkinson’s disease. *Neuropsychology*, 24(1), 1–8. <https://doi.org/10.1037/a0017433>
- Péron, J., Cekic, S., Haegelen, C., Sauleau, P., Patel, S., Drapier, D., ... Grandjean, D. (2015). Sensory contribution to vocal emotion deficit in Parkinson’s disease after subthalamic stimulation. *Cor-*

- tex; a Journal Devoted to the Study of the Nervous System and Behavior, 63, 172–183. <https://doi.org/10.1016/j.cortex.2014.08.023>
- Péron, J., Frühholz, S., Ceravolo, L., & Grandjean, D. (2016). Structural and functional connectivity of the subthalamic nucleus during vocal emotion decoding. *Social Cognitive and Affective Neuroscience*, 11(2), 349–356. <https://doi.org/10.1093/scan/nsv118>
- Péron, J., Frühholz, S., Vérin, M., & Grandjean, D. (2013). Subthalamic nucleus: a key structure for emotional component synchronization in humans. *Neuroscience and Biobehavioral Reviews*, 37(3), 358–373. <https://doi.org/10.1016/j.neubiorev.2013.01.001>
- Péron, J., Grandjean, D., Le Jeune, F., Sauleau, P., Haegelen, C., Drapier, D., ... Vérin, M. (2010). Recognition of emotional prosody is altered after subthalamic nucleus deep brain stimulation in Parkinson's disease. *Neuropsychologia*, 48(4), 1053–1062. <https://doi.org/10.1016/j.neuropsychologia.2009.12.003>
- Pessiglione, M., Guehl, D., Rolland, A.-S., François, C., Hirsch, E. C., Féger, J., & Tremblay, L. (2005). Thalamic Neuronal Activity in Dopamine-Depleted Primates: Evidence for a Loss of Functional Segregation within Basal Ganglia Circuits. *Journal of Neuroscience*, 25(6), 1523–1531. <https://doi.org/10.1523/JNEUROSCI.4056-04.2005>
- Phaf, R. H., Mohr, S. E., Rotteveel, M., & Wicherts, J. M. (2014). Approach, avoidance, and affect: a meta-analysis of approach-avoidance tendencies in manual reaction time tasks. *Frontiers in Psychology*, 5, 378. <https://doi.org/10.3389/fpsyg.2014.00378>
- Poldrack, R. A., Clark, J., Paré-Blagoev, E. J., Shohamy, D., Moyano, J. C., Myers, C., & Gluck, M. A. (2001). Interactive memory systems in the human brain. *Nature*, 414(6863), 546–550. <https://doi.org/10.1038/35107080>
- Luck, S. J. (n.d.). *An Introduction to the Event-Related Potential Technique, Second Edition*. Retrieved July 2, 2018, from <https://mitpress.mit.edu/books/introduction-event-related-potential-technique-second-edition>
- Pringsheim, T., Jette, N., Frolkis, A., & Steeves, T. D. L. (2014). The prevalence of Parkinson's disease: a systematic review and meta-analysis. *Movement Disorders: Official Journal of the Movement Disorder Society*, 29(13), 1583–1590. <https://doi.org/10.1002/mds.25945>
- Purves, D., Augustine, G. J., Fitzpatrick, D., Katz, L. C., LaMantia, A.-S., McNamara, J. O., & Williams, S. M. (2001). *Excitatory and Inhibitory Postsynaptic Potentials*. Neuroscience. 2nd Edition. Retrieved from <https://www.ncbi.nlm.nih.gov/books/NBK11117/>
- Rao, R. P., & Ballard, D. H. (1999). Predictive coding in the visual cortex: a functional interpretation of some extra-classical receptive-field effects. *Nature Neuroscience*, 2(1), 79–87. <https://doi.org/10.1038/4580>
- Rappel, P., Marmor, O., Bick, A. S., Arkadir, D., Linetsky, E., Castrioto, A., ... Eitan, R. (2018). Subthalamic theta activity: a novel human subcortical biomarker for obsessive compulsive disorder. *Translational Psychiatry*, 8(1), 118. <https://doi.org/10.1038/s41398-018-0165-z>
- Russell, J. A. (1980). A circumplex model of affect. *Journal of Personality and Social Psychology*, 39(6), 1161–1178. <https://doi.org/10.1037/h0077714>
- Sabatinelli, D., Keil, A., Frank, D. W., & Lang, P. J. (2013). Emotional perception: correspondence of early and late event-related potentials with cortical and subcortical functional MRI. *Biological Psychology*, 92(3), 513–519. <https://doi.org/10.1016/j.biopsycho.2012.04.005>
- Sabatinelli, D., Lang, P. J., Bradley, M. M., Costa, V. D., & Keil, A. (2009). The timing of emotional discrimination in human amygdala and ventral visual cortex. *The Journal of Neuroscience: The Official Journal of the Society for Neuroscience*, 29(47), 14864–14868. <https://doi.org/10.1523/JNEUROSCI.3278-09.2009>
- Sacchet, M. D., LaPlante, R. A., Wan, Q., Pritchett, D. L., Lee, A. K. C., Hämäläinen, M., ... Jones, S. R. (2015). Attention Drives Synchronization of Alpha and Beta Rhythms between Right Inferior Frontal and Primary Sensory Neocortex. *Journal of Neuroscience*, 35(5), 2074–2082. <https://doi.org/10.1523/JNEUROSCI.1292-14.2015>
- Sander, D., Grandjean, D., & Scherer, K. R. (2005). A systems approach to appraisal mechanisms in emotion. *Neural Networks: The Official Journal of the International Neural Network Society*, 18(4), 317–352. <https://doi.org/10.1016/j.neunet.2005.03.001>
- Santangelo, G., Barone, P., Trojano, L., & Vitale, C. (2013). Pathological gambling in Parkinson's disease. A comprehensive review. *Parkinsonism & Related Disorders*, 19(7), 645–653. <https://doi.org/10.1016/j.parkreldis.2013.02.007>

- Scherer, K. R. (2001). Appraisal considered as a process of multilevel sequential checking. In *Appraisal processes in emotion: Theory, methods, research* (pp. 92–120). New York, NY, US: Oxford University Press.
- Schreckenberger, M., Lange-Asschenfeldt, C., Lange-Asschenfeldt, C., Lochmann, M., Mann, K., Siessmeier, T., ... Gründer, G. (2004). The thalamus as the generator and modulator of EEG alpha rhythm: a combined PET/EEG study with lorazepam challenge in humans. *NeuroImage*, 22(2), 637–644. <https://doi.org/10.1016/j.neuroimage.2004.01.047>
- Seymour, B., & Dolan, R. (2008). Emotion, decision making, and the amygdala. *Neuron*, 58(5), 662–671. <https://doi.org/10.1016/j.neuron.2008.05.020>
- Sheeba, J. H., Stefanovska, A., & McClintock, P. V. E. (2008). Neuronal Synchrony during Anesthesia: A Thalamocortical Model. *Biophysical Journal*, 95(6), 2722–2727. <https://doi.org/10.1529/biophysj.108.134635>
- Shink, E., Bevan, M. D., Bolam, J. P., & Smith, Y. (1996). The subthalamic nucleus and the external pallidum: two tightly interconnected structures that control the output of the basal ganglia in the monkey. *Neuroscience*, 73(2), 335–357.
- Shohamy, D., Myers, C. E., Grossman, S., Sage, J., Gluck, M. A., & Poldrack, R. A. (2004). Corticostriatal contributions to feedback-based learning: converging data from neuroimaging and neuropsychology. *Brain: A Journal of Neurology*, 127(Pt 4), 851–859. <https://doi.org/10.1093/brain/awh100>
- Sieger, T., Serranová, T., Růžička, F., Vostatek, P., Wild, J., Šťastná, D., ... Jech, R. (2015). Distinct populations of neurons respond to emotional valence and arousal in the human subthalamic nucleus. *Proceedings of the National Academy of Sciences of the United States of America*, 112(10), 3116–3121. <https://doi.org/10.1073/pnas.1410709112>
- Smith, Y., Bevan, M. D., Shink, E., & Bolam, J. P. (1998). Microcircuitry of the direct and indirect pathways of the basal ganglia. *Neuroscience*, 86(2), 353–387.
- Spence, S., Shapiro, D., & Zaidel, E. (n.d.). The role of the right hemisphere in the physiological and cognitive components of emotional processing. *Psychophysiology*, 33(2), 112–122. <https://doi.org/10.1111/j.1469-8986.1996.tb02115.x>
- Steigerwald, F., Pötter, M., Herzog, J., Pinsker, M., Kopper, F., Mehdorn, H., ... Volkman, J. (2008). Neuronal activity of the human subthalamic nucleus in the parkinsonian and nonparkinsonian state. *Journal of Neurophysiology*, 100(5), 2515–2524. <https://doi.org/10.1152/jn.90574.2008>
- Steriade, M. (2001). Impact of network activities on neuronal properties in corticothalamic systems. *Journal of Neurophysiology*, 86(1), 1–39. <https://doi.org/10.1152/jn.2001.86.1.1>
- Suppa, A., Iezzi, E., Conte, A., Belvisi, D., Marsili, L., Modugno, N., ... Berardelli, A. (2010). Dopamine influences primary motor cortex plasticity and dorsal premotor-to-motor connectivity in Parkinson's disease. *Cerebral Cortex (New York, N.Y.: 1991)*, 20(9), 2224–2233. <https://doi.org/10.1093/cercor/bhp288>
- Suzuki, A., Hoshino, T., Shigemasa, K., & Kawamura, M. (2006). Disgust-specific impairment of facial expression recognition in Parkinson's disease. *Brain*, 129(3), 707–717. <https://doi.org/10.1093/brain/awl011>
- Swanson, L. W. (2003). *Brain architecture: Understanding the basic plan*. New York, NY, US: Oxford University Press.
- Talakoub, O., Neagu, B., Udupa, K., Tsang, E., Chen, R., Popovic, M. R., & Wong, W. (2016). Time-course of coherence in the human basal ganglia during voluntary movements. *Scientific Reports*, 6, 34930. <https://doi.org/10.1038/srep34930>
- Taylor, P. C. J., Nobre, A. C., & Rushworth, M. F. S. (2007). Subsecond changes in top down control exerted by human medial frontal cortex during conflict and action selection: a combined transcranial magnetic stimulation electroencephalography study. *The Journal of Neuroscience: The Official Journal of the Society for Neuroscience*, 27(42), 11343–11353. <https://doi.org/10.1523/JNEUROSCI.2877-07.2007>
- Temel, Y., Blokland, A., Steinbusch, H. W. M., & Visser-Vandewalle, V. (2005). The functional role of the subthalamic nucleus in cognitive and limbic circuits. *Progress in Neurobiology*, 76(6), 393–413. <https://doi.org/10.1016/j.pneurobio.2005.09.005>
- Tessitore, A., Hariri, A. R., Fera, F., Smith, W. G., Chase, T. N., Hyde, T. M., ... Mattay, V. S. (2002). Dopamine Modulates the Response of the Human Amygdala: A Study in Parkinson's Disease. *Journal of Neuroscience*, 22(20), 9099–9103. <https://doi.org/10.1523/JNEUROSCI.22-20-09099.2002>

- Torrence, C., & Compo, G. P. (1998). A Practical Guide to Wavelet Analysis. *Bulletin of the American Meteorological Society*, 79(1), 61–78. [https://doi.org/10.1175/1520-0477\(1998\)079<0061:APGTWA>2.0.CO;2](https://doi.org/10.1175/1520-0477(1998)079<0061:APGTWA>2.0.CO;2)
- Tzourio-Mazoyer, N., Landeau, B., Papathanassiou, D., Crivello, F., Etard, O., Delcroix, N., ... Joliot, M. (2002). Automated anatomical labeling of activations in SPM using a macroscopic anatomical parcellation of the MNI MRI single-subject brain. *NeuroImage*, 15(1), 273–289. <https://doi.org/10.1006/nimg.2001.0978>
- van Hartevelt, T. J., Cabral, J., Deco, G., Møller, A., Green, A. L., Aziz, T. Z., & Kringelbach, M. L. (2014). Neural plasticity in human brain connectivity: the effects of long term deep brain stimulation of the subthalamic nucleus in Parkinson's disease. *PloS One*, 9(1), e86496. <https://doi.org/10.1371/journal.pone.0086496>
- Van Veen, B. D., van Drongelen, W., Yuchtman, M., & Suzuki, A. (1997). Localization of brain electrical activity via linearly constrained minimum variance spatial filtering. *IEEE Transactions on Bio-Medical Engineering*, 44(9), 867–880. <https://doi.org/10.1109/10.623056>
- Varela, F., Lachaux, J. P., Rodriguez, E., & Martinerie, J. (2001). The brainweb: phase synchronization and large-scale integration. *Nature Reviews. Neuroscience*, 2(4), 229–239. <https://doi.org/10.1038/35067550>
- Verbruggen, F., & Houwer, J. D. (2007). Do emotional stimuli interfere with response inhibition? Evidence from the stop signal paradigm. *Cognition and Emotion*, 21(2), 391–403. <https://doi.org/10.1080/02699930600625081>
- Volkman, J., Allert, N., Voges, J., Weiss, P. H., Freund, H. J., & Sturm, V. (2001). Safety and efficacy of pallidal or subthalamic nucleus stimulation in advanced PD. *Neurology*, 56(4), 548–551.
- Walker, H. C., Watts, R. L., Schrandt, C. J., Huang, H., Guthrie, S. L., Guthrie, B. L., & Montgomery, E. B. (2011). Activation of subthalamic neurons by contralateral subthalamic deep brain stimulation in Parkinson disease. *Journal of Neurophysiology*, 105(3), 1112–1121. <https://doi.org/10.1152/jn.00266.2010>
- Wessel, J. R., & Aron, A. R. (2013). Unexpected events induce motor slowing via a brain mechanism for action-stopping with global suppressive effects. *The Journal of Neuroscience: The Official Journal of the Society for Neuroscience*, 33(47), 18481–18491. <https://doi.org/10.1523/JNEUROSCI.3456-13.2013>
- Wessel, J. R., Jenkinson, N., Brittain, J.-S., Voets, S. H. E. M., Aziz, T. Z., & Aron, A. R. (2016). Surprise disrupts cognition via a fronto-basal ganglia suppressive mechanism. *Nature Communications*, 7, 11195. <https://doi.org/10.1038/ncomms11195>
- West, T., Farmer, S., Berthouze, L., Jha, A., Beudel, M., Foltynie, T., ... Litvak, V. (2016). The Parkinsonian Subthalamic Network: Measures of Power, Linear, and Non-linear Synchronization and their Relationship to L-DOPA Treatment and OFF State Motor Severity. *Frontiers in Human Neuroscience*, 10, 517. <https://doi.org/10.3389/fnhum.2016.00517>
- Wieser, M. J., Mühlberger, A., Alpers, G. W., Macht, M., Ellgring, H., & Pauli, P. (2006). Emotion processing in Parkinson's disease: dissociation between early neuronal processing and explicit ratings. *Clinical Neurophysiology: Official Journal of the International Federation of Clinical Neurophysiology*, 117(1), 94–102. <https://doi.org/10.1016/j.clinph.2005.09.009>
- Yaari, Y., & Beck, H. (2002). "Epileptic neurons" in temporal lobe epilepsy. *Brain Pathology (Zurich, Switzerland)*, 12(2), 234–239.
- Yarnall, A., Rochester, L., & Burn, D. J. (2011). The interplay of cholinergic function, attention, and falls in Parkinson's disease. *Movement Disorders: Official Journal of the Movement Disorder Society*, 26(14), 2496–2503. <https://doi.org/10.1002/mds.23932>
- Yelnik, J., & Percheron, G. (1979). Subthalamic neurons in primates: a quantitative and comparative analysis. *Neuroscience*, 4(11), 1717–1743.
- Yoshimura, N., Kawamura, M., Masaoka, Y., & Homma, I. (2005). The amygdala of patients with Parkinson's disease is silent in response to fearful facial expressions. *Neuroscience*, 131(2), 523–534. <https://doi.org/10.1016/j.neuroscience.2004.09.054>
- Zavala, B., Damera, S., Dong, J. W., Lungu, C., Brown, P., & Zaghoul, K. A. (2017). Human Subthalamic Nucleus Theta and Beta Oscillations Entrain Neuronal Firing During Sensorimotor Conflict. *Cerebral Cortex (New York, N.Y.: 1991)*, 27(1), 496–508. <https://doi.org/10.1093/cercor/bhv244>
- Zavala, B., Zaghoul, K., & Brown, P. (2015). The subthalamic nucleus, oscillations, and conflict. *Movement Disorders: Official Journal of the Movement Disorder Society*, 30(3), 328–338. <https://doi.org/10.1002/mds.26072>

Zhang, G., Zhang, Z., Liu, L., Yang, J., Huang, J., Xiong, N., & Wang, T. (2014). Impulsive and compulsive behaviors in Parkinson's disease. *Frontiers in Aging Neuroscience*, 6, 318. <https://doi.org/10.3389/fnagi.2014.00318>

8. Appendix

Case	Age (years)/Sex	Disease duration (years)	Preoperative LEDD (mg)	Preoperative UPDRS OFF/ON (score)	Postoperative LEDD (mg)	Postoperative UPDRS OFF (medication) and ON (stimulation)	Striatal DD
wue03	63/m	18	2725	40/9	600	13	L < R
wue04	55/m	7	658	26/4	400	23	L < R
wue06	53/m	11	1133	47/12	180	9	L > R
wue07	62/m	10	650	43/24	220	19	L > R
wue09	56/m	19	1200	50/11	730	16	L < R
wue11	54/f	11	1300	55/4	460	9	L > R

Table A1 | **Patient information.**

	STN Signed Area Amplitudes ($\mu\text{V s}$)					
	Measurement window 1			Measurement window 2		
	unpleasant	neutral	pleasant	unpleasant	neutral	pleasant
OFF	1.08 (.046)	1.02 (.38)	1.11 (.41)	1.12 (.26)	.99 (.40)	1.11 (.35)
ON	.88 (.36)	1.08 (.56)	.83 (.35)	.70 (.32)	1.09 (.31)	.99 (.04)
Right STN	1.00 (.20)	1.18 (.28)	0.82 (.32)	.69 (.21)	1.04 (.35)	1.28 (.29)
Left STN	0.96 (.21)	.92 (.11)	1.12 (.27)	1.13 (.38)	1.04 (.31)	.82 (.22)
Most DD	.99 (.25)	.89 (.07)	1.12 (.29)	1.11 (.39)	1.02 (.31)	.87 (.29)
Least DD	.97 (.15)	1.21 (.26)	.82 (.29)	.71 (.24)	1.06 (.35)	1.23 (.30)

Table A2 | **STN Signed Area Amplitudes.** Mean values per condition combination, SD in parenthe-

	STN 50% Area Latencies (s)					
	Measurement window 1			Measurement window 2		
	unpleasant	neutral	pleasant	unpleasant	neutral	pleasant
OFF	.39 (.06)	.39 (.05)	.39 (.06)	.86 (.06)	.86 (.05)	.84 (.03)
ON	.39 (.03)	.40 (.03)	.39 (.03)	.88 (.04)	.83 (.02)	.92 (.02)
Right STN	.38 (.03)	.38 (.05)	.38 (.05)	.87 (.06)	.85 (.03)	.82 (.04)
Left STN	.40 (.07)	.40 (.06)	.40 (.07)	.87 (.05)	.85 (.03)	.83 (.02)
Most DD	.38 (.07)	.38 (.07)	.38 (.07)	.86 (.05)	.84 (.04)	.82 (.03)
Least DD	.40 (.03)	.41 (.03)	.40 (.03)	.88 (.06)	.86 (.02)	.84 (.03)

Table A3 | **STN 50% area latencies.** Mean values per condition combination, SD in parentheses.

	Virtual Amygdala					
	Signed Area Amplitudes ($\mu\text{V s}$)			50% Area Latencies (s)		
	unpleasant	neutral	pleasant	unpleasant	neutral	pleasant
OFF	.99 (.71)	1.06 (.79)	1.07 (.85)	.31 (.03)	.31 (.03)	.32 (.03)
ON	.74 (.96)	.64 (.85)	.79 (1.11)	.37 (.04)	.38 (.03)	.32 (.05)
Right	.88 (.77)	.97 (.73)	1.09 (.80)	.33 (.03)	.35 (.01)	.32 (.05)
Left	.68 (.47)	.72 (.48)	.61 (.65)	.34 (.02)	.34 (.02)	.32 (.03)
Most DD	.90 (.55)	.96 (.66)	1.07 (.78)	.34 (.03)	.35 (.02)	.32 (.04)
Least DD	.67 (.70)	.73 (.58)	.63 (.69)	.34 (.02)	.34 (.02)	.32 (.04)

Table A4 | **Virtual amygdala ERP parameter values.**

	Virtual ACC					
	Signed Area Amplitudes (μV s)			50% Area Latencies (s)		
	unpleasant	neutral	pleasant	unpleasant	neutral	pleasant
OFF	.84 (.57)	.81 (.49)	.84 (.53)	.35 (.02)	.34 (.01)	.35 (.02)
ON	.91 (.91)	.88 (1.08)	.88 (1.13)	.37 (.02)	.37 (.05)	.36 (.06)
Right	.87 (.83)	.86 (.85)	.86 (.89)	.35 (.03)	.35 (.03)	.34 (.04)
Left	.63 (.61)	.60 (.64)	.61 (.70)	.35 (.03)	.34 (.04)	.32 (.04)
Most DD	.80 (.85)	.79 (.85)	.81 (.90)	.35 (.03)	.35 (.03)	.34 (.04)
Least DD	.70 (.61)	.67 (.67)	.66 (.71)	.35 (.03)	.34 (.03)	.33 (.03)

Table A5 | **Virtual ACC ERP parameters.**

9. Curriculum Vitae

Persönliche Daten

Name	Uri E. Ramírez Pasos
Adresse	Neurologische Klinik und Poliklinik Josef-Schneider_Str. 11 97080 Würzburg
Mobil	0160 - 91665792
E-Mail	urieduardo@gmail.com
Geburtsdatum / -ort	24. November 1989 in Mexico City
Familienstand	ledig
Staatsbürgerschaft	mexikanisch

Ausbildung

01.09.13 – heute	Doktorand in Neurowissenschaften an der Universität Würzburg mit Dissertationsthema „Elektrophysiologie des nucleus subthalamicus von parkinsonischen Patienten bei limbischer Verarbeitung visueller Stimuli“.
01.09.13 – 31.8.14	Zusammenarbeit mit Dr. Pötter beim Projekt, „Single-Unit Activity in the Human Subthalamic Nucleus during Reach-to-Grasp Movements“. Arbeit präsentiert am Society for Neuroscience 2014 Kongress in Washington DC.
01.09.14 – 01.06.2016	Zusammenarbeit mit Dr. René Reese beim Projekt „Oral Levodopa Modulates Movement-Dependent Subthalamic Nucleus-Muscle Connectivity in Parkinson’s Disease“. Arbeit präsentiert am Movement Disorders Society 2016 Kongress in Berlin.

- 01.09.12 – 01.09.13 Qualifikationsprogram an der Universität Würzburg mit
Schwerpunkt auf Signalbearbeitung
- 22.08.08 – 10.08.12 B.Sc., Mathematik, University of Florida, Gainesville, FL
Universitätsabschluss: Bachelors of Science mit Durchschnittsnote
(GPA) 3.76.
- 12.09.06 – 10.05.08 International Baccalaureate, UWC of the Atlantic, Wales
Schulabschluss: International Baccalaureate mit 40 Punkten.

Weiterbildung

- 1.10.16– 15.10.16 Wissenschaftliche Weiterbildung an der Universität Mainz mit
Schwerpunkt auf Quellerekonstruktion für EEG
- 1.07.14– 31.07.14 Wissenschaftliche Weiterbildung an der Universität Kiel mit
Schwerpunkt auf higher order statistics

Kenntnisse

- EDV-Kenntnisse Python
Matlab
R
Photoshop
Microsoft Office

Sprachkenntnisse

Spanisch/Englisch/Deutsch: verhandlungssicher

Französisch: fließend in Wort und Schrift

Italienisch: Basiswissen